Investigation into the effects and mechanisms of rapamycin treatment in two mouse models of Complex I-deficient neurological pathology

Melana Yanos

A dissertation submitted in partial fulfillment of the
requirements for the degree of

Doctor of Philosophy

University of Washington

2014

Reading Committee:
Matt Kaeberlein, Chair
Sheri Mizumori, Chair
Jaime Diaz

Program Authorized to Offer Degree:
Psychology

University of Washington

Abstract

Investigation into the effects and mechanisms of rapamycin treatment in two mouse models of Complex I-deficient neurological pathology

Melana E Yanos

Chairs of the Supervisory Committee:
Matt Kaeberlein, Associate Professor
Department of Pathology

Sheri Mizumori, Professor
Department of Psychology

Treatments to stop or reverse the debilitating progression of early- and late-onset neurological diseases remain undiscovered. Collective evidence suggests that inhibition of the mechanistic target of rapamycin (mTOR) signaling pathway is effective at reducing markers of pathology in experimental models of age-related and developmental neurological diseases. These include, but are not limited to, models for Alzheimer's disease, Parkinson's disease, Huntington's disease, Fragile X syndrome, Tuberous Sclerosis Complex and Leigh syndrome. How regulation of mTOR activity

and its downstream effectors interact with underlying neural mechanisms of disease has been a topic of considerable debate.

The studies presented here investigate the potential therapeutic effects of the mTOR inhibitor rapamycin in two different mouse models for neurological disease: the NDUFS4 knockout (NDUFS4 KO) mouse for Leigh Syndrome and the MPTP mouse model for Parkinson's disease. In these models, mitochondrial electron transport chain complex I activity is reduced but results in distinct patterns of neuronal pathology. Our major objectives were (1) to identify previously unreported effects of rapamycin treatment in these models; and (2) to identify the potential cellular mechanisms that mediate these effects.

First, we demonstrate that daily treatment with high dose rapamycin effectively extends the short lifespan of NDUFS4 KO mice. Rapamycin treatment also resulted in prolonged healthspan in KO mice, as indicated by the offset of neurological damage, maintenance of weight and body fat, and the improvement of deleterious behavioral phenotypes. Systematic testing of potential mechanisms mediating these effects led us to favor a model in which rapamycin induces a metabolic shift in NDUFS4 KO brains toward amino acid catabolism and away from glycolysis, thus alleviating the buildup of glycolytic intermediates.

Following this set of discoveries, we expanded our findings to test whether dietary rapamycin delivered at higher doses than previously used could improve lifespan and abnormal weight phenotypes in NDUFS4 KO mice, similar to what was found for high dose injections. Dietary rapamycin doses were tested at 42 ppm, 126

ppm and 378 ppm, corresponding to 3-fold, 9-fold and 27-fold increases from the standard 14 ppm dosage used by the NIH Interventions Testing Program, respectively. As a result of these treatments, NDUFS4 KO lifespan was significantly extended, with successively higher dosages correlating with increased survival. We also found that dietary rapamycin at 126 and 378 ppm had significant effects on body weight and fat mass in male and female wild-type mice.

Finally, we conducted a pilot study investigating the effectiveness of high dose rapamycin treatment in treating the Parkinson's disease-like pathology of mice exposed to the toxic drug MPTP. Our results show that rapamycin treatment partially reduced neuron degeneration in the substantia nigra resulting from MPTP exposure, consistent with previous reports. In addition, MPTP mice showed evidence for hyperactive mTOR signaling compared to control mice, which could be potently reduced by rapamycin treatment. No significant changes in body weight or fast mass were found as a result of MPTP exposure, or as a result of an interaction between MPTP and rapamycin. When accounting for different age cohorts, middle aged mice that had been exposed to MPTP performed better on a rotarod task after receiving rapamycin treatment. Our young cohort, however, did not show any differences in performance between treatment groups. Thus, we believe that MPTP induces age-dependent phenotypes that may have been overlooked in previous studies utilizing young mice.

Thus far, comparison of these studies suggests that rapamycin treatment has both overlapping and distinct effects that contribute to attenuation of neural pathology of NDUFS4 and MPTP mouse models.

ACKNOWLEDGEMENTS

Completion of this doctoral thesis would not have been possible without the help and support of my colleagues, mentors, friends and family.

I would like to thank the Psychology department for sponsoring my enrollment in graduate school, over the course of a journey spanning almost 9 years. I admit there were times when it felt like completing of my PhD requirements were out of reach, but we managed to stick together. I'm very grateful that we did. I would also like to thank the NIH Genetics Approaches to Aging Training Grant for funding my research over the past four years.

Special thanks to my in-house Psychology adviser Dr. Sheri Mizumori, who so openly met with me even prior to my application to the UW psychology program. You have been a wonderful source of support, from start to finish. I appreciate so much your willingness to be my in-house adviser when I felt like I was a "homeless" graduate student! Thank you to Dr. Jim Diaz as well, for always been an advocate for graduate students, and for being such a positive addition to my thesis committee.

Certain members of my Psychology graduate student "cohort," who started the program with me those nine years ago, with whom I now have lifelong friendships – Yamile, Diane, Em and Jon – you guys understand this experience like no one else can. Thank you for always being there.

There are two specific research labs with whom I have had the special honor of collaborating with throughout my research. Special thanks first to the Rabinovitch lab – to Peter, for being a valuable addition to my faculty committee; and Jeanne, for answering my questions about how to do mouse research, and for letting me borrow things so that we weren't equipped with at the time. Many, many things. I would also like to thank past and present employees Ladiges lab for facilitating a positive research environment at the Foege mouse vivarium, Heather and Ruby in particular.

Of course, huge thanks to the Kaeberlein lab members, past and present, for your support, encouragement and collective sense of humor (not to mention the beers!). Simon, thank you so much for sharing your knowledge about mouse research with me, if it wasn't for all our hard collaborative work I don't know where I'd be right now. Thank you Fres for being my mentor when I first started out in the Kaeberlein lab, I will never forget how great a teacher you were. To Alessandro and Takashi, for being incredibly helpful resources to me just a couple of benches away. To the undergraduate mouse team, current and emeritus – Conner, Lanny, Nic, and Oliver – you guys have been the best helpers I could have asked for.

To my research adviser Dr. Matt Kaeberlein, I don't know how to thank you enough. You took a chance on recruiting a refugee graduate student from the Psychology department, and it has made all the difference for me in my academic pursuits these past few years. Through it all you have been a terrific source of encouragement, advice and support. I couldn't have asked for a better boss.

I've reserved my final thanks for my parents, Sally and Mel. I don't know really know how to express in words how grateful I am for you both. Perhaps my humble work can be at least a small expression of how honored I am to be your daughter. I dedicate this thesis to you.

TABLE OF CONTENTS

LIST OF FIGURES

LIST OF TABLES

CHAPTER 1 - INTRODUCTION

Dysregulation of mTOR pathway signaling in early- and late-onset neurological disorders: a potential therapeutic target

The mechanistic target of rapamycin (mTOR) is a highly conserved protein that has been identified as a key regulator of cellular growth, proliferation and survival in response to nutrient and hormonal cues [1–4]. A convergence of research over the past decade among both neuroscience- and aging-related fields has begun to identify the therapeutic potential of mTOR inhibition in the prevention and treatment of neurological diseases and disorders. In this chapter, I will briefly describe the mTOR signaling pathway and its known involvement in aging processes. Furthermore, I will discuss mTOR activity as it relates to general neuronal function as well as alterations in mTOR regulation in non-diseased aging brain. Finally, I will discuss how dysregulation of mTOR may be involved in a diverse panel of both early- and late-onset neurological diseases, and how inhibition of mTOR pathway components might be effective at protecting or restoring brain morphology and function in a neurological disease background.

PART 1. THE mTOR SIGNALING PATHWAY AND AGING

mTOR is a serine/threonine protein kinase that functions in a signaling pathway to detect and respond to changes in nutrients, cellular energy status, and stress to modulate cellular growth, proliferation and survival. Molecular components of mTOR signaling were originally identified through yeast studies involving rapamycin, a drug

that is known to specifically inhibit mTOR signaling, and for which mTOR has been named [5].

1.1. Regulation of mTOR signaling and downstream effectors

mTOR functions in two distinct complexes: mTORC1 and mTORC2. The mTORC1 complex consists of TOR kinase partnered with Raptor, PRAS40 (proline-rich AKT substrate 40 kDa), the DEP domain containing mTOR-interacting protein (DEPTOR) and mLST8. The mTORC2 complex is formed when mTOR interacts with rictor, DEPTOR mLST8 and hSIN[4,6]. mTORC1 regulates many cellular processes, including transcription, translation, autophagy, cell cycle and microtubule dynamics, whereas mTORC2 regulates actin cytoskeleton dynamics, cell metabolism and survival[7–10].

Generally, much more is known about upstream regulation of mTORC1 than mTORC2. An illustration of mTORC1 signaling pathway components is presented in **Figure 1.1.** A classical pathway for mTORC1 can be described in which inputs such as growth factors, hormones and cytokines lead to activation of phosphoinositide-3' kinase (PI3K), resulting in increased production of phosphatidylinositol 3,4,5-trisphosphate (PIP3). As a result, 3-phsophoinositide-dependent protein kinase (PDK1) is recruited to the cell membrane, where it phosphorylates and activates Akt. Activation of Akt removes inhibitory constraint on mTORC1 via phosphorylation of both TSC2 and PRAS40[11–13]. TSC2, along with TSC1 constitute the tuberous sclerosis complex TSC1/2, a GTPase-activating protein (GAP) that inhibits Rheb. Phosphorylation of TSC2 inhibits GAP activity, resulting in increased Rheb-GTP levels. Rheb-GTP binds

directly to the kinase domain of mTOR and thus stimulates mTORC1 activity[14–17]. In parallel, phosphorylation of PRAS40 releases it from the complex, thereby removing its inhibitory action from mTORC1[13]. In addition to extracellular stimulation through the PI3K pathway, intracellular signaling from AMP kinase (AMPK), which is activated in response to low cellular energy, inhibits mTORC1 activity through removal of TSC2 inhibition on GAP activity, or by phosphorylation of Raptor and its consequential dissociation from the mTORC1 complex[3,18,19]. mTORC2 also phosphorylates Akt, acting as a PKD2, indirectly modulating mTORC1 activity[9,20].

In addition, amino acids are required inputs for activation of mTORC1 through promotion of mTORC1 association with the Rag GTPases on the surface of lysosomes[10,21,22]. The four Rag proteins – Rag A, B, Rag C, and Rag D – form heterodimer pairs as RagA/B and Rag C/D with opposite nucleotide loading states, such that when GDP is bound to one pair, GTP is bound to the other. Amino acids promote loading of Rag A/B with GTP, which allows its interaction with the raptor component of mTORC1[22]. As a result, mTORC1 is recruited to the lysosomal surface, where it can be activated by Rheb. In addition, Rag GTPases dock on Ragulator, a multisubunit complex that is also required for activation of mTORC1 by amino acids[23]. The exact process by which Ragulator and Rag GTPases are localized to the lysosomal surface is not known, but an “inside out model” of amino acid sensing posits that amino acids accumulate in the lysosomal lumen and initiate signaling through a mechanism that requires the vacuolar H+-adenoside triphosphate ATPase (v-ATPase)[24]. The v-ATPase directly interacts with Ragulator on the surface of the lysosomes; furthermore,

its ATPase activity appears to be essential for relaying amino acid signals from the lysosomal lumen to Ragulator and Rag GTPases. Overall, it appears that the recruitment of mTOR to the lysosome surface through its interaction with Ragulator and RagGTPase components is dependent upon v-ATPase activity.[10]Activation of mTORC1 results in increased protein translation by phosphorylation of both 4E-binding protein (4EBP) and S6 kinase 1 (S6K1). Under basal conditions, hypophosphorylated 4EBP binds to and inhibits translation initiation factor 4E (eIF4E). Phosphorylation of 4EBP by mTORC1 activity releases 4EBP from eIF4E to initiate cap-dependent translation, in which eIF4E recruits eIF4G to the 5' end of most mRNAs[3,17–20]. Phosphorylation of S6K1 promotes mRNA translation by binding to and phosphorylating proteins involved in translation initiation and elongation, including eIF4B and elongation factor kinase 2 (eIF2K)[3,7,29,30].

In addition to promoting translation of proteins, mTORC actively suppresses autophagy, the process by which cellular materials are targeted to the lysosome to be degraded and recycled. mTORC1 phosphorylation of ATG13 and ULK1, the mammalian homologs of yeast Atg13 and Atg1, blocks autophagosome formation[31]. Conversely, inhibition of mTOR by pharmacological agents rapamycin or Torin1 strongly induces autophagy in cells [32,33].

Rapamycin inhibits mTORC1 by interacting with the receptor FK506-binding protein FKBP12 and blocking its interaction with Raptor[34]. As a consequence of mTORC1 inhibition, rapamycin has been shown to impair cell proliferation, reduce cell size, decrease global mRNA translation, and enhance autophagy[4,10]. Several reports have also indicated that rapamycin can modulate cellular metabolism and mitochondrial

function in a complex manner that is still poorly understood[35–37]. Although mTORC2 is considered "rapamycin insensitive," evidence has shown that chronic exposure to rapamycin in mice can sequester mTOR from mTORC2, thereby inhibiting mTORC2 assembly [38].

1.2. mTOR and aging

Because age is the most significant risk factor for onset of neurodegenerative diseases, interest in mTOR's involvement in aging processes has become relevant in the context of healthy brain aging and amelioration of neurodegenerative disease symptoms. Original research that identified the role of mTOR in longevity pathways were conducted in yeast, in which deletion of SCH9 – the yeast ortholog of S6K1 – resulted in a doubling of yeast chronological lifespan, or the duration of time that yeast cells in stationary phase remain viable[1,39]. Following this discovery, large scale analysis of single-gene deletion strains of yeast found that deletion of Tor1 or Sch9 increased replicative life span, or the number of daughter cells that are produced by a mother cell prior to senescence.[40] In the nematode worm *C. elegans*, RNA interference (RNAi) to block expression of mTOR homolog *let-363* or S6K1 homolog *rsks-1* results in increased lifespan.[41,42] In *drosophila*, overexpression of dTsc1 or dTsc2, or dominant-negative forms of dTOR and dS6k all result in lifespan extension[43]. S6K knockout in mice has similarly been shown to increase lifespan, although this effect appears to be specific for females[44]. In addition to studies examining the effects of genetic inhibition of mTOR on lifespan, pharmacological inhibition of mTOR by rapamycin has been shown to increase lifespan in fly, worm and mouse models[45–47].

Many of these studies suggest that inhibition of mTOR activity promotes longevity primarily through its effects on decreased translation and increased autophagy. Interestingly, these proposed mechanisms of aging are also implicated in mTOR's involvement in neurodegenerative disease pathology, which I will discuss in more detail later. Overall, research that further seeks to establish the role of mTOR as a modulator of aging processes is ongoing, and identification of additional downstream mechanisms affected by mTOR – including mitochondrial function, stress response, inflammation, and lipid synthesis – contribute to an increasingly complex understanding of its pro-longevity effects[1,3].

1.2.1. Interactions between mTOR and known longevity pathways

Consistent with its involvement in both nutrient sensing and regulation of longevity across species, substantial evidence supports a role for mTORC1 signaling in mediating the lifespan-extending effects of dietary restriction (DR). DR is defined as reduction of food intake without malnutrition. Similar to the conserved effects of mTOR inhibition, DR extends lifespan in yeast, worm, fly and rodent models[48–54]. Furthermore, DR has been shown to increase lifespan in non-human primates[48]. Current research on calorie restriction in humans has, thus far, shown evidence for improved cardiac health and protection against atherosclerosis, improved liver function, as well as decreased insulin levels and body temperatures, which are considered to be two biomarkers of longevity[55–58].

DR inhibits mTOR activity and fails to extend life span when mTOR activity is reduced in yeast, nematodes or flies[40,42,43,59]. Because of the highly conserved and

overlapping nature of both mTOR and DR longevity pathways, rapamycin's therapeutic potential as a "DR mimetic" is being widely explored in studies of aging and age-related disease.

However, the relationship between mTOR and aging is far more complex, as mTOR interacts with multiple longevity pathways in addition to DR. Reduced insulin/IGF-1-like signaling has been known to increase longevity in nematodes, flies and mice[60,61]. The IIS signaling cascade activates mTORC1, which in turn negatively regulates IIS through phosphorylation of S6K and inhibition of IRS-1[62]. Activation of AMP kinase (AMPK) through genetic overexpression or administration of the antidiabetic drug metformin increases lifespan in *C. elegans*[63,64]. Metformin has also been shown to enhance survival in short-lived, cancer-prone strains of mice[65]. Finally, mTORC1 is activated in response to hypoxia and regulates translation and stabilization of HIF1 along with HIF-1 target genes in mammals[66]; studies in *C. elegans* have implicated stabilization of HIF-1 acting downstream of mTOR to extend lifespan[67,68].

PART 2. mTOR FUNCTION IN THE BRAIN

2.1. mTOR involvement in synaptic plasticity, learning and memory

The role of mTOR (especially via mTORC1) in facilitating long-term synaptic plasticity has been extensively reported and reviewed[7,69–72]. Long-term synaptic plasticity is generally defined as a long-lasting change in synaptic efficacy in which the connection between pre- and post-synaptic neurons becomes stronger or weaker, through induction of long-term potentiation (LTP) or long-term depression (LTD),

respectively. Seminal work in *Aplysia* and crayfish established the involvement of protein synthesis in long-term facilitation (LTF) at specific synapses, and that LTF is sensitive to translation inhibition by rapamycin[73–76]. These discoveries were followed by strong evidence for the role of mTORC1-dependent translation in mammalian synaptic plasticity, particularly its requirement in the induction of hippocampal late-phase LTP (L-LTP), in which (1) rapamycin was found to inhibit mTOR activity and attenuate NMDA-R-dependent hippocampal L-LTP[77]; (2) stimuli that induced L-LTP also increased dendritic mTOR activity in a PI3K-dependent manner[78]; and (3) induction of L-LTP was sufficient to promote mTORC1-dependent translation[79].

Additional research has expanded upon these initial findings. A number of studies have identified several mRNAs that are translated in response to mTORC1 activation and also have well-characterized roles in synaptic function and plasticity[80–82]. mTORC1 can facilitate protein synthesis directly at the synapse, whereas application of general protein translation inhibitors or rapamycin in dendrites blocks induction of LTP[83,84]. Furthermore, induction of metabotropic glutamate receptor-mediated LTP or LTD has been shown to be dependent on mTORC1 inhibition of 4EBP2[85,86]. Although the involvement of mTOR activity in promoting translation of specific proteins at the synapse plays a significant role in plasticity, mTOR may also modulate neural activity through selective suppression of translation of some mRNAs. For instance, inhibition of mTORC1 activity results in synthesis of Kv1.1, a potassium channel whose expression is normally induced in dendrites during periods of low neuronal activity[87].

Synaptic plasticity is widely thought to provide the neural basis of learning and memory [88]. Consistent with inhibition of synaptic activity by rapamycin *in vitro*,

behavioral studies in rodents have shown that injection of rapamycin into specific brain regions interferes with consolidation of long-term memory (LTM) for auditory learning, fear conditioning and spatial memory tasks[89–91]. Experiments in rodent models have also demonstrated that areas of the brain that are involved in addiction formation are associated with increased mTOR activity, and rapamycin treatment may be useful in preventing the cognitive aspects of drug addiction[92]. Conversely, infusion of glucose in the hippocampus has been shown to be associated with stimulation of mTOR activity and enhanced spatial memory formation, an effect that is abolished by rapamycin treatment[91]. However, it is worth nothing here that glucose infusion may also have non-specific effects independent of mTOR activity. Genetic upregulation of mTOR activity through partial loss of TSC2 activity without causing neuropathological symptoms of TSC has also been reported to enhance performance on tests for episodic memory[93].

Recent studies have also suggested an involvement of mTORC2 in synaptic plasticity associated with learning and memory. Experiments in *Aplysia* have implicated phosphorylation of a novel PKC by Rictor in mediating LTF[94]. Work in 2013 by Huang et al. showed that contextual fear conditioning induced a temporary increase in hippocampal mTORC2 signaling in mice, and that conditional knockout of Rictor in the forebrain of mice impaired subsequent formation of hippocampal L-LTP and LTM[95]. A similar impairment in LTM correlating with reduced neural mTORC2 activity was found in a Rictor mutant fly model. Further observations revealed deficiency in proper actin dynamics as a result of reduced mTORC2 activity, and that pharmacological stimulation of actin polymerization was sufficient to restore deficient hippocampal L-LTP and LTM.

2.3. mTOR regulation of feeding behavior

Evidence from studies in mice and rats suggests that mTOR's nutrient sensing function, particularly in the hypothalamus, results in behavioral output through regulation of appetite and feeding. Cota et al. demonstrated that activation of hypothalamic mTOR signaling through direct administration of the amino acid L-leucine resulted in reduced feeding behavior; conversely, inhibition of hypothalamic mTOR signaling through administration of rapamycin, stimulated feeding. Additional studies suggest that regulation of feeding behavior by mTORC1 activity may be mediated, at least partially, through S6K1[96,97]. However, contradictory results regarding the role of mTOR activity have been reported by Mori et al. upon studying a transgenic mouse in which TSC1 in hypothalamic POMC neurons is knocked out[98]. POMC neurons are activated by leptin to repress feeding behavior, but stimulation of mTOR activity in these neurons through TSC1 knockout induced leptin resistance, increased feeding behavior and obesity. Chronic administration of rapamycin reversed these effects.

It is possible that upstream regulation of mTOR by either amino acids or TSC1 results in distinct downstream mechanisms that regulate feeding behavior. Furthermore, modulation of mTOR activity in different neuronal subtypes that regulate feeding behavior may partially explain contradictory results. Cota et al. reported that leucine stimulated hypothalamic activity primarily in NPY/AgRP neurons of the hypothalamus, which promote feeding behavior through expression neuropeptide-Y and agouti-related peptide (AgRP)[99]. NPY/AgRP neurons thus act in opposition to POMC neurons in regulation of appetite. Differential levels of mTOR activity in both neuronal populations may, perhaps, determine stimulation or suppression of feeding behavior. Methodological distinctions between studies may also explain contrasting effects of

rapamycin treatment; whereas Cota et al. utilized acute rapamycin treatment through intracerebroventricular administration of rapamycin, Mori et al. administered chronic and systemic rapamycin treatment to experimental mice via daily IP injection.

Collectively, these studies suggest that mTOR activity may influence both NPY/AgRP and POMC neural subtypes in promoting short- or long-term moderation of feeding behavior to maintain homeostatic balance.

2.4. Rapamycin treatment in the aging brain

Although acute rapamycin administration has been shown to interfere with processes of learning and memory, chronic rapamycin treatment may have beneficial effects on cognitive processes in the context of aging. A role for constitutive inhibition of mTOR in successful brain aging is consistent with its putative role in mediating the anti-aging effects DR, which has already been implicated in reduction of phenotypes in the aging brain and promotion of neuroprotective mechanisms against age-related cellular stress and damage[100,101]. Potential benefits of DR have been demonstrated in rodent models of stroke, Alzheimer's, Parkinson's' and Huntington's disease, in which regimens of caloric restriction and/or intermittent fasting have been shown to increase the resistance of neurons to dysfunction and degeneration[102–104]. Similar effects have also been documented in *C. elegans* models of proteotoxic diseases[105]. The role of mTOR activity in these diseases is discussed further in Part III.

Recent work utilizing rapamycin treatment in aged mice provides evidence in support of the positive cognitive effects of mTOR inhibition. In 2012, researchers from the Galvan group at the Barshop Institute reported that mice that had been treated with

a rapamycin diet for 4 months, beginning in mice at 8 months of age, performed significantly better on the Morris Water Maze task than mice that had been fed a control diet[106]. In addition, 25-month old mice that were fed a rapamycin diet for 40 weeks showed improved memory of an aversive stimulus, suggesting that late treatment with rapamycin may also have beneficial cognitive effects. An independent report that same year from the Oddo group, also based at the Barshop Institute, showed that long-term treatment of rapamycin (16 months) beginning at 2 months of age similarly improved spatial learning and memory, as indicated by MWM task performance[107]. However, this group also reported that short-term rapamycin treatment for 3 months, beginning at 15 months of age, did not result in improved MWM task performance; thus, a clear timetable for the onset and duration of rapamycin to yield effective treatment has yet to be determined. Furthermore, much work remains to be done to identifying the neural mechanisms that mediate rapamycin's effects on learning and memory, although correlational evidence suggests that long-term rapamycin treatment results in increased synaptic plasticity through NMDA signaling and enhanced phosphorylation of CREB[107] .

Inhibition of mTOR activity in the hypothalamus by rapamycin may also be effective in treatment of age-related obesity. Yang et al. reported that mTOR is hyperactive in POMC neurons in old (12-month) compared to young (1-month old) mice[108]. Consistent with previous work by Mori et al.,[98] conditional knockout of TSC1 in POMC but not NPGY/AgRP neurons resulted in dramatic weight gain and obesity shortly after weaning. Furthermore, the absence of TSC1 resulted in POMC neuronal silencing associated with obesity in old mice. Rapamycin administration via intraperitoneal (IP) injection or intracerebral infusion caused weight loss in 12-month-old

mice accompanied by a rescue in excitability of POMC neurons. Whether dysregulation of mTOR activity in the hypothalamus may be associated with age-dependent obesity in humans is still an open question for investigation.

PART 3. ALTERATIONS OF mTOR SIGNALING IN ADULT-ONSET NEURODEGENERATIVE DISEASES

Anti-aging effects induced by genetic or pharmacological inhibition of mTOR signaling could, in theory, delay onset and slow progression of age-related neurodegenerative diseases in generic fashion. This notion would be supported by research demonstrating that rapamycin confers neuroprotective effects in models of Alzheimer's disease, Parkinson's disease and Huntington's disease. However, an accumulation of evidence suggests that rapamycin-sensitive interactions between mTOR activity and cellular processes in specific neuronal populations may also contribute to the diverse pathology of these diseases.

3.1. Alzheimer's disease

The national prevalence of Alzheimer's disease (AD) for 2014 is an estimated 5.2 million people, with a vast majority of cases affecting individuals at ages of 65 and older. The total cost of health care for individuals with Alzheimer's is estimated to be more than $200 billion this year[109] The burden on the health care system is expected to become increasingly onerous as the incidence of AD and other types of dementia may nearly triple by 2050, with health care costs soaring to more than $1.2 trillion. Major symptoms of AD include significant deficits in memory and impaired judgment, with

brain pathology primarily characterized by the accumulation of proteinaceous amyloid-beta (Aβ) plaques and tau-containing neurofibrillary tangles (NFTs). Both hallmarks are associated with neural damage and cell death in the brain.

Postmortem analysis of tissue from AD patients has found that mTOR is activated in affected brain areas, as indicated by upregulation of phosphorylated S6K[110,111]. Studies involving a diverse array of fly, mouse and cell culture models have further implicated aberrant signaling of mTOR pathway components in AD pathology. Mechanistic models for mTOR signaling in AD have centered on (1) its regulation of autophagy, which can facilitate clearance of amyloid beta (Aβ) and neurofibrillary tangles (NFTs); and (2) its functional role in translation and hyperphosphorylation of tau. Emerging evidence also points to the involvement of feedback mechanisms between mTOR and upstream components, particularly within the PI3K/insulin signaling axis.

3.1.1 Regulation of autophagy by mTOR in AD

Research conducted at the Barshop Institute for Longevity and Aging by the Galvan group has previously shown that chronic inhibition of mTOR through long-term rapamycin treatment improves cognitive performance and lowered levels of $A\beta_{42}$ in the PDAPP transgenic mouse model for AD[112]. In this study, researchers also observed lower levels of LC3-II in hippocampi transgenic mice that had received rapamycin treatment, suggesting increased stimulation of autophagy. The Oddo group at the Barshop independently reported that rapamycin significantly reduced intracellular levels of $A\beta_{42}$ in the 3xTg-AD mouse model[113]. Furthermore, levels of autophagic components Atg7 and the Atg5/12 complex were found to be elevated as a result of rapamycin treatment. Their results were further supported by evidence that pharmacological

inhibition of autophagy in the 7PA2 cell culture model of AD was sufficient to block reduction of $A\beta_{42}$ levels by rapamycin. Dysregulation of mTOR and autophagy may even play a causal role in AD pathology, as subsequent studies has reported that genetic upregulation of mTOR activity in TSC2+/- mice results in reduced levels of Atg7 and Atg5/12 and increased levels of hippocampal tau[114].

A therapeutic role for mTOR-related autophagy in AD, however, is controversial. For instance, evidence for increased autophagy has been found in prefrontal cortex of AD patients, as well as in cortical and hippocampal neurons of the PS1/APP transgenic mouse model for AD[115]. Furthermore, stimulation of autophagy by rapamycin in non-neuronal cell cultures stably transfected with APP reportedly *increased* production of $A\beta_{40}$ and $A\beta_{42}$. Suppression of autophagy, in this case, appeared to reduce levels of Aβ.

Discordant research may be partially explained the relative role of autophagy in early versus late stage progression of AD. Research which examined the effects of rapamycin treatment in 3xTg mice beginning at either 2 or 15 months of age (prior to or following the onset of AD pathology, respectively), and continuing until the mice reached 18 months[113]. Impaired cognitive performance in 3xTg mice was rescued by early but not late treatment with rapamycin diet. Improved cognitive performance in early treatment groups was accompanied by reduction of amyloid plaques and neurofibrillary tangles. Interestingly, autophagy appeared to be activated in both early and late treatment groups, as indicated by increased levels of Atg7 and Atg5/12; however, activation of autophagy was not sufficient to reduce accumulation of Aβ and tau in late treatment groups. Thus, the effectiveness of rapamycin therapy may be limited to preventive and early treatments of AD.

3.1.2. mTOR and levels of tau in AD

Analysis of postmortem brains has shown that mTOR signaling is selectively increased in subpopulations of neurons predicted to develop NFTs, particularly in the entorhinal cortex, hippocampal complex and temporal cortex[110,116,117], and that such an increase correlated with tau phosphorylation. mTOR activity is upregulated and enhances tau-induced neurodegeneration in the tau^{R406W} *drosophila* model for tauopathy; furthermore, genetically increased activation of mTOR resulted in enhanced tau-induced neurotoxicity in the tau^{R406W} flies, while genetic or pharmacological inhibition of mTOR conferred neuroprotection against neural degeneration[118].

Additional studies have investigated the possibility of a causal link between aberrant mTOR signaling and hyperphosphorylation of tau, thus contributing to a major hallmark of AD pathology. *In vitro* experiments have shown that phosphorylation of tau is regulated by components of the PI3K/mTOR pathway[110,119]. Rapamycin treatment in P301S transgenic mice, which overexpress human tau, results in a signification reduction in tau pathology as indicated by the lack of NFTs and decrease in levels of hyperphosphorylated tau[114,120]. Researchers observed that TSC2+/- mice, which have increased mTOR activity, showed increase levels of hyperphosphorylated tau compared to WT mice [114]. The activity of GSK3B, which has been shown to phosphorylate tau[121], was also shown to be upregulated in TSC2+/- mice. Rapamycin is sufficient to reduce GSK3B activity in the P301S mouse model in addition to inducing autophagy genes. Thus, inhibition of mTOR might cause a reduction in tau pathology both by decreased phosphorylation and increased autophagy.

Experiments utilizing the 3xTg mouse model for AD Collective studies suggest that tau pathology is dependent on $A\beta_{42}$ accumulation[122–125]. Whether changes in tau pathology are directly due to an interaction between mTOR signaling and tau, or simply due to alteration in Aβ pathology, remains to be determined.

3.1.3. Insulin signaling and mTOR in AD

Metabolic dysfunction associated with insulin resistance and elevated blood glucose levels may be a significant factor contributing to the development of AD. Diabetes doubles the risk of developing AD[126,127], and patients with type-2-diabetes have evidence of hyperphosphorylated tau in their brains[128]. Examination of postmortem brain tissue from AD patients has shown that neurons, specifically, become increasingly resistant to insulin and insulin-like growth factor (IGF1)[129–131].

Aberrant insulin signaling is associated with sustained activation of the PI3-K/Akt/mTOR pathway in brains of patients with AD. Although insulin signaling and IGF-1 signaling bind to receptors and activate mTOR signaling downstream, an elegant feedback system is in place by which mTOR directly phosphorylates the insulin receptor, leading to its in internalization; this, in turn, shuts off its insulin-related activity. In this way mTOR modulates insulin signaling dependent on nutrient exposure.[131]

Chronic mTOR activity disrupts this feedback pathway, leading to insulin resistance. Aβ species, including monomers and soluble oligomers, can block insulin signaling by directly acting upon insulin receptors, thus reducing insulin sensitivity in AD brain. Furthermore, Aβ has been shown to influence mTOR activity through insulin pathway activation of Akt and subsequent phosphorylation of PRAS40[132]. Thus,

evidence of a reciprocal relationship between Aβ and mTOR supports a model in which sustained hyperactivation of the PI3K/Akt/mTOR signaling pathway in AD and consequently disrupting the feedback shut-off for normal activation.

Recently it was reported that increased sucrose intake exacerbates AD pathology, i.e. Aβ deposition and tau phosphorylation, in the hippocampus of 3xTg-AD mice [133]. 3xTg-AD mice receiving sucrose also showed induced insulin resistance in the brain and periphery, as well as increased activation of mTOR pathway components. Administration of a rapamycin diet, however, rescued total levels of IRS-1 and phosphorylation of several serine residue sites of IRS-1 to normal levels. Moreover, rapamycin treatment prevented sucrose-mediated deposition of Aβ and tau phosphorylation. Although corresponding effects on cognitive performance have yet to be demonstrated, emergent research supports a role for the mTOR pathway in modulation of insulin signaling in AD brain.

3.2. Parkinson's disease

Parkinson's disease (PD) is the second most common neurodegenerative disorder in the U.S. As of 2010, more than 600,000 individuals have been diagnosed with PD, or 0.3% of the general population. The prevalence of PD is much higher in the elderly population, affecting more than 1% of individuals over age 65 and 4-5% of individuals over 85[134–137] Major symptoms include slowness of movement ("bradykinesia"), rigidity, and postural instability, often presenting with nonmotor and neuropsychiatric symptoms such as cognitive decline and depression[134,138]. Major pathological hallmarks of PD include (1) degeneration of dopaminergic neurons in the

substantia nigra (SN); and (2) accumulation of α-synuclein protein in cytoplasmic inclusions called Lewy bodies. Administration of the DA precursor levodopa compensates for dopamine deficiency and alleviates symptoms in PD patients; however, therapies to cure or slow disease progression of PD remain undiscovered [134,139].

Diverse *in vitro* and *in vivo* models have been developed to study PD[138]. Toxin-based models utilizing 6-hydroxydopamine (6-OHDA) or complex inhibitors such as MPTP/MPP+ or rotenone result in cell death in neuronal cell culture. Administration of these same toxins to mice induces neurodegeneration in SN accompanied by varying deficits in locomotor behavior. Gene-based models are also widely used in PD research. Mutations expressing abnormal α-synuclein have been used to recapitulate disease pathology in mice and cell culture. Mutations in PINK1 or parkin genes, which are linked to the autosomal recessive form of PD in humans, have also been modeled in *drosophila*, resulting in DA neurodegeneration, locomotor deficits and mitochondrial dysfunction.

3.2.1. Protective mechanisms of mTOR inhibition in PD

Rapamycin's neuroprotective effects have been demonstrated in both fly and mouse models of PD[140–142]. Research in PINK1 and parkin mutant *drosophila* models for PD has shown that administration of rapamycin protected against neurodegeneration and rescued abnormal mitochondrial morphology in DA neurons[140]. Overexpression of 4EBP1 was also sufficient to confer neuroprotection in mutant flies, providing support for a possible mechanism of reduced cap-dependent translation. Experiments utilizing

the MPTP mouse model for PD have also shown that rapamycin treatment reduces neurodegeneration of DA neurons in the substantia nigra after acute MPTP insult[141,142]. Evidence for reduced levels of alpha-synuclein, along with increased levels of LC3II and the appearance of autophagosomes in the SN region, suggests that rapamycin-induced autophagy may play a role in neural rescue[142].

Experiments in cell culture reveal a more complex role for mTOR activity in PD-related neuronal cell death. Malagelada et al. found that inhibition of mTOR activity by RTP801 *promoted* OHDA-induced cell death in PC12 neuronal cells, whereas increased mTOR activity reduced toxicity[143]. However, a later study by their group also demonstrated rapamycin to be neuroprotective in the same cell culture model[141]. Thus, rapamycin's specific actions in reducing some, but not all, of mTOR's activity may underlie its therapeutic effects. Overall, their research supports a model in which RTP801 and rapamycin might differentially affect feedback signaling between mTOR and upstream Akt.

3.2.2 Rapamycin-induced autophagy in PD

Conflicting reports from *in vitro* studies have called into question the relative importance of autophagy in mediating the therapeutic effects of rapamycin in PD models. Rapamycin-stimulated autophagy has been shown to degrade accumulation of alpha-synuclein in cell culture[144]; furthermore, rapamycin can alleviate rotenone-induced apoptosis in neuronal SH-SY5Y cell cultures, an effect that is partially blocked by suppression of Atg5 [145]. However, MPP+ toxicity has also been shown to reduce autophagy in SH-SY5Y neuroblastoma cells[146]. In addition, stimulation of autophagy was observed to contribute to neuron death in PC12 cells expressing mutant A53T

alpha-synuclein[147], or in dopaminergic cell lines subjected to oxidative stress[148]. Overall, a firm causal link between rapamycin-induced autophagy and alleviation of PD pathology has yet to be established. Future investigation of signaling pathway components linking mTOR to regulation of autophagy in PD models may help to resolve contradictory findings.

3.2.3. Impact of rapamycin on mitochondrial function and oxidative stress in PD models

There is growing evidence that dysfunctional mitochondria and oxidative stress play a significant role in PD cell death[100,138,149]. Research from the Buck Institute for Research in Aging showed that oxidative stress resulting from increased levels of monoamine oxidase B (MAO-B) in cell culture results in reduced activity of parkin, which targets damaged mitochondria for autophagic degradation[150]. The resulting accumulation of damaged mitochondria was reduced by co-treatment of cells with rapamycin, perhaps through a mechanism of increased mitophagy independent of parkin function. In addition, deficiencies in respiration and mitochondrial complex I activity resulting from MAO-B-induced oxidative stress were rescued by rapamycin co-treatment. This study is consistent with previous work demonstrating that rapamycin enhanced clearance of mitochondrial load after apoptotic insult in cell culture and blocked downstream signaling cascades that would otherwise induce cell death [151]. Furthermore, pre-treatment with rapamycin could increase survival in flies exposed to paraquat toxicity, dependent upon function of essential autophagy gene Atg1.

Rapamycin may also protect against oxidative stress and downstream apoptotic signaling through its promotion of antioxidant activity. It has previously been shown that

rapamycin pre-treatment resulted in improved locomotor behavior and reduced DA neurodegeneration in SN after administration of 6-OHDA to rats[152]. In this study, rapamycin was also observed to reduce 6-OHDA-induced injury to mitochondria and decreased levels of malondialdehyde, an indicator of oxidative stress. Conversely, antioxidant levels of SOD and GSH-PX were decreased in PD rats. Rapamycin also increased expression of anti-apoptotic gene Bcl-2 and decreased expression of pro-apoptotic gene Bax in 6-OHDA rats. However, a contradictory report from experiments suggest that mTOR inhibition promotes oxidative stress resulting from nucleolar disruption, leading to PD pathology[153].

3.3. Huntington's disease

Huntington's disease is an inherited neurodegenerative disorder in which a CAG expansion mutation (beyond 35 repeats) is translated into an abnormally long polyglutamine tract at the N terminus of huntingtin.[154] It is the most common type of polyglutamine disease. Onset of debilitating neurological symptoms usually begins in adulthood at 30-40 years of age, although early onset Huntington's disease affects a small number of cases in childhood and teens. Principal symptoms include chorea (involuntary jerking or twitching movements) and progressive cognitive dysfunction[154]. There is currently no effective treatment for Huntington's disease.

Degeneration is primarily found in the medium spiny neurons of the striatum and other brain regions in the cortex of HD patients[155]. Mutant proteins accumulate into proteinaceous aggregates in the nuclei of HD patients as well as mouse models. The significance of these aggregates in HD pathogenesis has come under some debate

among researchers; research in the years immediately following the discovery of neuronal aggregates in HD published contradictory results, with some in support of the "aggregation theory" of neural toxicity and others supporting the view that aggregates are innocuous or may even be employed as part of a protective mechanism[156]. Further work to dissect the process of htt aggregation and identify toxic intermediate products contributed to the construction of a more elegant model that could explain disparity in views [157]. Generally, the model proposes that soluble and insoluble toxic species result from polyglutamine-expanded protein misfolding, and that formation of visible aggregates may be protective for sequestering the soluble and insoluble toxic species[156].

A significant paper from the Rubinsztein group published in 2004 demonstrated that (1) mTOR signaling is altered in *in vitro* models of HD; and (2) that inhibition of mTOR by rapamycin can confer neuroprotective effects *in vivo* in mouse and fly models for Huntington's disease[158]. Researchers found colocalization of mTOR with cytoplasmic and nuclear huntingtin aggregates in an htt-mutant cell culture model, as well as in brains of transgenic mice and postmortem tissue of individuals with Huntington's disease. This colocalization appeared to impair mTOR activity, as indicated by downregulation of phospho-4EBP1 and phospho-s6 appeared in mutant cells; however, overexpression of Rheb to enhance mTOR signaling in mutant cells resulted in increased aggregate formation and cell death. Rapamycin treatment reduced neurodegeneration in a fly model in which mutant huntingtin with 120 glutamine repeats was expressed in photoreceptors; rapamycin slowed the consequential neurodegeneration of rhabdomeres in these flies. Furthermore, treatment of

Ross/Borchelt mice expressing mutant Huntington with rapamycin ester CC1-779 showed improvement in behavioral testing for tremors, wire maneuvering, grip strength and rotarod performance. CCC1-779 was shown to reduce mTOR activity in vivo (as indicated by IHC for phospho-s6 in mouse brains) and also appeared to reduce aggregate load of mutant huntingtin.

Researchers proposed a model in which autophagy is activated in response to HD-related neurotoxicity, and that inhibition mTOR facilitates autophagic clearance of aggregates. Western blots indicated that levels of LC3-II, which can correlate with autophagosome number, were higher in mutant cell lines than in wild-type. Immunofluorescence assays also showed an increased number of mutant cells containing aggregates that were positive for LC3-GFP compared to wild-type. Recently, it was reported that nucleolar stress in the R6/2 mouse model for Huntington's disease activates p53/PTEN, which in turn inhibits downstream mTOR activity and induces autophagy[159]. Additional studies have reported that rapamycin is effective at reducing neurodegeneration in fly models for non-HD-polyglutamine diseases[158,160,161]; furthermore, these studies have reported that neural rescue is dependent upon the presence of atg1 or atg12, factors that are critical for autophagy.

A similar dependence on autophagy-related genes in mediating rapamycin's neuroprotective protects has not yet been demonstrated in mammalian models of polyglutamine disease. Furthermore, additional functions regulated by mTOR activity may influence HD pathology. For instance, research with a cellular model of HD found that rapamycin could reduce accumulation of insoluble polyQ proteins in an atg-5-

independent manner[162]. Researchers proposed that mTOR could, alternatively, reduce the amount of soluble protein required for polyQ aggregation.

PART 4. TARGETING THE mTOR PATHWAY IN TREATMENT OF EARLY-ONSET NEUROLOGICAL DISORDERS

Because of the mTOR pathway's implications in aging processes, much of the research hoping to unlock the therapeutic potential in neurodegenerative disease has focused on disorders affecting middle-aged adults and the elderly. However, evidence for hyperactive mTOR signaling has also been found in neurological disorders affecting individuals during development or childhood; thus, mTOR-regulated mechanisms that cause cell death or synaptic dysfunction late in life may overlap with early-onset pathology (and vice versa). Furthermore, therapeutic interventions to inhibit mTOR activity may play a pivotal role in treating these diseases; indeed, rapamycin has been shown to be effective at attenuating pathology in models for several childhood disorders, which I discuss below.

4.1. Early-onset Epilepsy

Epilepsy is a neurological condition that is characterized by recurrence of epileptic seizures. Genetic etiology of epilepsy has been highly associated with "TORopathies," or disorders relating to defective components of the mTOR signaling pathway. Comorbidity of epilepsy with tuberous sclerosis complex (TSC) has been especially studied in this regard.

TSC is an autosomal dominant disorder, resulting from mutations in either TSC1 or TSC2, and is estimated to occur in approximately 1 in 6000 newborns[163–165]. The

most common neurological manifestations of TSC are epilepsy, mental retardation, and autistic behavior, with epilepsy occurring in up to 80-90% of TSC patients[166]. Predictions regarding removal of TSC1/2 inhibition on mTORC1 signaling are consistent with actual disease pathology, as hyperactive mTOR signaling is indeed evident in both cortical tubers and subependymal giant cell astrocytomas (SEGAs) of TSC patients[167,168]. A number of genetic mouse models for TSC also show evidence for elevated mTOR activity in brain, and have proved useful in investigating the effects of mTOR inhibition in treatment of epileptogenesis[169–172].

Neuron-specific TSC1 knockout mice development of neuropathological features similar to those of TSC patients, including enlarged and dysplastic neurons, reduced myelination, and epileptic seizures[169]. These mice are also short-lived, with a median survival of 33 days. Treatment with mTOR inhibitors rapamycin or RAD001 by intraperitoneal injection beginning at postnatal day 7 dramatically improved survival, with 90-100% survival at 100 days when the study was terminated[170]. Furthermore, treatment resulted in the complete absence of seizures. Neurofilament abnormalities, myelination and cell enlargement were also improved in knockout mice as a result of rapamycin/RAD001 treatment, changes which are consistent with observed attenuation of mTOR hyperactivity and restoration of phospho-Akt levels.

Similarly dramatic anti-epileptogenic and pro-survival effects of early rapamycin treatment have been observed in the TSC1 conditional knockout mouse for glial cells ($Tsc1^{GFAP}CKO$) (Zeng et al. 2008). In addition, late rapamycin treatment beginning at 6 weeks, after onset of epileptic phenotype, was also effective at suppressing seizures and improving survival. Early and late rapamycin treatment were effective at reducing

astrogliosis, enlarged brain pathology and hippocampal disorganization, although late treatment did not completely reverse these histological abnormalities.

The role of mTOR signaling and therapeutic potential of rapamycin may extend to early-onset epileptogenesis that is not related to TSC. For instance, rapamycin has been shown to reduce seizures a rat model of non-genetic etiology for infantile spasms, or IS[173]. In this "multiple-hit" model, suppression of spasms correlated with the ability of rapamycin to normalize otherwise hyperactive TORC1/ps6 activity in perilesional cortical neurons. In addition, rapamycin treatment decreased subsequent development of cognitive deficits, as indicated by performance on a Barnes radial maze.

Given converging evidence based on studies in TSC patients and animal models for TSC, rapamycin and its analogs (rapalogs) have already undergone clinical trials for TSC in adults and children[174,175]. The rapalog everolimus has been approved by the USDA to treat SEGAs, and both rapamycin and everolimus have been reported to decrease seizures in TSC patients with established epilepsy[174,176,177]. Although clinical trials are underway, little is known about the potential mechanisms by which inhibition of mTOR signaling counteracts epileptogenesis associated with TSC. Evidence for the role of ketogenesis as a result of reduced mTOR signaling might offer some explanation; liver-specific deletion of TSC1 in mice results in defective ketogenesis in response to fasting, a phenotype that can be reversed by rapamycin treatment[178]. Ketogenic diet is already a well-established treatment for epilepsy[179], and has also been shown to affect levels of phospho-s6 and phospho-Akt in hippocampus and liver of normal rats[180]). A possible connection between mTOR inhibition and production of

ketones might induce a systemic effect on liver and brain in treatment of TSC-related epilepsy, but has yet to be demonstrated.

4.2. Fragile X syndrome

Fragile X syndrome is an inherited form of mental retardation caused by loss-of-function mutation in the RNA binding protein fragile X mental retardation protein (FMRP). Mutation in FMRP is also the most common single gene mutation associated with autism. Patients diagnosed with Fragile X display a wide range of neurological symptoms such as cognitive and behavioral problems, attentional deficits, emotional dysregulation, seizures; along with non-neurological symptoms that include facial dysmorphism, connective tissue anomalies, and macro-orchidism[181–183]. Incidence of Fragile X is an estimated 1 in 4000 boys and 1 in 8000 girls, and is typically diagnosed in early childhood[184,185].

Fragile X mutation is caused by an expansion of a CGG repeat sequence in the 5' untranslated region of FMR1, which results in gene silencing[186–188]. Deficiency in FMRP, which acts as a translational repressor, results in abnormal translation of dendritic mRNAs in response to stimulation of metabotropic glutamate receptors (mGluRS) and aberrant induction of LTD[8585,183,189]. The Fmr1 knockout (KO) mouse model for Fragile X syndrome resembles many aspects of the disease in humans, including impaired cognitive function, abnormalities in dendritic spine morphology and exaggerated mGLUR-LTD[190–194,194].

Mounting evidence suggests that activation of the mTOR signaling pathway is involved in Fragile X syndrome. Hyperactive mTOR signaling has been identified in lymphocytes of Fragile X patients, as indicated by increased phosphorylation of mTOR, S6K, 4EBP1 and Akt[193]. In a study utilizing Fmr1 KO mouse model, elevation of mTOR activity was found in hippocampal slices; however, rapamycin was not sufficient to block induction of hippocampal mGLUR-LTD by application of mGlu receptor agonist 3,5 dihydroxyphenylglycine (DHPG)[195]. Analysis of upstream components of the PI3K/Akt/mTOR pathway suggests that rapamycin-independent inhibition of mTOR through pharmacological blockade of PI3K was effective at attenuating DHPG-induced LTD. Overall, our understanding of mTOR's involvement in the pathology of Fragile X syndrome is still in its nascent stages, and these seminal studies have laid the groundwork for further investigation.

4.3. Mitochondrial disease: Leigh Syndrome

Leigh syndrome (LS) is the most common mitochondrial disease, affecting 1 in 40,000 newborns, with symptoms typically presenting in the first 2 years of life[196,197]. It is a severe neurological disorder characterized by the loss of motor function, weakness, lactic acidosis, respiratory failure and incidence of seizures. The prognosis for Leigh syndrome is poor; most cases of LS die within the first few years of life, and rare cases surviving into their teens[198–200]. To date, treatment of LS is limited to palliative care and amelioration of lactic acidosis. No effective cure for LS currently exists[201].

There is considerable genetic and clinical heterogeneity in diagnosis of Leigh syndrome, but patients most typically manifest a pattern of focal, necrotizing lesions in the basal ganglia, diencephalon, cerebellum or brainstem[200,202]. Deficits in the

mutations in genes encoding for subunits or assembly factors of the mitochondrial electron transport chain (ETC) predominantly underlie LS pathology, with deficiency in ETC complex I considered to be the most common genetic cause[200].

A recent report from our group revealed the novel therapeutic potential of rapamycin in treatment of LS[203]. In this study, we utilized a transgenic knockout mouse deficient in the NDUFS4 subunit of Complex I which had been developed by the Palmiter lab[204]. These NDUFS4 knockout (NDUFS4 KO) mice develop severe phenotypes that closely resemble symptoms of LS, including a profound neurodegenerative phenotype, impaired growth, and progressive deficits in movement[204]. Moreover, these mice show early death at 50 days of age.

Based on previous work in yeast which identified extension of replicative lifespan in mutants that are deficient for genes associated with mitochondrial disease, we reasoned that the DR mimetic effects of rapamycin might similarly extend lifespan in a mammalian model for LS. Indeed, we found that rapamycin treatment beginning at postnatal day 10 doubled median lifespan and tripled maximum lifespan in NDUFS4 KO mice[203]. Moreover, we found that rapamycin treatment attenuated the appearance of lesions in cerebellum and vestibular nuclei, and correspondingly offset the presentation of neurological phenotypes such as clasping. Western blotting of whole brain lysates for phospho-s6 indicated hyperactive mTOR activity in NDUFS4 KO mice compared to age-matched WT controls. In contrast, levels of phospho-s6 were dramatically reduced in both WT and NDUFS4 KO mice as a result of rapamycin treatment. Although we found evidence for increased autophagy in the brain, we did not observe a

corresponding rescue in complex I assembly or function as a result of rapamycin treatment.

Experimental evidence suggests that inhibition of mTOR by rapamycin may induce metabolic adaptation to effectively treat disease phenotypes. We discovered that rapamycin treatment rescued fat storage in NDUFS4 KO mice, as evidenced by restored staining of lipid droplets in liver and increased fat mass in overall body composition. Moreover, metabolomic analysis of whole brain of 30-day old NDUFS4 KO mice before the onset of neurological symptoms, we observed an abnormal increase in levels of glycolytic intermediates and a corollary decrease in free amino acids and fatty acids. Rapamycin treatment reversed this abnormal metabolic profile. Currently, our lab favors a model in which accumulation of toxic metabolites (i.e. glycolytic intermediates and lactate) may underlie critical aspects of neural pathology in NDUFS4 KO mice, and that rapamycin restores metabolic homeostasis perhaps through regulation of mTOR-related nutrient sensing. Although much remains to be done to further establish the causal factors that underlie rapamycin's benefits, our results may open promising new lines of investigation in development of targeted interventions for LS.

5. Conclusions and research purpose

Previous research has shown that mTOR activity is important for normal brain functions such as formation of long-term memory and regulation of feeding behaviors. Inhibition of mTOR activity by acute rapamycin treatment has also been shown to disrupt neural mechanisms that underlie these behaviors. Paradoxically, aberrant upregulation of mTOR activity is associated with several early- and late-onset

neurological diseases, as well as general age-related deficiencies in neuronal function. Inhibition of mTOR activity by chronic rapamycin treatment has been shown to have vast neuroprotective properties, which correlates with its attenuation of behavioral symptoms in neurological disease models. Regulation of mTOR and its downstream effectors by common or distinct pathways across various neurological diseases is critical for understanding how rapamycin treatment works, and thus may lead to development of more optimal, targeted therapies.

The studies presented here investigate the therapeutic effects of rapamycin in two different mouse models for neurological disease: the NDUSF4 KO model for Leigh Syndrome, and the MPTP mouse model for Parkinson's disease. Both mouse models are characterized by deficiency of mitochondrial electron transport complex I activity in the brain, which is believed to contribute to the appearance of their respective neuropathological phenotypes. The general purpose of these studies is as follows: (1) to investigate the effectiveness of high-dose rapamycin treatment in reducing neural pathology and symptoms; and (2) to identify and compare potential mechanisms of rapamycin-induced neuroprotection.

CHAPTER 2

mTOR Inhibition Alleviates Mitochondrial Disease in a Mouse Model of Leigh Syndrome

The contents of this chapter were published in: Johnson SC, Yanos ME, Kayser EB, Quintana A, Sangesland M, Castanza A, Uhde L, Hui J, Wall VZ, Gagnidze A, Oh K, Wasko BM, Ramos FJ, Palmiter RD, Rabinovitch PS, Morgan PG, Sedensky MM, Kaeberlein M. mTOR inhibition alleviates mitochondrial disease in a mouse model of Leigh syndrome. *Science* 342, 1524-1528 (2013).

OVERVIEW

Mitochondrial dysfunction contributes to numerous health problems, including neurological and muscular degeneration, cardiomyopathies, cancer, diabetes, and pathologies of aging. Severe mitochondrial defects can result in childhood disorders such as Leigh syndrome, for which there are no effective therapies. We found that rapamycin, a specific inhibitor of the mechanistic target of rapamycin (mTOR) signaling pathway, robustly enhances survival and attenuates disease progression in a mouse model of Leigh syndrome. Administration of rapamycin to these mice, which are deficient in the mitochondrial respiratory chain subunit NDUFS4 [NADH dehydrogenase (ubiquinone) Fe-S protein 4], delays onset of neurological symptoms, reduces neuroinflammation, and prevents brain lesions. Although the precise mechanism of rescue remains to be determined, rapamycin induces a metabolic shift toward amino acid catabolism and away from glycolysis, alleviating the buildup of glycolytic intermediates. This therapeutic strategy may prove relevant for a broad range of mitochondrial diseases.

INTRODUCTION

Leigh syndrome is a clinically defined disease resulting from genetic defects that disrupt mitochondrial function. It is the most common childhood mitochondrial disorder, affecting 1 in 40,000 newborns in the United States[198]. Leigh syndrome is characterized by retarded growth, myopathy, dyspnea, lactic acidosis, and progressive encephalopathy primarily in the brainstem and basal ganglia[205,206]. Patients typically succumb to respiratory failure from the neuropathy, with average age of death at 6 to 7 years[198].

We recently observed that reduced nutrient signaling, accomplished by glucose restriction or genetic inhibition of mTOR, is sufficient to rescue short replicative life span in several budding yeast mutants defective for mitochondrial function[207], including four mutations associated with human mitochondrial disease (Figure 2.1). These observations led us to examine the effects of rapamycin, a specific inhibitor of mTOR, in a mammalian model of Leigh syndrome, the NDUFS4 knockout (NDUFS4 KO) mouse[208]. NDUFS4 encodes a protein involved in assembly, stability, and activity of complex I of the mitochondrial electron transport chain (ETC)[209,210]. NDUFS4 KO mice show a progressive neurodegenerative phenotype characterized by lethargy, ataxia, weight loss, and ultimately death at a median age of 50 days[204,208]. Neuronal deterioration and gliosis closely resemble the human disease, with primary involvement of the vestibular nuclei, cerebellum, and olfactory bulb.

METHODS

Animal Care

NDUFS4 +/- breeders were obtained from the Palmiter laboratory at the University of Washington. Following colony expansion by backcrossing to C57Bl/6 CR mice, obtained from the NIA, NDUFS4 +/- mice were bred as harems with heterozygous parents bred to produce NDUFS4 KO offspring. All mice were weaned at 20-21 days of age. NDUFS4 KO animals were always housed with a minimum of one control littermate for warmth and stimulation. All mice were weighed daily and food and gel were provided on the bottom of each cage so that ability to find food or water did not become a limiting factor for survival. Mice were euthanized if they showed a 20% loss in maximum body weight, immobility, or were found prostrate or unconscious. Mice used for rotarod and QMR were separate from those used in the lifespan so that the any stress resulting from these assays would not be a complicating factor in determining survival. NDUFS4 heterozygous mice and wild-type mice were identical in each assay described here and thus were pooled as controls for the experiments described.

All care of experimental animals was in accordance with the University of Washington institutional guidelines and experiments were performed as approved by the Institutional Animal Care and Use Committee.

Rapamycin Administration

Rapamycin was dissolved in DMSO to 100 mg/mL. This was diluted in 5% PEG-400/5% Tween-20 (vehicle) to a concentration of 1.2mg/mL, sterile filtered, aliquoted into 1mL portions, and stored at -80 for long-term storage. Rapamycin treated mice were injected with 66 microliters / 10g body weight for a final dosage of 8.0 mg/kg. Vehicle mice were injected with vehicle containing an equal volume of diluent and

DMSO lacking rapamycin. Injections were performed intraperitoneally using 29 gauge, 3/10cc insulin syringes. The abdomen was briefly swabbed with an alcohol wipe prior to injection.

Rotarod

Rotarod parameters were set at beginning speed of 0 rpm with an acceleration rate of 0.1 rpm/s and a maximum speed of 40 rpm. Mice underwent practice sessions on two consecutive days, with one session per day. The animals were tested 24 hours after the second practice day; mice underwent three rotarod sessions on the testing day, and latency-to-fall times were recorded. Median and maximum times were then calculated. The number of mice used for each data point is as indicated in Figure S5.

Western Blotting

Whole-organs were rinsed of blood and flash-frozen in liquid nitrogen. Tissues were cryohomogenized on dry ice and the homogenized frozen powder was split for protein and RNA extractions. Protein was extracted by sonicating powdered tissue in RIPA buffer (10mM Tris-HCl pH 8.0, 1mM EDTA, 1% Triton X-100, 0.1% sodium deoxycholate, 0.1% SDS, 140mM NaCl) with Roche cOmplete Ultra protease inhibitor and PhosSTOP phosphatase inhibitor tablets added prior to use. Protein lysates were BCA'd using standard techniques and 20 micrograms protein per sample were run using 3 Novex minigels. Antibodies used were ordered from the following companies: Hsp60:Cell Signaling Technology #4870, LC3: Cell Signaling, #4108, Akt: Cell Signaling, #2920, pAkt: Cell Signaling, #4060, IGFR: Cell Signaling, #3027, pIGFR: Cell

Signaling, #4568, Beclin: Novus Biologicals, NBP1-00088, CytC: MitoSciences, #MSA06, CoxIV: Cell Signaling, #4844, GAPDH: Novus Biologicals, NB300-322, Ndufs3:Invitrogen, #439200, Ndufs9 MitoSciences (MS Catalog Number MS111), p62: Cell Signaling, #5114, S6: Cell Signaling, #5317, pS6: Cell Signaling, #4856. Blots were blocked in 3% milk-TBST and all primary antibodies were used at 1:1000 in 0.3%-TBST milk.

Tissue Staining

Tissues were fixed overnight in 4% formalin in PBS and cryoprotected by soaking in 30% sucrose in PBS until floating (24-48 hours). Oil-red-o staining was performed by the University of Washington Histology and Specialized Pathology Services core facilities by standard methods. Staining for Iba1 and GFAP were performed using 30-µm free-floating sections were used. Paraffin sections were rehydrated through a series of graded ethanol solutions and boiled for 20 min in sodium citrate buffer, pH 6.0, for antigen unmasking. Sections were blocked with 10% normal donkey serum (NDS) in PBS-0.2% Triton X (PBST) for 1 h at room temperature and then incubated overnight at 4 °C in a wet chamber with primary antibodies diluted in 1%NDS-PBST (1:1,000 anti-GFAP, Sigma #G3893 , or 1:1,000 anti–Iba-1, Cell Signaling #019–19741). Slides were washed in PBST and incubated for 1 h at RT with Cy2- or Cy3-conjugated secondary antibodies (1:200 in 1% NDS-PBST; Jackson Immunoresearch). Sections were washed in PBS and counterstained with DAPI (Sigma) and coverslipped with aqueous mounting media (Fluo romount G; Electron Microscopy Science).

Microscopy

All images were gathered with a Nikon Eclipse E600 bright field and fluorescence microscope at the University of Washington Keck Microscopy center. All image analysis was performed using the free analysis program ImageJ (http://rsbweb.nih.gov/ij/).

Respiration assays

Respiration of freshly isolated mitochondria was measured with a Seahorse XF24 flux analyzer (Seahorse BioScience, Billerica, MA) following the manufacurers guidelines (http://www.seahorsebio.com/resources/tech-writing/iso-mito-xf24.pdf). Briefly: 5ug of mitochondria were adsorbed to the bottom of each sample well by spinning 50ul of mitochondrial suspension at 2000g for 20min at 4°C. The medium was MAS (70mM sucrose, 220mM mannitol, 10mM KH2PO4, 5mM MgCl2, 2mM HEPES, 1mM EGTA, 0.02% fatty acid-free BSA, pHed to 7.2 with KOH at 37°C) supplemented with electron donor substrate. Electron donor combinations for complex I dependent respiration were 5mM malate plus either 10mM pyruvate, 10mM glutamate or 10mM α-ketoglutarate. For measuring complex I-independent respiration the complex II substrate succinate (13mM) in combination with the complex I inhibitor rotenone (2μM) was utilized. Before loading the plate into the Seahorse the assay volume of all wells, samples, and blanks was adjusted to 500ul by adding more of the same medium (MAS plus electron donors).

The instrument was programmed to execute the following protocol at 37°C: wait 10 min, mix 1min, wait 3 min, mix 1 min, wait 3 min, mix 1 min, measure 3 min, mix 1

min, measure 3 min state 2 respiration, mix 1min, inject ATP synthetase substrate ADP (4mM, pH'd to 7.2), mix 1min, measure 3min state3 respiration, mix 1min, inject ATP synthetase inhibitor oligomycin (2.5ug/ml), mix 1min, measure 3min state 4 respiration, mix 1min, inject uncoupler carbonyl cyanide 4-(trifluoromethoxy)-phenylhydrazone (= FCCP) (5uM), mix 1min, measure 3min uncoupled respiration, mix 1min, inject complex III inhibitor antimycin A (4uM), mix 1min, measure 3min respiratory chain-independent respiration. Concentrations given signify concentrations after injection in assay. Respiration rates for each well were determined using the Akos algorithm for OCR (oxygen consumption rate) (2009 Gerencser et al. AnalChem81 6868 - Seahorse - quantitative microplate-based respirometry with correction for oxygen diffusion), background corrected and normalized to µg of loaded protein. State3 and uncoupled respiration rates declined during the 3min measurement interval and were therefore determined as the initial (maximum) respiration rate measured. State2 and state4 rates were stable and therefore reported as the average over the respective measurement interval. For each mitochondrial preparation these parameters were reported as the mean of 5 technical replicates.

Blue Native Gels (BNG)

BNG-PAGE was performed as described by Wittig et al. (2006 Nature Protocols 1(1) 418) with the modification that precast minigels (Novex, NativePAGE 3-12% Bis-Tris, BN2011BX10, 1mm thick) were used in an XCell SureLock Mini-Cell (Invitrogen). Key features of the sample treatment: 150ug of previously frozen mitochondria samples were extracted with either digitonin (6:1 detergent:protein w:w) or Triton X-100 (5:1

detergent:protein w:w) and protein complexes in the 15,000g supernatant were negatively charged with Coomassie Blue G-250 (1:8 detergent:dye w:w). Key features of the run: After 1h electrophoresis at 100V blue cathode buffer was replaced by cathode buffer without Coomassie blue and 300V were applied for an additional 1.5h. At the end of the run the overall protein distribution in the gel could be imaged without any additional Coomassie staining. Complex I in-gel activity (IGA) staining: Gels were incubated at room temperature with 2.5mM NADH and 0.5mM nitroblue tetrazolium (mod. of Sabar et al. PlantJ44 893). The purple-ish hue of the formazan reaction product identifies bands with NADH dehydrogenase activity were. (A prominent cross reactivity at about 200 kD is probably caused by dehydrolipoamide dehydrogenase (2009 EH Meyer et al. PlantPhysiol151 603)).

Metabolomics

Approximately 150 micrograms of cryohomogenized frozen tissue powder from each sample were sonicated, with 50 micron glass beads in 500 microliters of 80:20 methanol:H20 on dry ice, incubated for 30 minutes, then centrifuged for 10 min at 14,000 rpm in a microcentrifuge at 4 degrees C. Supernatant was moved to a new tube, on dry ice, and the extraction was repeated two more times. The total volume of extract was combined and lyophilized using a microcentrifuge rotovac at 14,000 rpm, 30 degrees C, with carbon dioxide filling the rotovac chamber prior to applying the vacuum and starting centrifugation. Samples were submitted to the University of Washington Nutrition Obesity Research Center Analytic Core facility for analysis.

Dried samples were reconstituted in 5 mM ammonium acetate in 95% water/5% acetonitrile + 0.5% acetic acid and filtered prior to LC-MS analysis. The filtered samples were injected to the LC system which was composed of two Agilent 1260 binary pumps, an Agilent 1260 auto-sampler and Agilent 1290 column compartment containing a column-switching valve (Agilent Technologies, Santa Clara, CA). The chromatography was performed using Solvents A (5 mM ammonium acetate in H2O + 0.5% acetic acid + 0.5% acetonitrile) and B (acetonitrile + 0.5% acetic acid + 0.5% water), with 5% B for 2 min, 5% B to 80% B in 3 min, 80% B for 3 min, 80% B to 5% B in 3 min, and 5% B for 7 min. After the chromatographic separation, MS ionization and data acquisition was performed using an AB Sciex QTrap 5500 mass spectrometer (AB Sciex, Toronto, ON, Canada) equipped with electrospray ionization (ESI) source. Multiple-reactionmonitoring (MRM) mode was used for targeted data acquisition of 158 metabolites. The extracted MRM peaks were integrated using MultiQuant 2.1 software (AB Sciex, Toronto, ON, Canada). Reproducibility of the quality control samples indicated excellent technical reproducibility with an average CV of 7% for positive ion mode and 10% for negative ion mode detected metabolites.

Statistical Analysis

All data were presented as means +/- SEM. Comparisons between groups were performed using student t-tests, 2-tails. $P<0.05$ was considered significant and $p<0.005$ considered highly significant (designated * and ** on bar graphs, respectively). Statistical comparisons of lifespan curves were performed using the log-rank test as indicated.

Metabolomic data q-value multiple testing correction was performed using the R plugin qvalue available at http://genomics.princeton.edu/storeylab/qvalue/.

Rapamycin Blood Level Analysis

Whole-blood samples were collected through cardiac puncture immediately following euthanasia into tubes containing EDTA. Samples were frozen and shipped on dry ice to the Javors lab in the Department of Psychiatry at the University of Texas Health Science Center San Antonio for analysis by HPLC.

RESULTS/DISCUSSION

We first examined the effects of delivering rapamycin (8 mg/kg) every other day by intraperitoneal injection beginning at weaning [approximately postnatal day 20 (P20)]. This treatment reduces mTOR signaling in wild-type mice[211] and provided significant increases in median survival of male (25%) and female (38%) knockout mice (Figure 2.2A). A slight reduction in maximum body size and a delay in age of disease onset were also observed (Figure 2.2B and Figure 2.3). Although these results showed that NDUFS4 KO mice benefit from rapamycin treatment, we noted that by 24 hours after injection, rapamycin levels in blood were reduced by more than 95% (Figure 2.4). We therefore performed a follow-up study delivering rapamycin (8 mg/kg) daily by intraperitoneal injection starting at P10, which resulted in blood levels ranging from >1800 ng/ml immediately after injection to 45 ng/ml trough levels (Figure 2.4). For comparison, an encapsulated rapamycin diet that extends life span in wild-type mice by about 15% achieves steady-state blood levels of about 60 to 70 ng/ml, and trough levels

between 3 and 30 ng/ml are recommended for patients receiving rapamycin[47]. In the daily-treated cohort, we observed a striking extension of median and maximum life span; the longest-lived mouse survived 269 days. Median survival of males and females was 114 and 111 days, respectively (Figure 2.4C).

Vehicle-injected knockout mice first displayed neurological symptoms around P35, coinciding with a body weight peak (Figure 2.2B to D, and Figure 2.3D). After this point, disease symptoms progressively worsened and weight declined. Daily rapamycin treatment dampened developmental weight gain and prevented the progressive weight loss phenotype (Figure 2.2B and Figure 2.3E). This effect was robust, even among mice from the same litter (Figure 2.5). Incidence and severity of clasping, a commonly reported and easily scored phenotype that progresses with weight loss and neurological decline, was also greatly attenuated in rapamycin-treated knockouts (Figure 2.2, C to E). Performance in a rotarod assay, which measures balance, coordination, and endurance, was assessed in a separate cohort of mice. Vehicle-treated knockout mouse performance worsened as the disease progressed, whereas rapamycin-treated knockout mice maintained their performance with age (Figure 2.2F and 2.6). Dyspnea, previously observed in vehicle-treated knockout mice[208], was not observed in the mice injected daily with rapamycin.

Rapamycin-treated knockout mice also did not develop the neurological lesions associated with this disease (red arrows in Figure 2.7). The lesions, characterized by astrocyte activation and glial reactivity [detected by glial fibrillary acidic protein (GFAP) and Iba1 staining, respectively] were detectable in all vehicle-treated knockout mice over 50 days of age[208]. We were unable to detect lesions in the cerebellum of age-

matched rapamycin-treated knockout mice. GFAP, Iba1, and laminin (a marker of neovascularization) were markedly increased in olfactory bulbs of vehicle-treated but not in rapamycin-treated knockout mice (Figure 2.7B and Figure 2.8). Rapamycin did not affect GFAP, Iba1, or laminin levels in wild-type mice (Figure 2.8). Western blotting for GFAP using whole-brain lysates from ~50-day-old mice revealed a significant increase in GFAP in knockout mice that was attenuated by rapamycin (Figure 2.7C). Furthermore, no lesions were detected in 100-day-old and 268-day-old rapamycin-treated knockout mice (Figure 2.9). Overall, the percentage of mice showing neurological symptoms was much reduced at every age point after P35 in rapamycin-treated knockout mice, with about half never exhibiting overt signs of neurological disease before death (Figure 2.7D and E).

Given the pleiotropic effects of mTOR inhibition[10,212], we sought to identify downstream mechanisms associated with attenuation of mitochondrial disease. Rapamycin has well-documented immune-modulatory effects, so we first considered that the benefit might arise from reduced neuroinflammation. To test this model, we treated mice with FK-506 (tacrolimus), a clinically approved immunosuppressive drug that binds the same target as rapamycin, FKBP12, but inhibits calcineurin signaling rather than mTOR[213]. FK-506 did not affect disease onset or progression (Figure 2.10 A and B, Figure 2.11), indicating that neither immunosuppression nor off-target disruption of calcineurin by binding of FKBP12 are likely to account for the effects of rapamycin. We next considered that rapamycin might improve mitochondrial function by increasing macroautophagy, removing the least functional components of the mitochondrial network. Although we were able to detect evidence of induction of autophagy in the liver

and brain of rapamycin-treated mice (Figure 2.12), there was no corresponding rescue of mitochondrial function (Figure 2.10C and Figure 2.13). Complex I assembly and stability, assessed by blue native gel electrophoresis, were also unaltered by rapamycin (Figure 2.10D and Figure 2.14), as were levels and localization of ETC proteins (Figure 2.10E and F, Figure 2.15). We found no evidence for induction of HSP60, a component of the mitochondrial unfolded protein response, either by NDUFS4 loss or by rapamycin (Figure 2.10F and Figure 2.15).

As a central coordinator of nutrient sensing and growth, mTOR regulates metabolism by integrating levels of amino acids at the lysosome, energetic sensing by adenosine monophosphate–activated protein kinase (AMPK), and extracellular signals through insulin and insulin-like growth factor (IGF)[212,214]. We reasoned that loss of NDUFS4 might perturb metabolic signaling and affect mTOR activity. Consistent with this idea, phosphorylation of ribosomal protein S6, a target of mTOR complex 1 (mTORC1) signaling, was significantly increased in the brains of knockout mice (Figure 2.16A), and rapamycin reduced phosphorylation of S6 in both wild-type and knockout mice. IGF1 receptor (IGF1R) phosphorylation was also increased in NDUFS4 KO mice and reduced by rapamycin (Figure 2.16A). Whole-body quantitative magnetic resonance revealed a progressive loss in body fat in the NDUFS4 KO mice that was ameliorated by daily rapamycin injections (Figure 2.16B). Furthermore, Oil Red O staining and metabolomic analysis of liver indicated that knockout mice had a marked deficiency in liver fat droplets and free fatty acids that was partially rescued by rapamycin (Figure 2.16C and D, Figure 2.17). Whole-brain metabolomics of 30-day-old mice revealed an abnormal metabolic profile in the NDUFS4 KO mice that included an

accumulation of pyruvate, lactate, and all detected glycolytic intermediates, consistent with clinical reports of Leigh syndrome[205,215] (Figure 2.16E). The metabolomic signature of the NDUFS4 KO mouse brain includes a decrease in free amino acids, free fatty acids, nucleotides, and products of nucleotide catabolism, increased oxidative stress markers, and reduced levels of γ-aminobutyric acid (GABA) and dopamine (Figure 2.18). Rapamycin rescued many of these metabolomic defects associated with NDUFS4 deficiency, including levels of GABA, dopamine, and free fatty acids. Increased amino acids, metabolites of amino acid and nucleotide catabolism, and free fatty acids accompanied the decrease in glycolytic intermediates, whereas markers of oxidative stress were unchanged. Moreover, hexokinase—the first enzyme in glycolysis—was increased in NDUFS4 KO mice and reduced by rapamycin in knockout and control mice, consistent with the decrease in glycolytic intermediates (Figure 2.16A).

Taken together, our results demonstrate that inhibition of mTOR improves survival and health in the NDUFS4 KO model of Leigh syndrome. These findings raise the possibility that mTOR inhibitors may offer therapeutic benefit to patients with Leigh syndrome and potentially other mitochondrial disorders. Rapamycin derivatives have several adverse effects, however, including immunosuppression, hyperlipidemia, and decreased wound healing, which may limit their utility in this context, particularly in very young patients. Thus, a more detailed understanding of the mechanisms by which rapamycin alleviates disease in NDUFS4 KO mice should allow for the development of more targeted interventions to improve health in patients suffering from mitochondrial diseases for which there are no effective treatments.

CHAPTER 3

Dietary rapamycin alleviates mitochondrial disease and alters body composition in a dose-dependent manner

The contents of this chapter will be submitted for publication as: Yanos ME, Johnson SC, Letexier NJ, Jarvie CM, McCanta LM, Tamis O, Hui J, Sangesland M, Gagnidze A, Van-Den-Ende A, Kaeberlein M. Dietary rapamycin alleviates mitochondrial disease and alters body composition in a dose-dependent manner. *Journal to be determined*.

OVERVIEW

The drug rapamycin has been shown to extend lifespan and improve several measures of healthspan in mice when provided in the diet at 14 ppm using an encapsulation strategy designed for release in the small intestine. In a recent report, daily intraperitoneal (IP) injection of rapamycin at 8 mg/kg was found to more than double survival and greatly attenuate disease progression in the NDUFS4 KO mouse model of the severe mitochondrial disease Leigh Syndrome. Here we report the effects of dietary delivery of encapsulated rapamycin at doses ranging from 42 ppm to 378 ppm on health and survival in Leigh Syndrome mice and on body composition in wild type mice. We conclude that the highest dose of dietary rapamycin tested, approximately 27-fold greater than that previously shown to extend the lifespan of wild type mice, achieves effects comparable to daily injection with no adverse effects noted during the course of the experiments.

INTRODUCTION

Rapamycin, a specific inhibitor of the mechanistic target of rapamycin (mTOR), is the only pharmacological intervention thus far shown to robustly and reproducibly extend lifespan in budding yeast, nematode worms, fruit flies, and mice[212]. Rapamycin was first shown to increase murine lifespan by the National Institute on Aging Interventions Testing Program (ITP) in a study where genetically heterogeneous UMHET3 mice were fed a diet supplemented with 14 ppm encapsulated rapamycin beginning at around 600 days of age[47]. Since then, a similar rapamycin-supplemented diet initiated in young animals has also been shown to extend lifespan in UMHET3 mice[216], and in C57Bl/6 inbred mice when initiated at either 19 months of age[217] or mixed ages[218]. An intermittent treatment protocol where rapamycin is injected subcutaneously at 1.5 mg/kg three times per week for two weeks out of every month beginning in young animals has also been shown to extend lifespan in the inbred 129/Sv background[219].

In addition to increasing lifespan, several studies have indicated that rapamycin can improve a variety of healthspan measures in mice. At least three studies have attempted to comprehensively evaluate the effects of rapamycin on healthspan by quantifying multiple age-sensitive traits[217,218,220]. In each study, rapamycin treatment was associated with improvements in many, but not all, of the age-associated phenotypes examined. The failure to detect positive effects from rapamycin for some age-sensitive traits has resulted in ongoing discussion in the literature regarding whether rapamycin increases lifespan in mice by generally slowing aging or primarily through anti-cancer effects[218,221–223]. Despite some differences in interpretation, there is

general consensus that, in addition to reducing or delaying cancer progression, rapamycin also attenuates age-associated declines in some measures of cardiac, immune, muscular, and cognitive function[224].

Leigh Syndrome (LS) is a severe mitochondrial disease that occurs in about 1:40,000 newborns, is typically diagnosed during early childhood, and is characterized by retarded growth, myopathy, dyspnea, lactic acidosis, and progressive encephalopathy mainly localized to the vestibular nuclei, cerebellum, and olfactory bulb[198]. The NDUFS4 KO knockout (KO) mouse has been developed as a murine model of LS[204]. NDUFS4 encodes a subunit of Complex I of the mitochondrial electron transport chain, and mutations in the NDUFS4 gene are associated with Leigh Syndrome in people[225–228]. NDUFS4 KO mice have decreased Complex I abundance and activity in multiple tissues; however, disease progression and death appear to result primarily from central nervous system defects[208,218].

In a recent study, we observed a striking suppression of Leigh Syndrome phenotypes by rapamycin in NDUFS4 KO animals[229]. Every other day intraperitoneal (IP) injection of 8 mg/kg rapamycin beginning at weaning (~P20) resulted in a roughly 30% increase in survival, while daily IP injection of the same dose of rapamycin beginning at P10 was sufficient to more than double median survival and triple maximum survival. In addition to enhancing survival, daily injection of rapamycin also improved coordination and greatly reduced neurodegeneration, neuroinflammation, and neurological behavioral phenotypes, such as clasping and slowness of movement in the NDUFS4 KO animals. Suppression of disease phenotypes by rapamycin in NDUFS4 KO mice was not accompanied by restoration of Complex I activity in brain; however, at

least some aspects of the underlying metabolic defect, including accumulation of glycolytic intermediates and lactate, were reversed. Daily injection of rapamycin also had an unexpected effect on body composition in both wild type (WT) and KO animals, resulting in increased percent body fat despite a reduction in body weight.

Based on these findings in combination with the prior studies using encapsulated rapamycin in the diet, we set out to determine whether oral delivery of encapsulated rapamycin could achieve effects similar to daily IP injection in NDUFS4 KO mice. Here we report that feeding mice standard chow supplemented with rapamycin at 378 ppm, a dose 27-fold higher than that shown to extend lifespan of WT animals, is sufficient to achieve effects on survival and body composition in NDUFS4 KO mice comparable to daily IP injection of 8 mg/kg rapamycin. Effects of short-term high-dose oral delivery of rapamycin in WT animals are also presented.

MATERIALS AND METHODS

Animals

NDUFS4 +/- breeders were obtained from the Palmiter laboratory at the University of Washington, and procedures to obtain and care for knockout mice have been previously described[203]. NDUFS4 heterozygous mice and wild-type mice obtained through NDUFS4 +/- breeding show identical phenotypes here, and thus were pooled as wild-type controls for the experiments described.

Encapsulated rapamycin was obtained from the Barshop Institute at the University of Texas Health Science Center at San Antonio and Rapamycin Holdings, Inc. Standard mouse chow was ground to a power and mixed with rapamycin dosage amounts at 14, 42, 126 or 378 ppm. Approximately 300 mL of 1% bulk food agar in autoclaved water was added per kilogram of powdered chow. Powdered chow was then hand formed into pellets and incubated at 55°C for 2-3 hours. Pellets were allowed to dry before being sealed for short-term (4°C) or long-term (-20°C) storage.

Mice began receiving assigned diet treatments upon weaning, at 20-21 days of age. Mice assigned to rapamycin (8 mg/kg) or vehicle injection groups began treatments at postnatal day 10 (P10) as previously described.

All care of experimental animals was in accordance with the University of Washington institutional guidelines and experiments were performed as approved by the Institutional Animal Care and Use Committee.

Body composition measurements

Body composition measurements were measured at indicated time points using quantitative nuclear magnetic resonance imaging (QNMR) with an EchoMRI 3-in-1 Animal Tissue Composition Analyzer at the University of Washington In Vivo Services Core.

Rapamycin Blood Level Analysis

Whole-blood samples were collected from decapitated trunk or cardiac puncture immediately following euthanasia into tubes containing EDTA. Samples were frozen and shipped on dry ice to the Javors lab in the Department of Psychiatry at the University of Texas Health Science Center San Antonio for analysis by HPLC.

Statistical Analysis

Wilcoxon Mann-Whitney Rank Sum tests were performed to analyze survival data. Parametric tests including independent sample t-tests, one-way ANOVA and two-way ANOVA tests were all used as indicated in the results. All tests were two-tailed and assumed equality of variance, with an alpha level of significance set at $p<0.05$. Statistical analysis was performed using IBM SPSS Statistics 22 or R-3.1.0 software.

RESULTS

Dietary rapamycin during development attenuates weight gain and promotes body fat accumulation in a dose-dependent manner.

To assess the effect of oral dietary delivery of rapamycin at higher doses than previously administered, small cohorts of WT animals were fed chow containing 42, 126 or 378 ppm rapamycin beginning at weaning (~P20, see Materials and Methods). The amount of rapamycin present in whole blood or plasma was measured after at least 7 days on the rapamycin diet (Figure 3.1A and Figure 3.1B). For comparison, the levels

of rapamycin detected following intraperitoneal injection of 8 mg/kg at 1 hour, 24 hours, and 48 hours are also shown[229].

At day 30, or after 10 days of receiving diet treatments, ANOVA tests showed that body weights for male and female WT mice were significantly different between conditions, respectively (Figure 3.2A and 3.2B). Post-hoc pairwise comparisons showed that female weights for all three rapamycin treatments were significantly reduced compared to control treated animals (Figure 3.2B). At this time point, body weights of male WT mice were significantly reduced for 126 ppm and 378 ppm rapamycin doses, but not 42 ppm (Figure 3.2A). By day 60, statistical analysis by t-test showed that control treated animal weights had increased significantly for both males and females (Figure 3.2A and 3.2B). Dietary rapamycin at 126 ppm and 378 ppm appeared to attenuate body weight gain of both male and female WT mice (Figure 3.2A and 3.2B). At day 60, females receiving 126 or 378 ppm rapamycin treatments showed a significant increase in percent body fat compared to control treated mice (Figure 3.3A). Percent body fat in 60 day old males was consistent with this trend, although pairwise comparisons did not show a significant effect (Figure 3B.)

Dietary rapamycin promotes survival and alters body mass in NDUFS4 *knockout mice*

We next assessed survival of NDUFS4 KO animals fed a diet containing either 42, 126 or 378 ppm rapamycin beginning at weaning. Relative to control fed animals, a significant increase in median survival was detected for all three rapamycin-treated cohorts (Figure 3.4A and B).

Rapamycin treatment also altered the weight gain profiles of KO mice, which show a characteristic pattern of weight gain between P20 and P35 followed by a rapid decline in body weight, concomitant with the presentation with neurological symptoms[229]. This pattern of weight gain followed by weight loss was observed in the KO animals treated with 42 ppm dietary rapamycin, although the age at which weight peaked was delayed roughly proportionally to the increase in survival for this cohort (Figure 3.5A). Interestingly, a weight peak was never observed in the 126 or 378 ppm rapamycin-treated cohorts (Figure 3.5A), which is strikingly similar to the weight profiles of animals treated with 8 mg/kg/day of rapamycin by IP injection[229]. Furthermore, diet containing 378 ppm of rapamycin chow appeared to rescue loss of fat mass relative to total body weight in KO mice similar to 8 mg/kg/day rapamycin by IP injection (Figure 3.6A and B). These observations are consistent with the effects of daily IP injection of 8 mg/kg rapamycin beginning around weaning[229].

DISCUSSION

The data presented here suggest that dietary delivery of encapsulated rapamycin at 126 to 378 ppm can achieve biological efficacy comparable to daily IP injection of 8 mg/kg rapamycin in young WT and NDUFS4 KO animals. Median survival of NDUFS4 KO animals fed 378 ppm rapamycin diet beginning at weaning was not significantly different from animals treated by daily injection beginning at P10. In addition, the effects of 126 or 378 ppm rapamycin diet on body weight and body composition in WT mice appeared similar to the effects of daily injection. Based on these observations we estimate that between 126 to 378 ppm rapamycin must be delivered orally in the diet in order to obtain biological efficacy comparable to 8 mg/kg/day delivered by IP injection in

C57BL/6N mice. Based on prior estimates for dietary delivery of this form of rapamycin[47], this equates to between 20 and 60 mg/kd/day rapamycin.

Our observation that dietary doses of rapamycin much higher than have been previously tested for effects on normative aging are not only well-tolerated, but can result in significantly reduced disease burden, raise the possibility that high doses may also have larger positive effects on longevity and healthspan in mice. Suboptimal dosing regimens may explain the lack of aging phenotypes previously found in rapamycin-treated mice[218]. Rapamycin diet at the standard ITP dose of 14 ppm may be sufficient to induce anti-cancer and other age-independent effects on survival, but we believe that higher doses are likely to induce anti-aging effects that have not been previously detected.

High levels of circulating rapamycin in the blood may be necessary to induce tissue-specific metabolic changes in order to attenuate aging phenotypes. Previously, we found that daily IP injection of 8 mg/kg could effectively cross the blood-brain barrier to reduce whole brain levels of phospho-s6, an indicator of mTOR activity, in both KO and WT mice[229]. Lower doses of rapamycin may not be sufficient to cross the blood-brain barrier. This is further supported by evidence that 6 mg/kg of rapamycin delivered by IP injection induced high blood levels of circulating rapamycin (>1000 ng/ml) but yielded relatively low penetrance in the brain (approximately 100 ng/g) compared to liver (approximately 1000 ng/g). This high dosage of rapamycin was also shown to be sufficient to inhibit mTOR activity in whole brain lysates[230]. Thus, we hypothesize that a substantial reduction of mTOR activity in the brain of NDUFS4 KO mice is likely required for the metabolic shift we observed as a result of rapamycin treatment.

Identification of a minimum threshold of pharmacological effectiveness also has implications for inducing changes in the aging brain. For instance, daily IP injection of rapamycin at 8 mg/kg has been reported to alter neural activity involved in age-dependent obesity in mice[231].

Age-related changes in liver metabolism might also respond to rapamycin a dose-dependent manner. Administration of the ITP dose of rapamycin diet at 14 ppm for 6 months has been shown to simulate aspects of DR in liver by inhibiting lipogenesis, increasing lipolysis, and increasing serum levels of nonesterified fatty acids.[232] However, long-term rapamycin treatment at this dosage could not mimic the effects of DR on induction of β-oxidation of fatty acids and consequential production of ketone bodies. In contrast, acute rapamycin treatment of 10 mg/kg delivered by IP injection has been shown to maintain elevated levels of ketone bodies in liver upon refeeding mice after a 24 hour fast.[233] Observed defects in ketogenesis associated with aging may thus be responsive to a chronic high dose of rapamycin.

Differential effects of rapamycin treatment on lifespan and healthspan have previously been reported[47]. Low dosage at 14 ppm appears to have sex-specific effects on lifespan and age-related changes in the liver transcriptome, with female mice responding more robustly to rapamycin treatment.[234] Our lab has reported that high doses of rapamycin treatment delivered via IP injection or chow induces robust lifespan extension in both male and female KO mice. Treatment of dietary rapamycin also appeared to induce changes in body weight and fat mass in both male and female WT mice, although observed effects were more pronounced in females. Thus, effects of

rapamycin treatment in both males and females may partially depend on whether mice have a disease background.

In summary, it appears that oral delivery of rapamycin can attenuate symptoms associated with LS in NDUFS4 KO comparably to daily injection of the drug, and that high blood levels of rapamycin from either IP injection or chow are required to induce significant effects on lifespan and body composition. The optimal dosage required for circulating blood levels of rapamycin to have noticeable therapeutic effects on aging phenotypes is yet to be determined, but we believe that the standard ITP dosage of 14 ppm is below the minimum threshold for detecting these effects. Some concern has been raised that high levels of rapamycin in the blood for sustained periods of time results in symptoms of diabetes such as hyperglycemia and glucose intolerance.[35] However, preliminary data from our lab has shown that 90 day chronic IP injection of rapamycin in adult WT mice does not appear to significantly affect circulating glucose levels in the blood (data not shown), and suggests that tolerance to the drug may be developed over the course of prolonged treatment.

CHAPTER 4

Investigation of mTOR inhibition in treatment of pathology and symptoms of the MPTP mouse model of Parkinson's disease

The contents of this chapter will be submitted for publication as Yanos ME, Letexier NJ, Jarvie CM, McCanta LM, Kaeberlein M. Investigation of mTOR inhibition in treatment of pathology and symptoms of the MPTP mouse model of Parkinson's disease (working title). *Journal to be determined*.

OVERVIEW

Parkinson's disease (PD) is the second most common neurodegenerative disease in the U.S., affecting more than 1% of individuals over the age of 65. Effective treatment to halt or reverse progression of the disease does not currently exist. Previous reports suggest that inhibition of the mechanistic target of rapamycin (mTOR) pathway is effective at reducing markers of neural pathology in models of PD and other neurodegenerative diseases. We conducted a study to further investigate the known effects of mTOR inhibition by high dose rapamycin in treating the PD-like pathology of mice exposed to the toxic drug MPTP. Our preliminary results show that rapamycin treatment partially reduced neuron degeneration in the substantia nigra resulting from MPTP exposure, consistent with previous reports. In addition, MPTP mice showed evidence for hyperactive mTOR signaling compared to control mice, which could be potently reduced by rapamycin treatment. Assessment of motor behavior was assessed by performance on a rotarod task, and results suggest that MPTP induces age-dependent, rapamycin-sensitive phenotypes that may have been overlooked in previous studies utilizing only young mice. Overall, we speculate that hyperactive mTOR may be associated with neural pathology of PD, and that inhibition of mTOR may be particularly effective at reducing age-specific factors underlying symptoms of the disease.

INTRODUCTION

Parkinson's disease (PD) is the second most common neurodegenerative disorder in the U.S. As of 2010, more than 600,000 individuals have been diagnosed with PD, or 0.3% of the general population. The prevalence of PD is much higher in the elderly population, affecting more than 1% of individuals over age 65 and 4-5% of individuals over 85[134–137] Major symptoms include slowness of movement ("bradykinesia"), rigidity, and postural instability, often presenting with nonmotor and neuropsychiatric symptoms such as cognitive decline and depression[134,138]. Major pathological hallmarks of PD include (1) degeneration of dopaminergic neurons in the substantia nigra (SN); and (2) accumulation of α-synuclein protein in cytoplasmic inclusions called Lewy bodies. Administration of the DA precursor levodopa compensates for dopamine deficiency and alleviates symptoms in PD patients; however, therapies to cure or slow disease progression of PD remain undiscovered[134,139].

The neurotoxic drug 1-methyl-4-phenyl-1,2,3,6-tetrahydropyridine (MPTP) is regarded as a powerful tool to study the underlying mechanisms of PD pathology in animal models. Symptoms of MPTP toxicity in humans were initially reported in 1983, when several drug users developed a rapidly progressive parkinsonian syndrome traced to intravenous administration of MPTP contaminants[235]. Observations of MPTP-related patterns of neurodegeneration largely resembling that of PD followed with studies in spider monkeys[236]. In addition to in MPTP-treated primate models have since proved invaluable for testing potential treatments for PD. Acute or chronic administration of MPTP has also been shown to induce dopaminergic

neurodegeneration and movement deficits in mice. Generally, the MPTP mouse model is a more tractable model for investigation of PD-related pathology at the cellular and molecular level.[138]

The exact mechanism by which MPTP induces PD-like dopaminergic neurodegeneration has not been firmly established, but strong evidence suggests that mitochondrial dysfunction plays a causal role. MPTP crosses the blood-brain barrier and is converted to the actively toxic metabolite MPP+[237,238]. MPP+ is transported into neurons through the plasma membrane, where it is concentrated into mitochondria and potently inhibits ETC complex I activity[239,240]. The negative impact on neuronal ATP production may be particularly harmful in dopaminergic nerve terminals, which are rich in synaptic mitochondria.[138] Furthermore, MPP+ may stimulate production of reactive oxygen species (ROS) by disrupting the flow of electrons through complex I, resulting in mitochondrial damage[241,242]. Mice that are deficient for superoxide dismutase-1 (SOD1), a key ROS scavenging enzyme, are resistant to MPTP-induced dopaminergic neuron degeneration[243]. Consistent with both of these hypotheses, significant ATP depletion and oxidative damage have been observed in postmortem brain tissue of PD patients[244,245].

Inhibition of the mechanistic target of rapamycin (mTOR) pathway appears to have therapeutic potential for treatment of PD. Administration of rapamycin, a specific inhibitor for mTOR, has been reported to attenuate neurodegeneration of DA neurons in the SN after acute MPTP insult[141,142]. Rapamycin treatment appears to result in increased autophagy, which may play a role in neural rescue through removal of alpha-synuclein in brains of MPTP-treated mice[142]. However, a corresponding improvement in

locomotor behavior in the MPTP mouse model as a result of rapamycin treatment has not yet been reported. Furthermore, it is not known whether MPTP induces aberrant mTOR activity, similar to what has been reported in patients and animal models of Alzheimer's and Huntington's disease[246–251]. Previous work from our lab has shown evidence for increased mTOR activity in complex I-deficient NDUFS4 knockout (NDUFS4 KO) mouse model for Leigh Syndrome compared to wild-type mice[229]. Thus, we predict that pharmacological inhibition of complex I activity through MPTP exposure might similarly induce hyperactive mTOR signaling.

The purpose of this study is to further characterize the therapeutic effects of rapamycin treatment in the MPTP mouse model for PD and to draw comparisons with results from our previous work with the NDUFS4 KO mouse. To do this, we investigated the effects of high dose daily rapamycin injections on MPTP-induced dopaminergic neuron degeneration in the substantia nigra in mice, similar to what has been previously reported with different MPTP and rapamycin dosing regimens (Table 4.1). In addition, we compared rapamycin- and vehicle-treated MPTP mice in tests for (1) levels of mTOR activity in whole brain tissue; (2) performance on the rotarod behavioral tasks; and (3) body mass composition.

METHODS

Animals and tissue collection

A total of 37 C57BL/6 males were obtained from non-transgenic crosses of mice originating from Charles River Laboratories. All mice were 11 to 26 weeks of age at the

time of MPTP treatment. Mice were divided into three groups: Saline/Vehicle (S/V), MPTP/Vehicle (M/V), and MPTP/Rapa (M/R). Mice received either acute treatment of MPTP (18 mg/kg MPTP-HCl dissolved in saline; Sigma) or saline in a series of four intraperitoneal (IP) injections at 2-hour intervals.

Rapamycin was dissolved in DMSO to 100 mg/mL. This was diluted in 5% PEG-400/5% Tween-20 (vehicle) to a concentration of 1.2mg/mL. Daily administration of rapamycin (8 mg/kg) or non-rapamycin vehicle solution by IP injection began 24 hours after acute MPTP or saline treatment and continued for the duration of experiments. All care of experimental animals was in accordance with the University of Washington institutional guidelines and experiments were performed as approved by the Institutional Animal Care and Use Committee.

Two to three weeks after acute MPTP or saline administration, mice were euthanized by cervical dislocation, decapitated, and brains were quickly removed. Midbrain and striata were both dissected for further processing.

Rotarod

Rotarod (Rotamex 5, Columbus Instruments) performance was assessed before and after MPTP treatment. Rotarod parameters were set at beginning speed of 0 rpm with an acceleration rate of 0.1 rpm/s and a maximum speed of 40 rpm. Mice underwent one day of orientation consisting of a single session, followed by two practice days consisting of two sessions per day. Animals were tested 24 hours after the second practice day; mice underwent three rotarod sessions on the testing day, and latency-to-fall times were recorded. Median and maximum times were then calculated.

Body composition measurements

Body composition measurements were measured using quantitative nuclear magnetic resonance imaging (QNMR), with an EchoMRI 3-in-1 Animal Tissue Composition Analyzer, at the University of Washington In Vivo Services Core. Measurements were taken before and after MPTP treatment.

Immunohistochemical (IHC) staining

Dissected midbrains from 4-5 animals per group were fixed in 10% neutral buffered formalin for at least 24 hours, cryoprotected by soaking in 30% sucrose until floating (24-48 hours) then embedded in OCT. IHC staining was performed at the University of Washington Histology and Imaging Core at the South Lake Union campus. Consecutive Coronal sections (8 μm) were obtained using a freezing microtome. Sections were immunolabeled with a monoclonal anti-TH antibody (Millipore, MAB318; 1:1000), incubated with a polymerized HRP-conjugated secondary antibody and developed with DAB.

Western blotting

Remaining brain tissue was frozen separately for western blotting. For tissue homogenization, frozen tissue was placed into the pre-chilled chamber of a cryogenic tissue pulverizer (RPI) and instantly turned into fine powder with the compression force of a pestle struck by a mallet. The finely ground tissue was transferred to a Dounce homogenizer containing ice-cold RIPA homogenization buffer (10mM Tris-HCl pH 8.0, 1mM EDTA, 1% Triton X-100, 0.1% sodium deoxycholate, 0.1% SDS, 140mM NaCl)

with Roche cOmplete Ultra protease inhibitor and PhosSTOP phosphatase inhibitor tablets added prior to use. Supernatants were collected and protein concentration was determined by BCA protein assay (Thermo Scientific 23227). Equal amounts of protein (20 μg) were resolved by SDS–polyacrylamide gel electrophoresis (4 to 12% gel), and Western blot analysis was performed with protein/phosphoprotein-specific antibodies. Densitometry analysis was performed as previously described using ImageJ software.

Statistical methods

Rotarod performance, total body weight and fat mass normalized to body weight underwent statistical analysis testing for both between-groups and within-subjects effects. These tests included t-tests for independent groups, one-way and two-way ANOVAs for independent groups, and mixed two-way ANOVA with repeated measures. All tests were two-tailed and assumed equal variances with significance levels of $\alpha=0.05$. To examine possible interactions with age effects, data was grouped into juvenile (11-16 weeks of age) and adult (22-26 weeks of age) cohorts. All statistical analysis was performed using IBM SPSS Statistics 22 software.

RESULTS

High dose rapamycin treatment rescues SN dopaminergic neuron loss

Two to three weeks after acute MPTP (or saline) treatment, mice were sacrificed and midbrains tissue containing the SN was dissected and cryofixed. Midbrain sections were then immunostained for tyrosine hydroxylase (TH), an enzyme which catalyzes the rate limiting step in synthesis of dopamine[252]. Through qualitative analysis of TH immunostaining, we observed that acute MPTP treatment resulted in SN dopaminergic

neuron loss (Figure 4.1). Rapamycin appeared to at least partially rescue the neuron loss resulting from MPTP treatment.

Rapamycin abolishes hyperactive mTOR activity in MPTP-treated mice

Western blotting of whole brain lysates revealed that normalized protein levels of phosphorylated s6, an indicator of mTOR activity, were increased in M/V mice compared to S/V control group (Figure 4.2A and B). In contrast, M/R mice showed significantly reduced levels of phospho-s6 compared to both M/V and S/V groups.

MPTP treatment and age-dependent effects on rotarod performance

Analysis of rotarod performance following MPTP or saline treatment did not show a significant difference between groups, for either median, $F(2,29)=0.176$, $p=0.840$, or maximum, $F(2,29)=0.520$, $p=0.601$, latency times, (Figure 4.3A). Gross plotting suggests that acute MPTP insult may impair rotarod performance in relation to individual baseline latency times (Figure 4.3B); however, a within-subjects mixed ANOVA test did not show a significant interaction between treatment groups and testing days, $F(2,29)=0.313$, $p=0.735$. Post-hoc pairwise comparisons between groups also did not show any significant results.

We reasoned that differences in rotarod performance might be masked by age-dependent variability. Thus, we separated data into adult (22-26 week old) and juvenile (11-16 week old) cohorts. Independent samples t-test comparison of adult vehicle- and rapamycin-treated mice after acute MPTP insult approach significance for both median and maximum latency times, $t(8)=2.301$, $p=0.05$ and $t(8)=2.23$, $p=.052$, respectively (Figure 4.4A). In contrast, independent sample t-test comparison of vehicle- and

rapamycin-treated juvenile mice after MPTP was highly non-significant for median and maximum latency times, t(11)=0.428, 0.670 and t(11)=0.449, p=0.662, respectively (Figure 4.4B).

MPTP does not affect total weight or body mass composition

NDUFS4 KO mice show progressive loss total body weight and fat mass, effects that are partially rescued by rapamycin treatment[229]. We were interested in whether MPTP treatment might result in similar systemic effects on body mass composition. One-way ANOVA statistical test did not find any significant difference between treatment groups for either body weight or fat mass, F(2,29) = 0.248, p=0.781 and F(2,29) =0.268, p=0.767, respectively (Figure 5A and B). We then tested for whether different age groups might significantly interact with treatment type; however, two-way ANOVA did not show a significant interaction between these variables for fat mass, F(2,30)=0.220, p=0.804, or total body weight, F(2, 30)=0.237, p=.790 (Figure 4.6A and B).

DISCUSSION

Consistent with previous research, we found evidence that rapamycin treatment rescued MPTP-induced neural degeneration in the SN. Moreover, we found evidence for hyperactive mTOR signaling in whole brain of MPTP treated mice. Although there are many upstream or feedback components that might drive hyperactive mTOR signaling in PD models, the PI3K/Insulin signaling pathway may be of particular interest. Incidence of PD is associated with insulin resistance and high rates of type II diabetes[253]. Adult mice that develop obesity and insulin resistance as a result of high

fat diet show exacerbated effects of SN dopaminergic neurodegeneration after exposure to MPTP[254]. Aberrant insulin signaling could potentially correlate with sustained activation of the PI3-K/Akt/mTOR pathway, similar to what has been found in brains of patients with Alzheimer's disease[131]. Although insulin and IGF-1 bind to receptors and activate mTOR signaling downstream, an elegant feedback system is in place by which mTOR directly phosphorylates the insulin receptor, leading to its in internalization; this, in turn, shuts off its insulin-related activity. Chronic mTOR activity disrupts this feedback pathway, leading to insulin resistance. Insulin has been shown to regulate dopamine transporter mRNA in SN and brain dopamine concentration in rats[255]. Thus, chronic mTOR activation might indirectly influence dopamine levels through a mechanism of insulin resistance.

Perhaps our most surprising result was the lack of an obvious impairment in rotarod performance following MPTP exposure. Previous research utilizing the rotarod as a behavioral test for MPTP exposure has yielded mixed results[256]. We believe that age-dependent factors could account for high amount of variability among our treatment groups. The adult subset of mice showed impairment on rotarod performance as a result of MPTP exposure, and effect that appeared to be partially rescued by rapamycin treatment. Although juvenile mice 8-10 week olds have been widely used for MPTP experiments in order to improve survival rates[257], previous research has shown that 21-month old mice show more severe behavioral deficits in response to MPTP compared to 3-month old young mice[258]. In addition to neurodegeneration in the SN, 21-month old mice exposed to MPTP also showed loss of dopaminergic cell bodies in the locus coeruleus and ventral tegmental area regions of the brain. Furthermore, it has been

reported that old mice aged 9-12 months show more dramatic dopaminergic neuron loss in the SN than 3 month old young mice, correlated with prolonged microglial activation[259]. Thus, we believe that future experiments in fully developed adults or aged mouse cohorts could reduce variability, improve statistical power, and have more salient interpretations for the highly age-dependent incidence of PD in humans.

A mere dose-dependent effect could also possibly explain the high amount of variability in our behavioral results. The total amount of MPTP administered to each mouse was based on individual body weight. Our adult cohort of mice weighed, on average, 3 grams more than the juvenile cohort of mice upon receiving MPTP treatment, and thus received more total amount of drug. It is possible that a "threshold" dosage of total MPTP is required to induce the amount of SN dopaminergic neuron loss that would result in a robust behavioral phenotype.

Our previous work in the NUDFS4 KO mouse supports a model in which rescued metabolic function, but not autophagy, mediates the therapeutic effects of rapamycin in neural pathology resulting from complex I inhibition. Specifically, rapamycin induces a metabolic shift toward amino acid catabolism and away from glycolysis, alleviating the buildup of glycolytic intermediates. This metabolic shift may be reflected by alterations in body composition in NDUFS4 KO mice, which show a progressive loss of fat mass that could be rescued by rapamycin treatment. Although we found evidence for increased autophagy NDUFS4 KO mice in both brain and liver as a result of rapamycin treatment, we did not find a corresponding rescue of complex I activity or assembly that would result from removal of dysfunctional mitochondrial components.

Our current data suggests that systemic effects of complex I inhibition differ in MPTP treated mice compared to what we previously found in NDUFS4 KO mice. Measurements of total weight and fat mass were not significantly different across treatment groups. The data indicate that MPTP does not induce any major alterations in physiological state that would echo the aberrant metabolic phenotype found in NDUFS4 KO mice. Effects of Complex I deficiency on body weight and composition may be a developmental feature unique to NDUFS4 KO mice. Alternatively, it is possible that assessment of body weight and fat mass at a later timepoint after MPTP exposure would reveal significant effects. It is also possible that alterations in body composition is independent of whole brain metabolism in NDUFS4 KO mice; thus future metabolomic analysis of whole brain lysates from mice exposed to MPTP may help to determine whether this is indeed the case.

Body weight and fat mass appeared to be reduced in M/R mice compared to either S/V or M/V groups. A significant caveat to this observation, however, is that the data does not include a fourth Saline/Rapamycin (S/R) treatment group; thus, whether rapamycin-induced weight loss is the result of an interaction with MPTP treatment cannot be determined at this time. We did not test for indicators of autophagy or complex I activity in this particular set of experiments, so it is possible that rapamycin-induced autophagy may at least partially contribute to dopaminergic neuron rescue. Furthermore, it should be noted that these results are preliminary and larger sample sizes are needed in order to confirm these observations.

In summary, it appears that either genetic or pharmacological inhibition of Complex I activity in NDUFS4 KO and MPTP mouse models, respectively, leads to a

sustained increase in mTOR activity. Similar mechanisms of upstream regulation of mTOR such as PI3K/insulin signaling may overlap between these models. Interestingly, our previous work showed increased phosphorylation of insulin-like growth factor (IGF-1) in NDUFS4 KO mice, a phenotype which could be rescued by rapamycin treatment. Downstream effects of mTOR hyperactivity on metabolism and physiology, however, may be distinct between NDUFS4 KO and MPTP mice, as the differences in our body mass composition data suggest. Specific downstream components of mTOR activity that are differentially activated during development versus adulthood could also help to explain why complex I inhibition might affect distinct neuronal populations in these models.

CHAPTER 5

Conclusions and future work

The research presented in this dissertation provides a comparative framework for understanding the mechanisms of rapamycin in treatment in neurological disease. A model in which "one mechanism fits all" is largely ignorant of the complex cellular functions regulated by mTOR activity. Previous reports have implicated autophagy, in particular, as a common mechanism of rapamycin-induced neuroprotection against a broad spectrum of neurodegenerative diseases, although conflicting reports have also challenged this view. It is possible that observations of rapamycin-induced autophagy and neuroprotection in *in vivo* models represent a correlative, rather than causal relationship, as was described in Chapter 2. Furthermore, most data pertaining to autophagy are difficult to interpret, as autophagy can result in either increased or decreased autophagosome numbers based on the rate of autophagic flux and turnover.

Systematic testing and comparison of potential mechanisms of mTOR inhibition in models of neurological disease can identify both distinct and overlapping components to inform the development of targeted therapies. Furthermore, dose dependent effects of chronic rapamycin treatment should also be tested. This is especially important for systemic treatment, in which high circulating blood levels of rapamycin are required for penetration of the drug through the blood-brain barrier.

It should also be noted that the clinical implications for high dose rapamycin treatment in diseased patients may be limited by its potential side effects. Rapamycin has already been FDA-approved for its immunosuppressive effects in prevention of kidney transplant rejection, its anti-tumoregenic effects in several types of cancers, and

a wide variety of other clinical uses[1,260]. Side effects such as hyperlipidemia, hyperglycemia, anemia and reduced wound healing have been reported by patients[1,261] Furthermore, the involvement of mTOR activity in supporting normal brain function should be considered. Whereas acute rapamycin treatment may impair formation of long-term memory, chronic rapamycin treatment has been shown to reduce both age-related and disease-related cognitive defects. Thus, specific treatment paradigms may have beneficial effects in some contexts, and detrimental effects in others.

A major goal of future work to expand upon the studies presented here would be to identify how mTOR activity and the neuronal pathology resulting from deficiency in complex I are linked. I am particularly interested to know whether upstream regulation of mTOR by insulin signaling might influence the susceptibility of neurons to damage as a result of complex I deficiency. One experiment to test this possibility would be to induce insulin resistance in mice through sucrose treatment prior to MPTP exposure, a similar paradigm to that of a previous study by the Oddo group in 3xTg AD mice[133]. Furthermore, proposed mechanisms of rapamycin-induced neuroprotection in NDUFS4 KO and MPTP-treated mice should be further tested in *in vitro* models of cultured neural cells.

In addition, the question as to whether rapamycin can halt or reverse disease progression has critical relevance for neurological disease patients, as most individuals are diagnosed after the appearance of debilitating symptoms. Experiments to investigate whether rapamycin can improve survival in NDUFS4 KO mice after the onset of disease symptoms at approximately 35 days of age are currently under way,

and our preliminary results suggest that delayed rapamycin treatment is also effective at extending lifespan in these animals. Future work in this and other models of neurological diseases should further investigate the relative contribution of reparative versus preventative cellular processes in mediating the therapeutic effectiveness of mTOR inhibition.

FIGURES

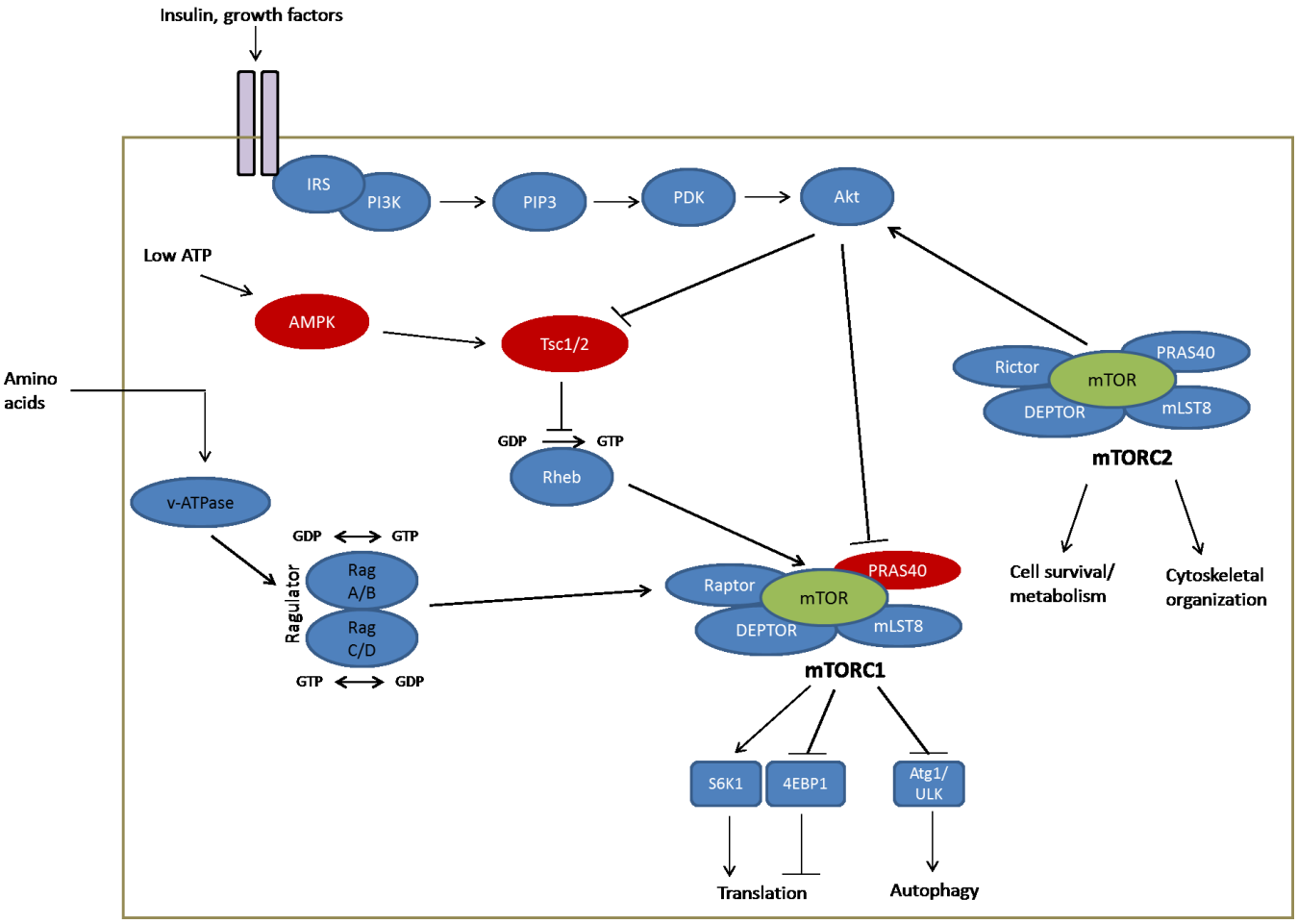

Figure 1.1. Simplified model of the mTOR signaling network. mTOR is assembled into two discrete complexes, rapamycin-sensitive mTORC1 and rapamycin-insensitive mTORC2. Extracellular signals such as nutrients, growth factors or cytokines determine activation of mTORC1, which in turn regulates reciprocal mechanisms of protein translation or autophagy. Intracellular signals such as levels of ATP also regulate mTORC1 activity; low levels of ATP are sensed by AMPK, an inhibitor of mTORC1. mTORC2 activity phosphorylates Akt, and thus indirectly inhibits mTORC1.

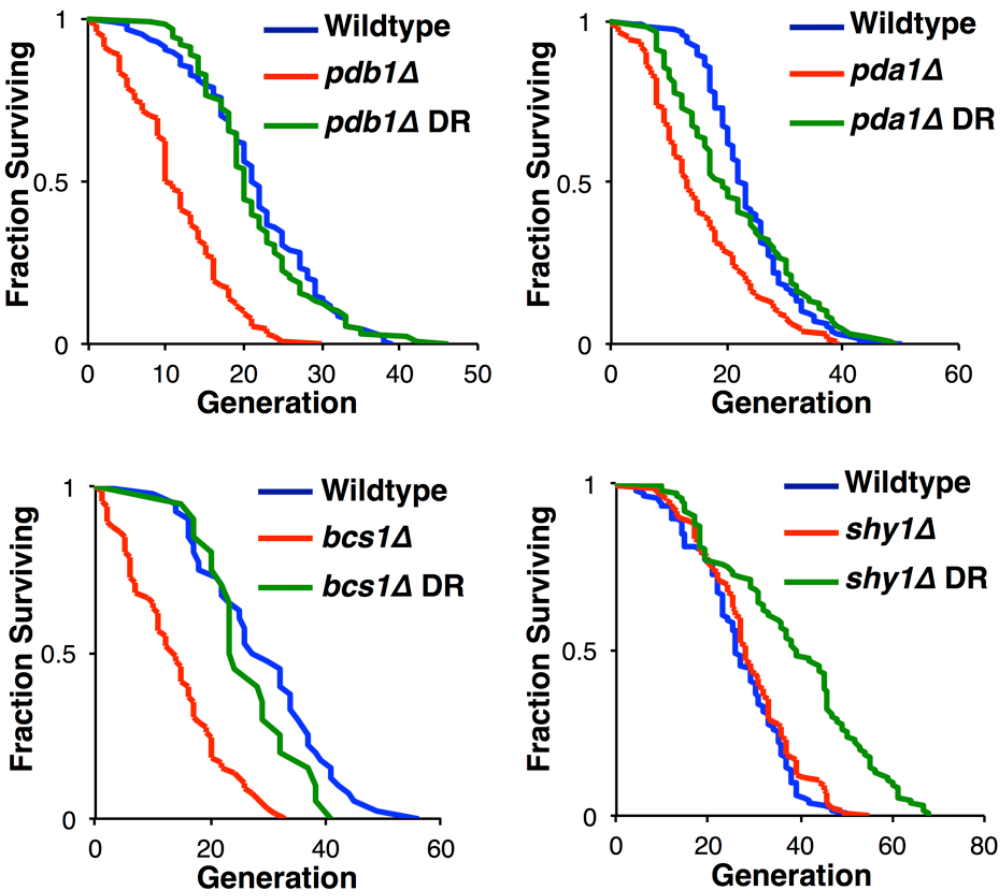

Figure 2.1. Glucose Restriction Extends the Replicative Lifespan of Leigh Syndrome Homolog Mutants in Yeast. Glucose restriction at 0.05% extends the replicative lifespan of *pdb1Δ*, *pda1Δ, bcs1Δ*, and *shy1Δ* cells. *pdb1Δ*, *pda1Δ, bcs1Δ* are short-lived compared to WT cells on regular media (2% glucose) while *shy1Δ* cells have a WT lifespan on regular media. Each plot shows experiment-

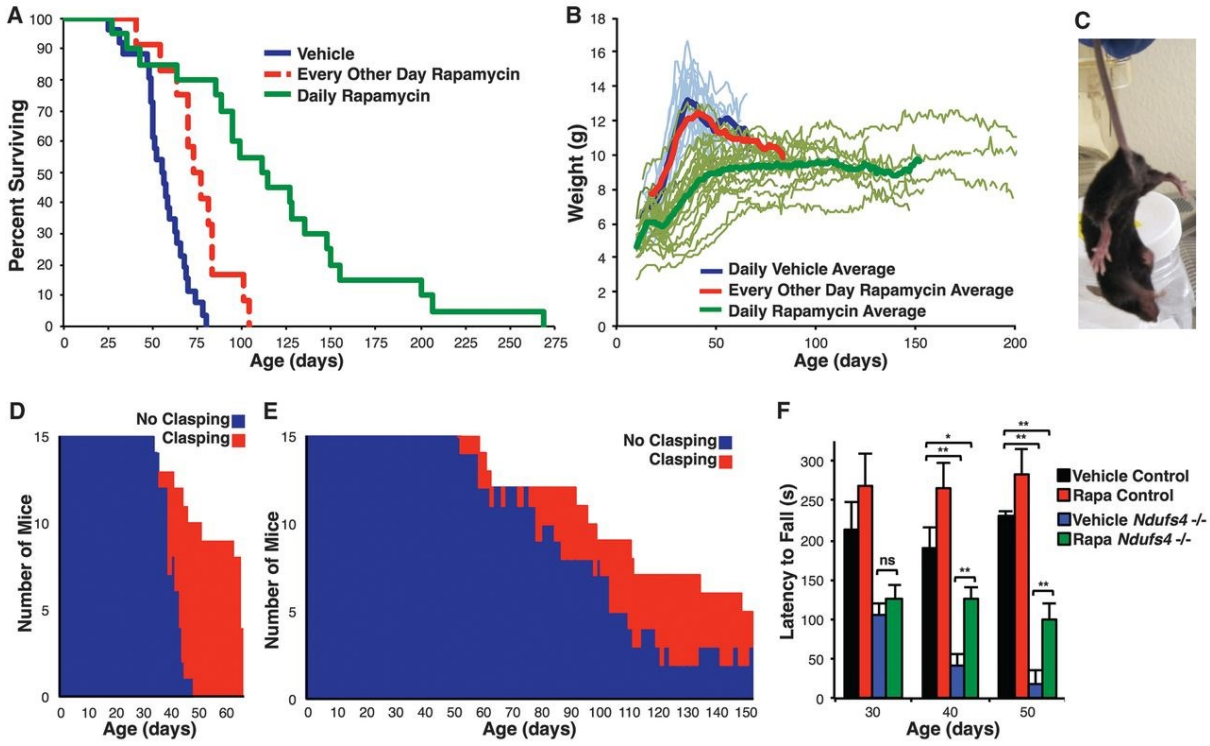

Figure 2.2. Reduced mTOR signaling improves health and survival in a mouse model of Leigh syndrome. (A) Survival of the *Ndufs4*$^{-/-}$ mice was significantly extended by rapamycin injection every other day; life span more than doubled with daily rapamycin treatment (log-rank $P = 0.0002$ and $P < 0.0001$, respectively). (B) Body weight plots of *Ndufs4*$^{-/-}$ mice. (C) Representative forelimb clasping behavior, a widely used sign of neurological degeneration. Clasping involves an inward curling of the spine and a retraction of forelimbs (shown here) or all limbs toward the midline of the body. (D and E) Clasping in vehicle-treated (D) and daily rapamycin-treated (E) *Ndufs4*$^{-/-}$ mice as a function of age. A total of 15 mice were observed for clasping daily for each treatment. Age of onset of clasping behavior is significantly delayed in rapamycin-treated mice (**$P < 0.001$ by log-rank test). (F) *Ndufs4*$^{-/-}$ mice show a progressive decline in rotarod performance that is rescued by rapamycin (*$P < 0.05$, **$P < 0.005$, Student's *t* test; error bars are ±SEM). (See also fig. S5, which indicates replicate numbers)

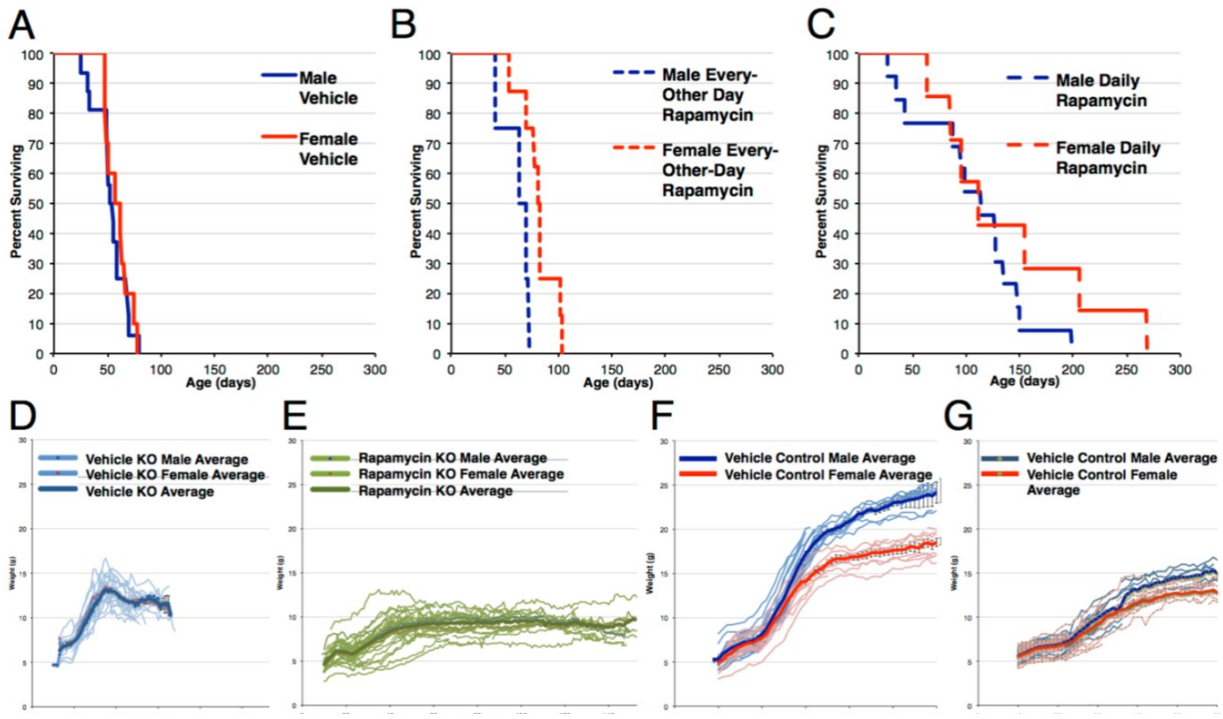

Figure 2.3. Lifespan and weight tracking data split by gender. (A) Vehicle treated Ndufs4 -/- mouse lifespan split by gender (n=16 and 10 for males and females, respectively). (B) Every-other-day rapamycin injected Ndufs4 -/- mouse lifespan split by gender (n=4 and 8 for males and females, respectively). (C) Daily rapamycin injected Ndufs4 -/- mouse lifespan split by gender (n= 13 an 7 for males and females, respectively). (D-G) Weight tracking of vehicle treated Ndufs4 -/- (E), daily rapamycin treated Ndufs4 -/- (F), vehicle treated control (G), and daily rapamycin treated control mice.

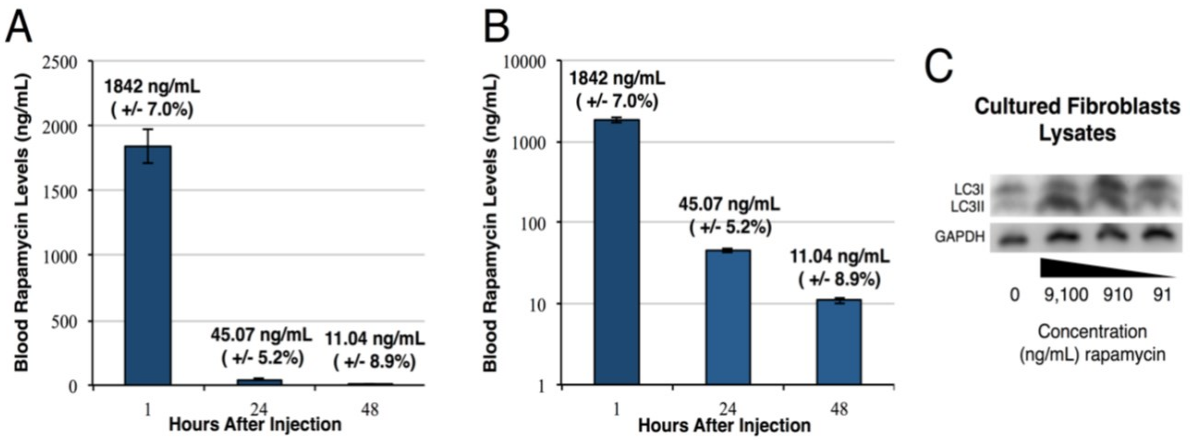

Figure 2.4. Blood levels of rapamycin following injection of 8mg/kg. (A-B) Analysis of blood levels of rapamycin show a rapid decrease in blood levels by 24 hours post-injection (shown in linear (A) and log (B) scale). (C) Western blotting for LC3, a marker of mTOR inhibition, treated with rapamycin for 6 hours suggests that levels of rapamycin in mice at 24 hours post-injection are below levels necessary to induce pathways downstream of mTOR. Error bars represent +/- standard error of the mean (SEM), n=3 animals per data point.

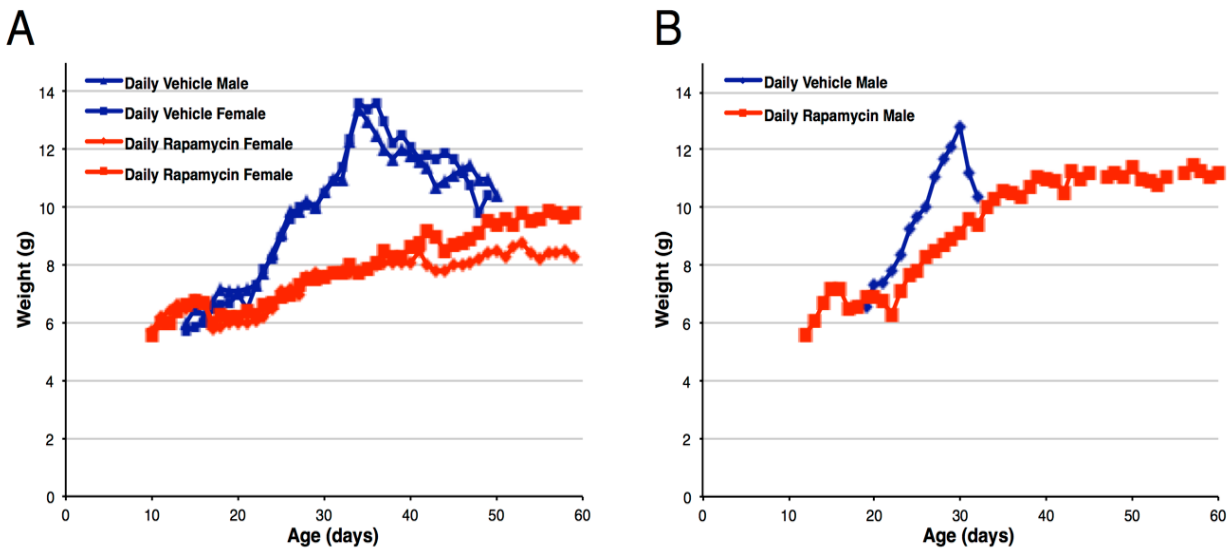

Figure 2.5. Daily rapamycin injection effect highly reproducible even among mice within the same litter. (A-B) Two representative litters where pups were randomly assigned to vehicle or rapamycin treatment. In both litters the rapamycin response was robust. Response was also gender independent at this dose (see also Figure 2.3).

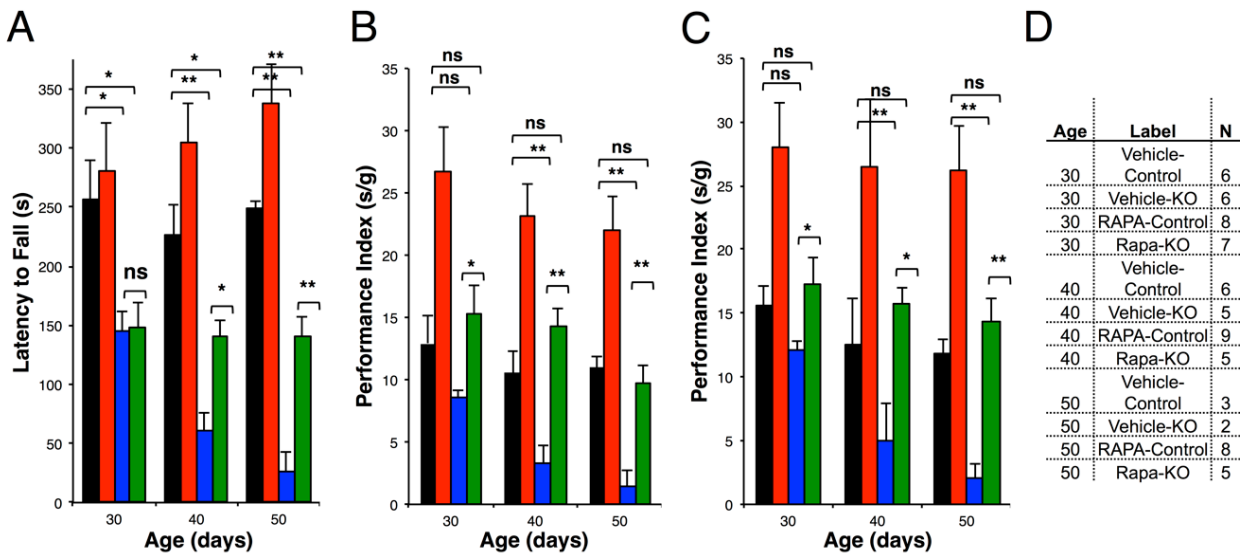

Age	Label	N
30	Vehicle-Control	6
30	Vehicle-KO	6
30	RAPA-Control	8
30	Rapa-KO	7
40	Vehicle-Control	6
40	Vehicle-KO	5
40	RAPA-Control	9
40	Rapa-KO	5
50	Vehicle-Control	3
50	Vehicle-KO	2
50	RAPA-Control	8
50	Rapa-KO	5

Figure 2.6. Additional Rotarod Data. (A) Maximum latency to fall. (B) Weight-normalized medianlatency to fall (see Figure 1 for raw median latency to fall data). (C) Weight-normalized maximum latency to fall. (D) Number of mice assayed for each condition.

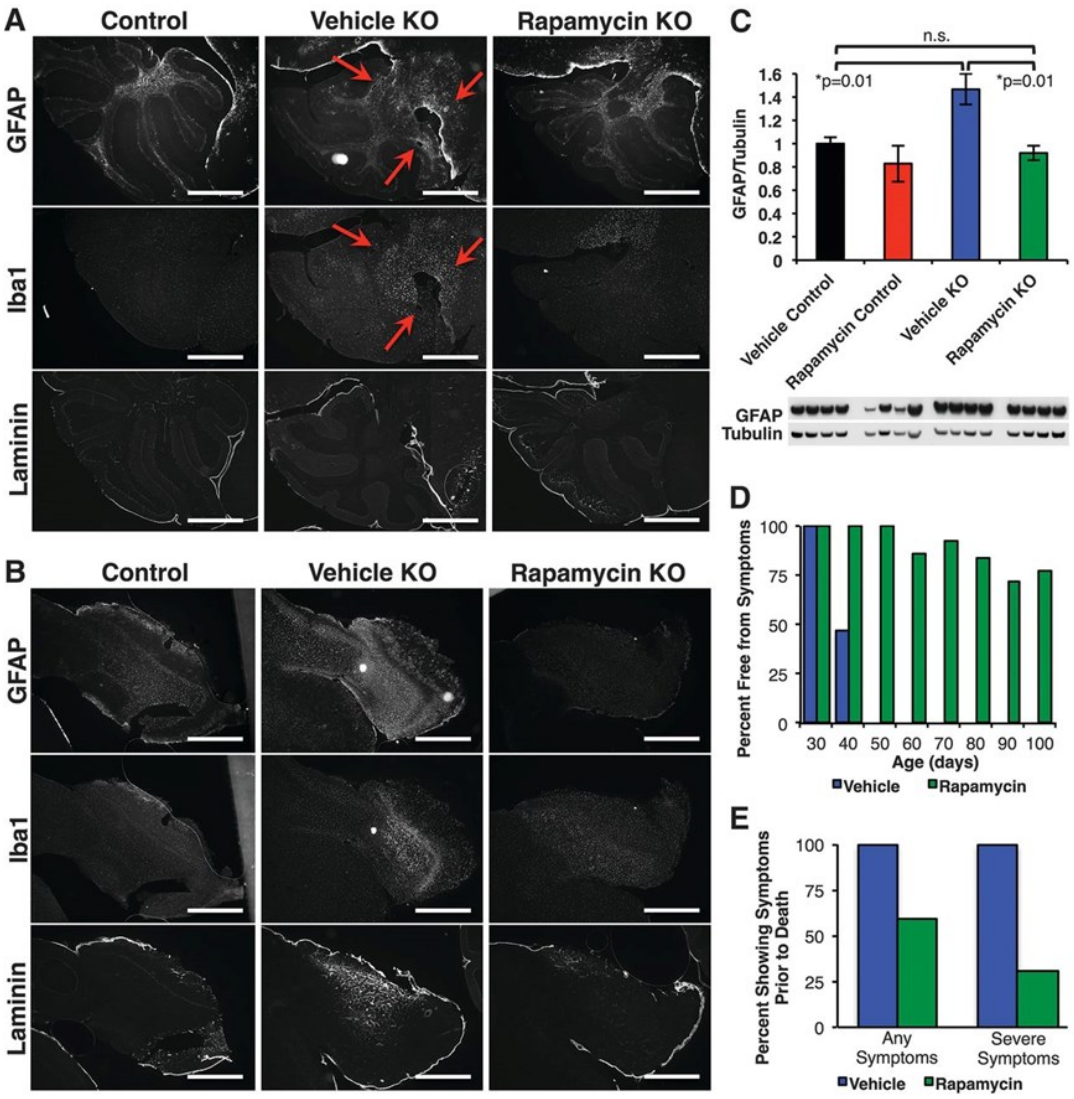

Fig. 2.7 Rapamycin reduces neurological disease *in Ndufs4*$^{-/-}$ mice. (A) Representative cerebellar staining for neurological lesions in 55- to 60-day-old mice. All vehicle-treated mice showed glial activation and lesions at this age, whereas lesions were not detected in age-matched daily rapamycin-treated mice (n = 6; scale bars, ~500 μm) (see also figs. S6 and S7). (B) Representative olfactory bulb staining shows activation of glia by GFAP staining and neovascularization by laminin staining in vehicle-treated knockout (KO) mice and a robust attenuation in rapamycin-treated KO mice (n = 6 per treatment; scale bars, ~500 μm). (C) Western blotting of whole-brain lysates from a separate cohort of mice shows increased GFAP in vehicle KO mice and rescue to control levels by rapamycin (*P < 0.05, Student's t test; error bars are ±SEM). (D and E) The percentage of living mice showing neurological symptoms is greatly reduced by daily rapamycin treatment (D), as is the number of mice showing neurological symptoms at the time of death (E).

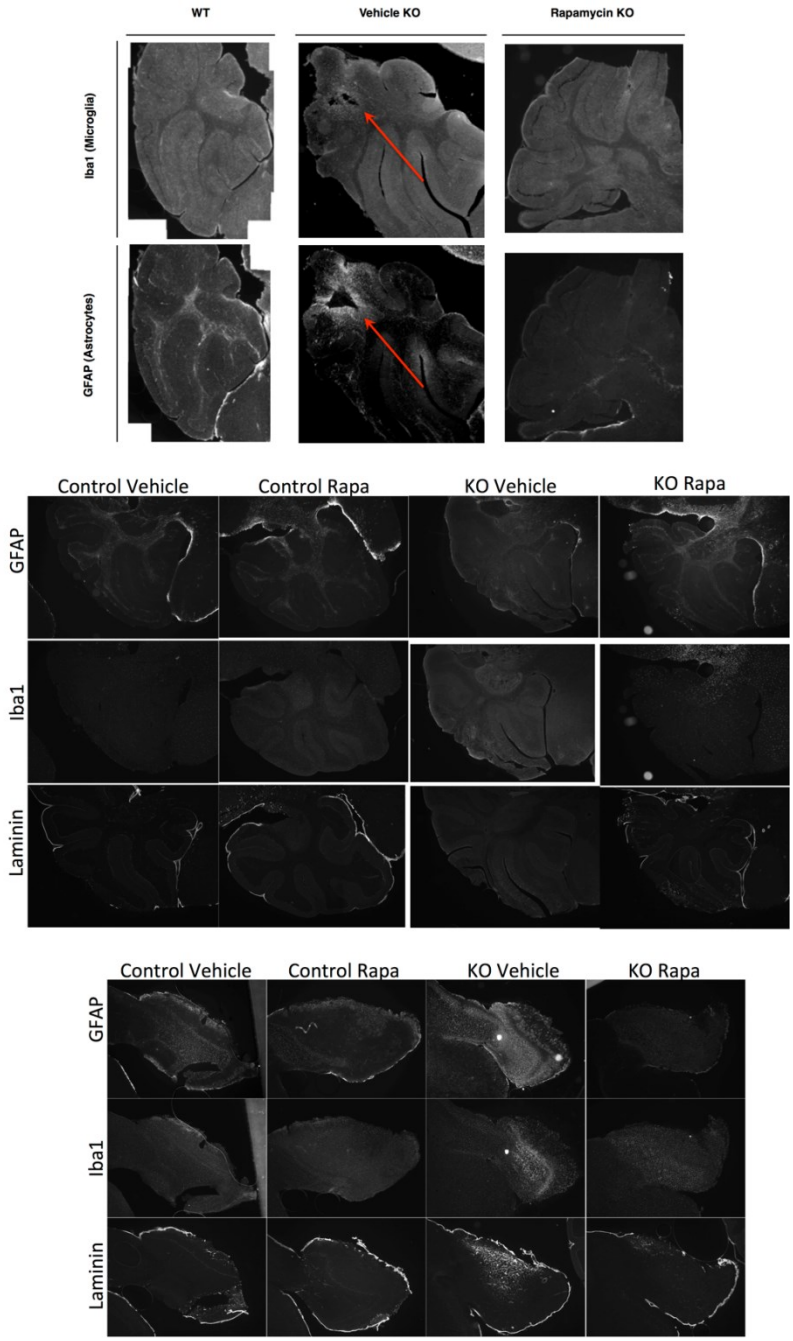

Figure 2.8. Additional Histology Images. (Top two panels) Additional age-matched samples showing rescue of lesions in the cerebellum by rapamycin. (Bottom panels) Rapamycin has no overt effects on staining pattern or intensity in control animals.

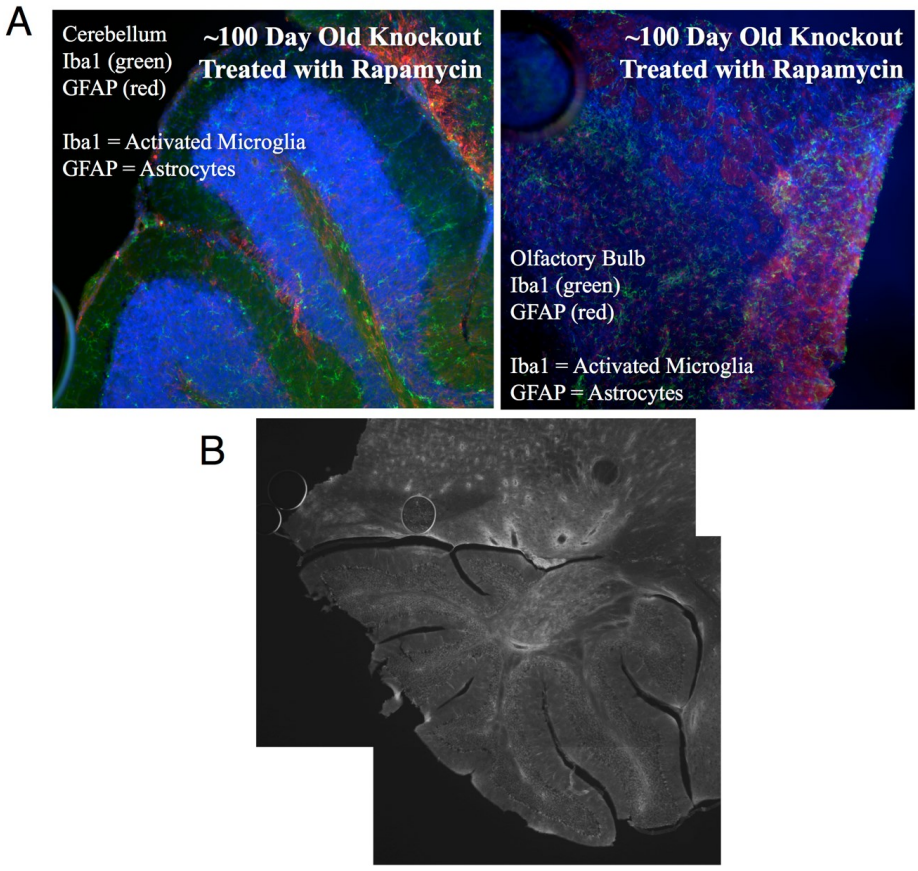

Figure 2.9. Absence of Overt Lesions in Brains from Very Long-Lived Rapamycin Treated Knockout Animals. Brains from two very long-lived rapamycin treated knockout mice found dead in cage (FDIC) were removed from the corpse, fixed, stained, and imaged. The quality of stain and imaging is limited by the post-mortem condition, however in each of these cases there were no apparent lesions present at time of death. (A) A brain from an FDIC 100 day old rapamycin treated KO stained with Iba1 (green), GFAP (red), and DAPI (blue). (B) A brain from a 268 day old animal stained with Laminin. Compare to the overt lesions in Figure 2.8. .

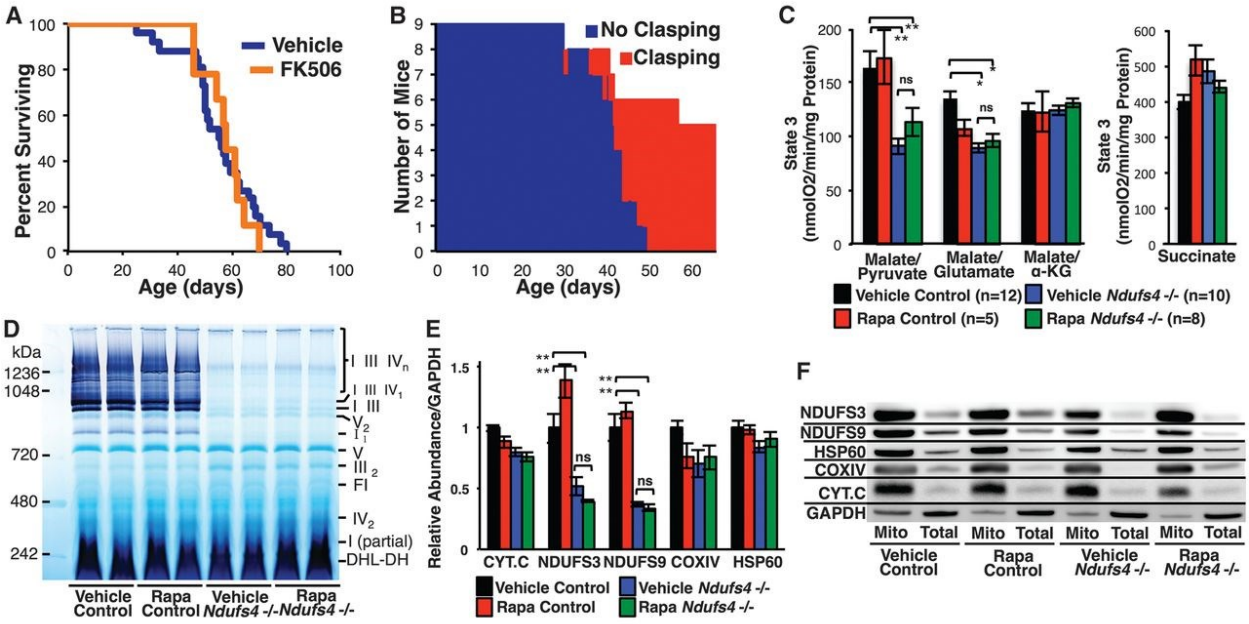

Figure 2.10 Rapamycin does not substantially alter mitochondrial function or complex I assembly. (A and B) FK-506 delivered at the highest tolerated dose (see fig. S8) failed to enhance survival (A) or attenuate disease (B) in*Ndufs4*$^{-/-}$ mice. (C) Rapamycin has no observed effect on respiratory activity or complex I deficiency of mitochondria isolated from ~50-day-old *Ndufs4*$^{-/-}$ mice; *n* = 4 to 6 mice per data point. (see also fig. S10). (D) Native-in-gel activity assays reveal that rapamycin does not influence assembly or stability of complex I (see also fig. S11). (E and F) Complex I subunits (NDUFS3 and NDUFS9) are significantly reduced in *Ndufs4*$^{-/-}$ mice, and rapamycin has no effect on their total levels (F) or subcellular localization (E) in brain. Levels of other mitochondrial proteins (cytochrome c, the complex IV subunit COXIV, and HSP60) are independent of both *Ndufs4* genotype and treatment (see also fig. S9). **P* < 0.05,***P* < 0.005, Student's *t* test; ns, not significant. Error bars are ±SEM. neurological symptoms at the time of death (E).

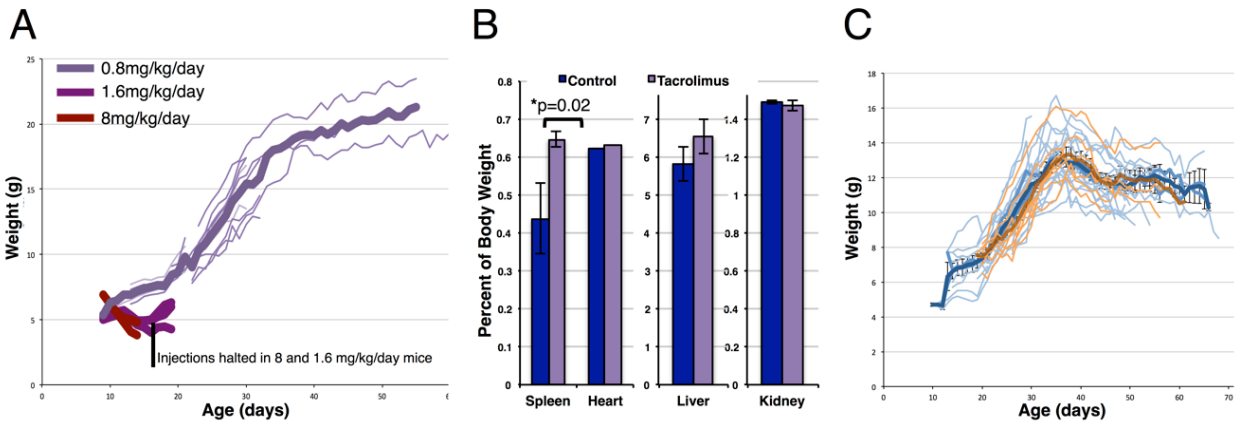

Figure 2.11. Highest tolerable dose of tacrolimus (FK-506) determined in control mice. (A) Initial dose of 8 and 1.6 mg/kg/day were not tolerated by control mice as determined by weight loss during treatment. 0.8 mg/kg/day was tolerated and induced splenomegaly at 30 days (B). (C) Tacrolimus also had no effect on the weight phenotype of Ndufs4 -/- mice. Error bars represent +/- SEM, p-value determined using students t-test, n=4 per data point.

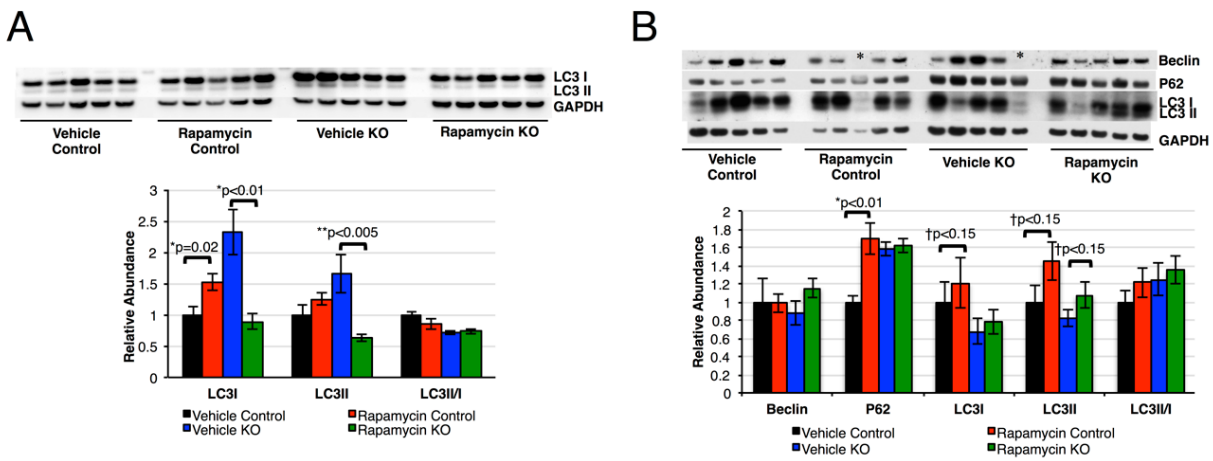

Figure 2.12. Daily rapamycin increases activation of autophagy in brain and liver. (A) LC3 isincreased in the brains of rapamycin treated control animals. *Ndufs4 -/-* animals show an accumulation of LC3I and II, as has been observed in models associated with overactive mTOR, while rapamycin rescues LC3I and II to WT levels. No significant changes in LC3II/I ratio were observed in brain. (B) Liver homogenates from rapamycin treated animals show increases in P62 and LC3 and a trend toward increases in LC3I and LC3II. Outliers in the Beclin blot are denoted with (*) and were excluded from the analysis, though changes were non-significant regardless of their inclusion. All values were normalized to GAPDH to account for variation in loading, with the exception of LC3II/I ratios. Error bars represent +/- SEM, p-values calculated using students t-test.

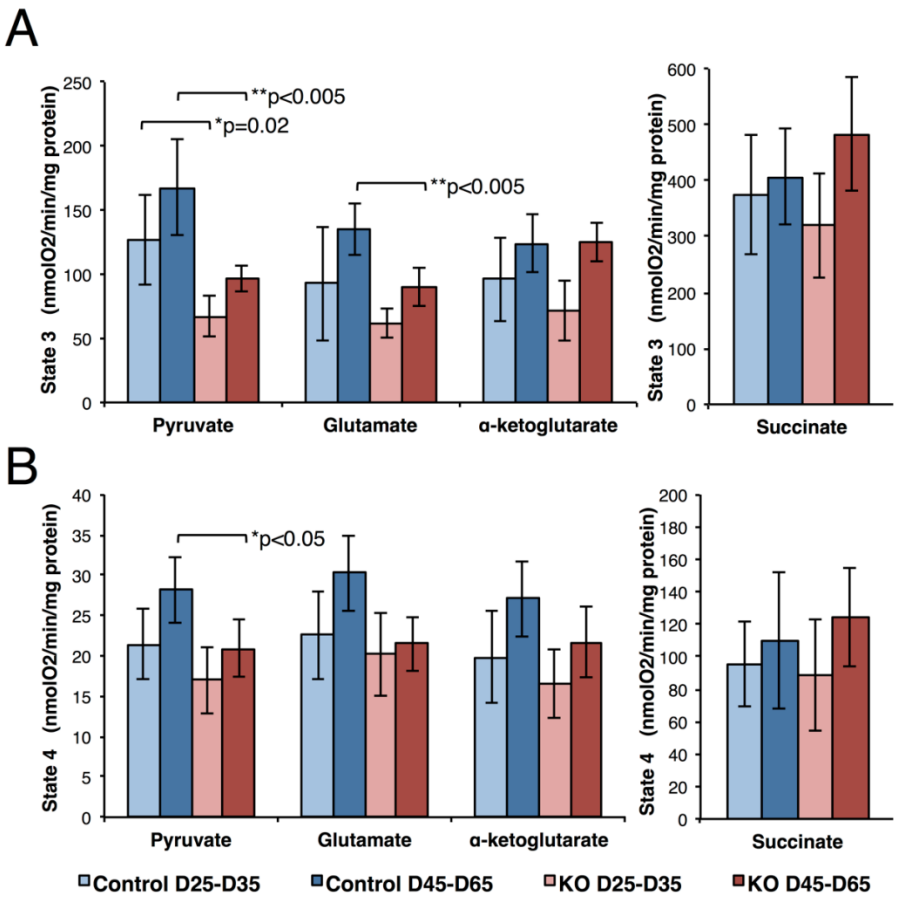

Figure 2.13. State 3 and state 4 defects in complex I driven respiration in *Ndufs4 -/-* mice. Complex I deficiency was similar when analyzed by state 3 (A) or state 4 (B), althoughthe state 3 deficiency appeared slightly more pronounced. Mitochondrial respiration through complex I appeared to increase with age but pyruvate and glutamate drivenrespiration were deficient at each age. Malate provided with each complex I substrate indicated. α–dicated. ient and succinate driven respiration were not effected by NDUFS4 deficiency. Error bars represent +/- SEM, p-values calculated using students t-test, n=4-6 animals per datapoint.

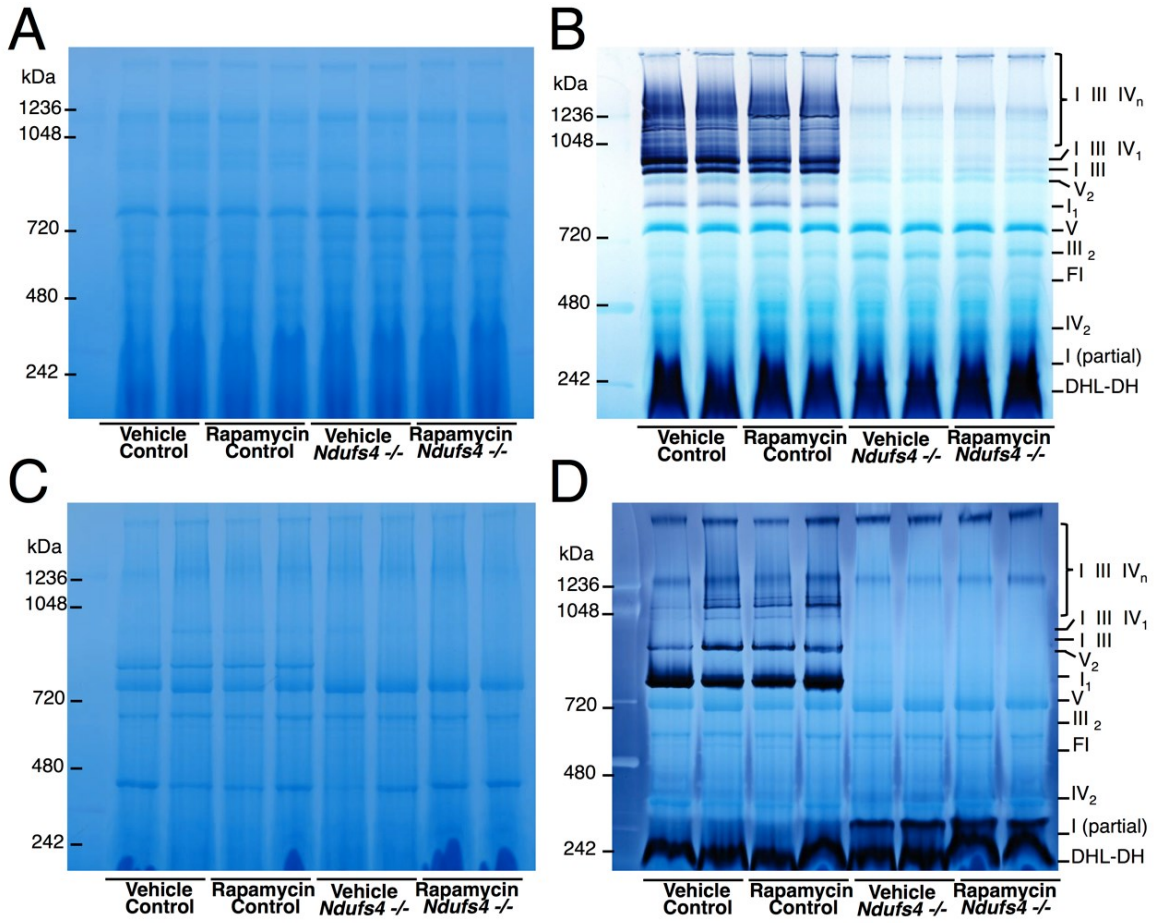

Figure 2.14. Additional blue-native in gel activity assay data. Isolated brain mitochondria were analyzed by blue native gel (A,C) and stained using in gel staining for complex I activity (B,D). A mild, non-ionic detergent (digitonin) was used to analyze supercomplex formation (A-B), while a stronger detergent (Triton X-100) was used to analyze free complex I. The *Ndufs4 -/-* mice had deficient complex I assembly and supercomplex incorporation and rapamycin had no effect on these features.

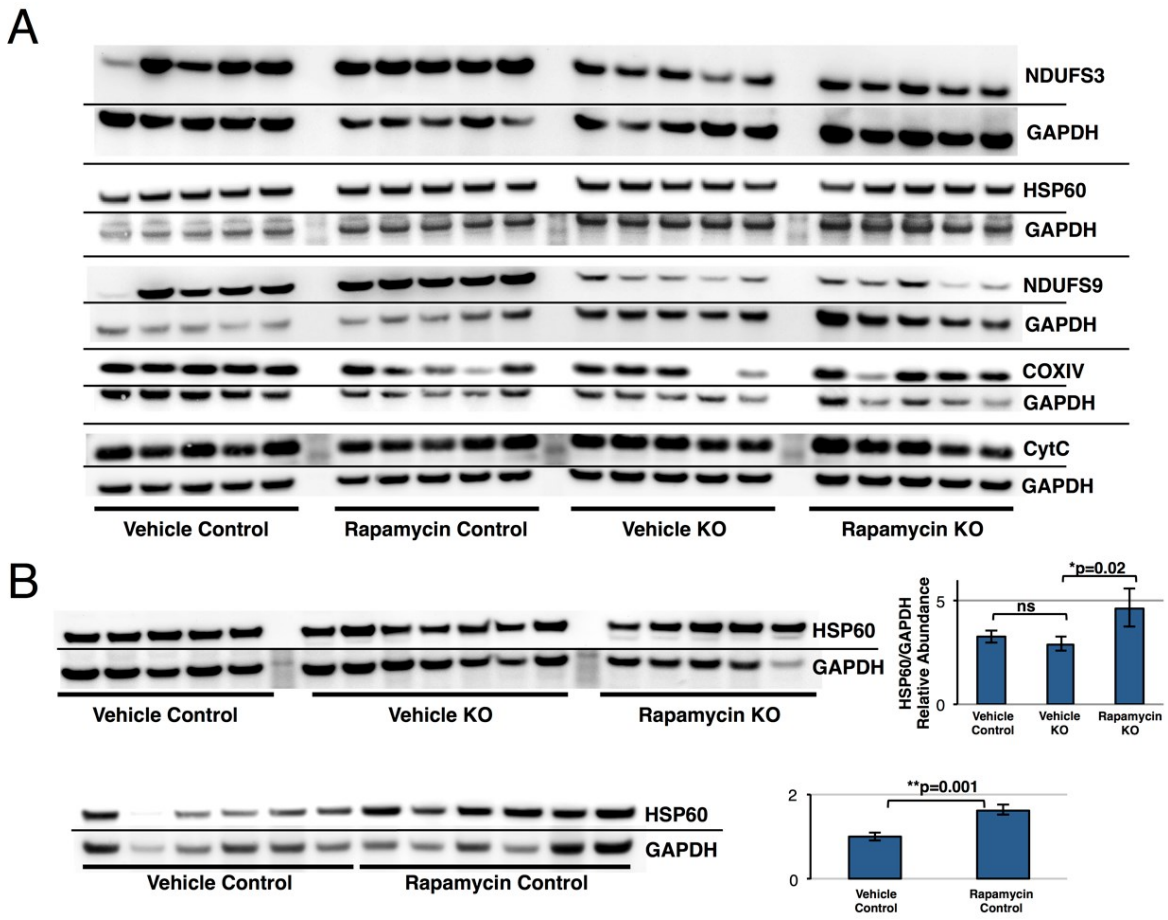

Figure 2.15. Additional western blot data. (A) Western blots of whole-brain lysates corresponding to Figure 2.10. (B) HSP60 is induced in liver by rapamycin but is not induced in the *Ndufs4 -/-* mice without treatment. Error bars represent +/- SEM, p-values calculated using students t-test.

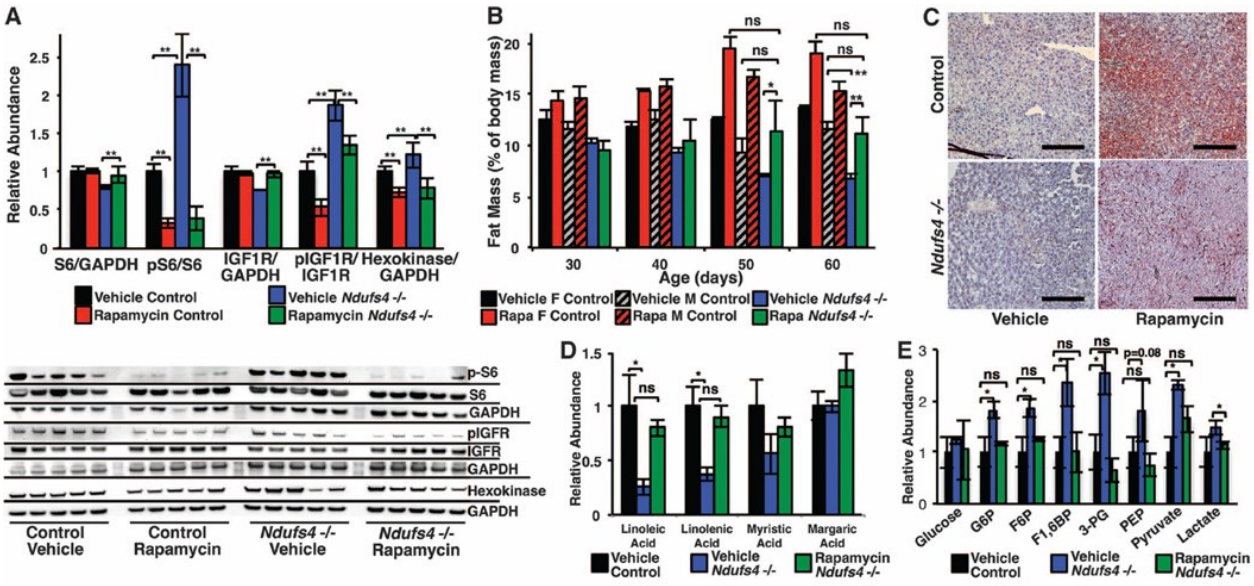

Figure 2.16. Ndufs4–/– mice exhibit mTOR activation and metabolic defects that are suppressed by rapamycin. (A) mTOR activity, as indicated by phosphorylation of S6, is increased in Ndufs4–/– mouse brain. Total IGF1R and S6 are decreased in Ndufs4–/– mice, suggesting feedback inhibition from chronic mTOR activation. Rapamycin potently inhibits phosphorylation of S6 and rescues levels of IGF1R and S6. (B) Total body fat progressively decreases in Ndufs4–/– mice but is maintained in rapamycin-treatedmice. Fatmass differs by sex in control but not Ndufs4–/– mice (n = 4 to 6 mice per data point). (C and D) Liver fat droplets are deficient in vehicle-treated Ndufs4–/– mice and partially rescued by rapamycin (representative images, n > 6 stained per treatment; scale bar, ~100 mm) (C), as are free fatty acids detected by metabolomics (D) (n = 4 per treatment). (E) Accumulation of glycolytic intermediates in Ndufs4–/– brain is suppressed by rapamycin (n = 4 per treatment) (see fig. S14 and tables S1 to S3). *P < 0.05, **P < 0.005, Student's t test; error bars are TSEM.

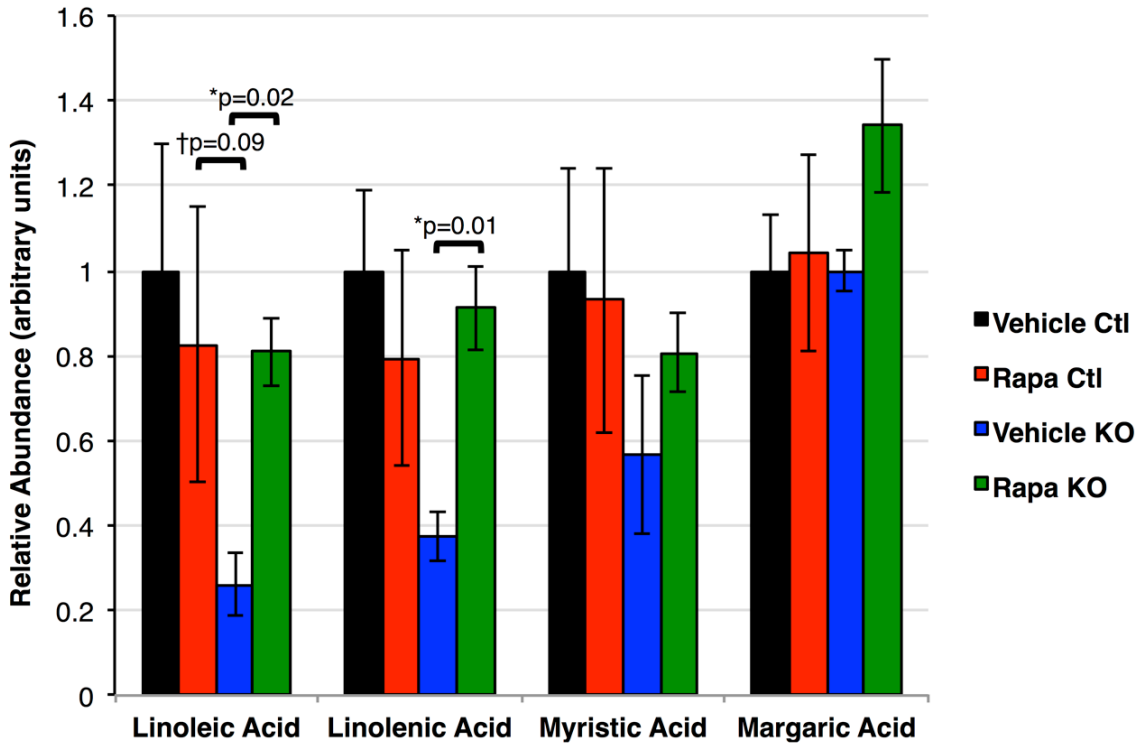

Figure 2.17. Free fatty acids in liver detected by metabolomics. Free fatty acids are low in *Ndufs4 -/-* animal liver and rescued by rapamycin. Error bars represent +/- SEM, p-values calculated using students t-test. n = 4 animals per treatment.

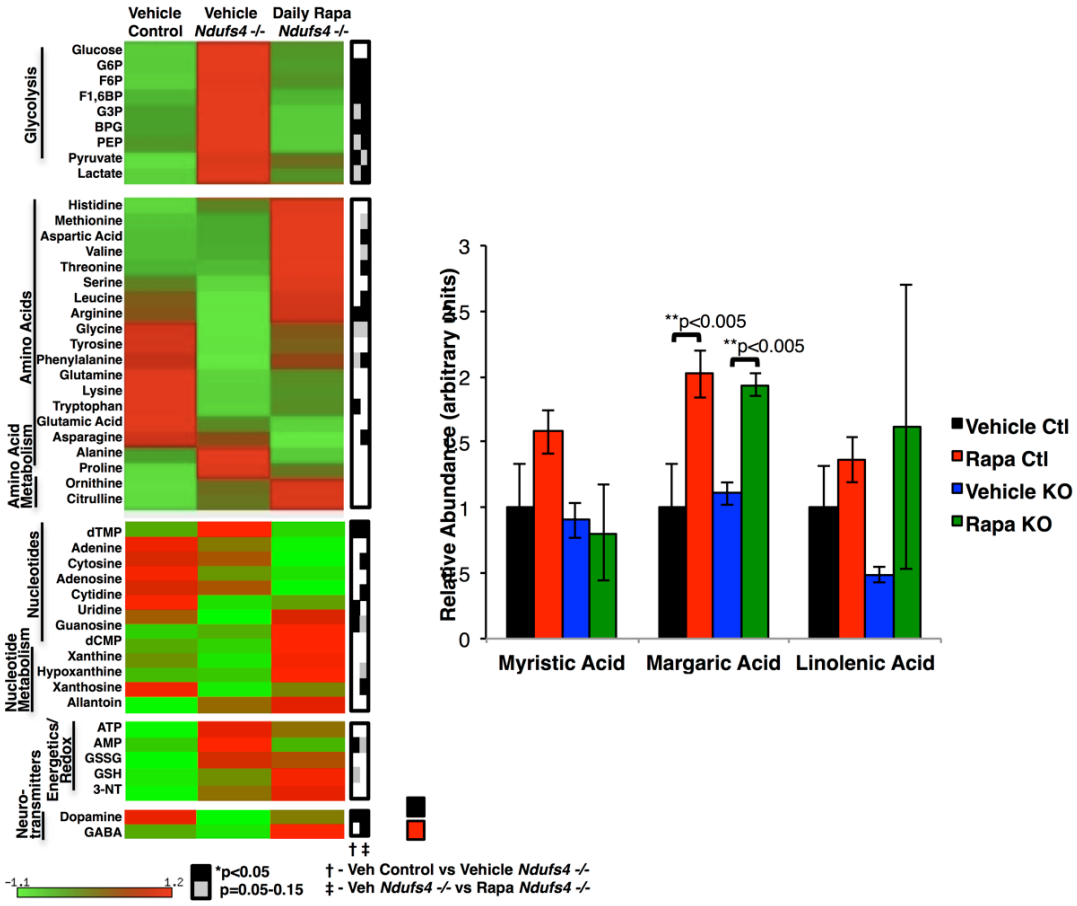

Figure 2.18. Metabolic profiling of *Ndufs4 -/-* brains. Metabolomic analysis of *Ndufs4 -/-* mouse brains revealed an accumulation of glycolytic intermediates that is rescued by rapamycin. Rapamycin treatment also increases levels of free-amino acids and free-fatty acids, overall consistent with a shift from glycolysis to amino acid and fat catabolism pathways. The effects of rapamycin on KO animals is distinct from those on control animals and the effects on control mice are not intuitively informative in the setting of the KO animals and will require further study (See also **Supplemental Table 1** for data, statistics, and rapamycin treated control mouse data). Error bars represent +/- SEM, p-values calculated using students t-test. n = 4 animals per treatment.

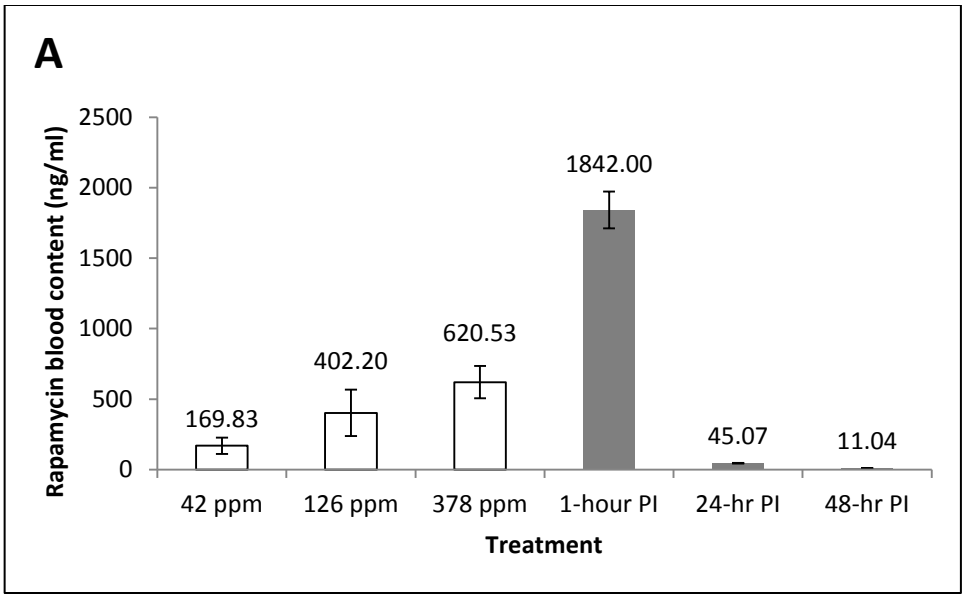

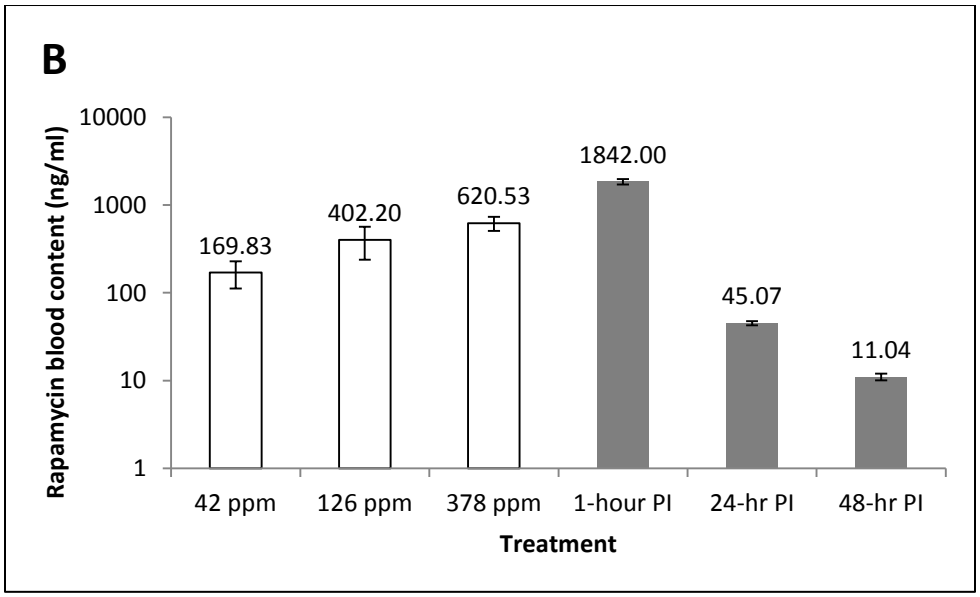

Figure 3.1. Levels of rapamycin in the blood as a result of dietary treatment. Blood levels were collected from mice fed 42 ppm, 126 ppm or 378 ppm of encapsulated rapamycin, or 3, 9 and 27 times the rapamycin dosage previously used by the Interventions Testing Program(ITP), respectively. Blood level measurements are represented on both linear (A) and logarithmic (B) scales. Open columns represent dietary rapamycin dosages, whereas filled columns represent post-injection (PI) blood levels at varying time points after 8 mg/kg rapamycin injection. N=3 to 7 mice per group, error bars represent SEM.

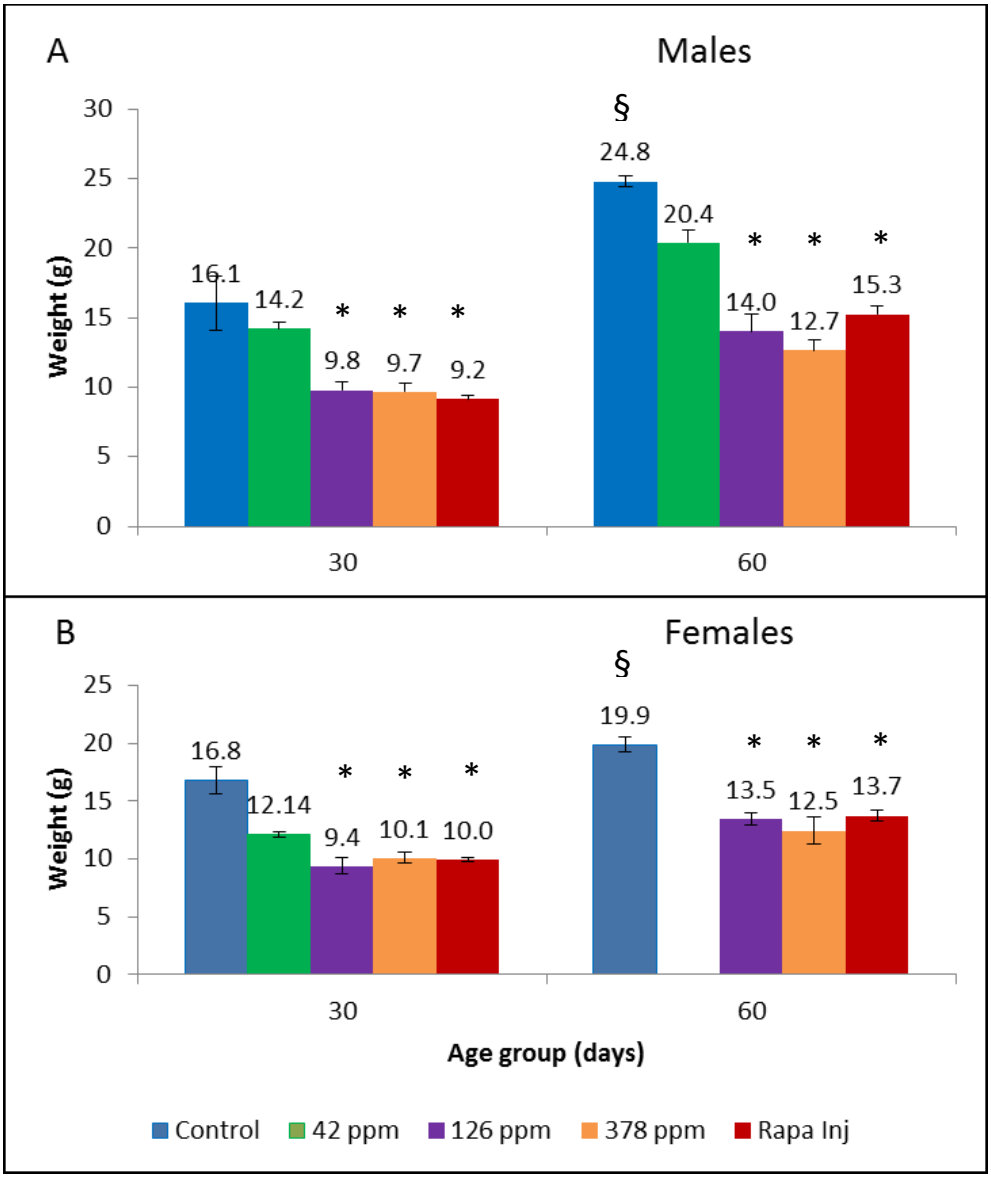

Figure 3.2. Body weights of WT mice receiving dietary rapamycin treatments. Average body weights are compared at postnatal day 30 and 60 time points, or 20 and 40 days after weaning. By day 30, both male (A) and female (B) animals receiving 42, 126 or 378 ppm dietary rapamycin treatment since weaning appeared to show reduced weights compared to control mice. At day 60, male and female control treated mice had gained more than 30% and 18% of their original weights, $F=16.680$, $p<0.001$ and $F=23.912$, $p<0.001$. Only modest weight gain was observed for male and female mice receiving dietary treatment at 126 and 378 ppm. Weights at both 30 and 60 day time points for both genders were similar to what we had previously observed for animals receving daily rapamycin treatment by injection. Data for female mice receiving 42 ppm rapamycin diet at day 60 was not available. N=2 to 13 mice for all conditions, error bars represent SEM. *indicates significant against same day control treated animals as tested through post-hoc pairwise comparison. $p<0.05$. §indicates significant difference between 30 and 60 day time points, $p<0.05$.

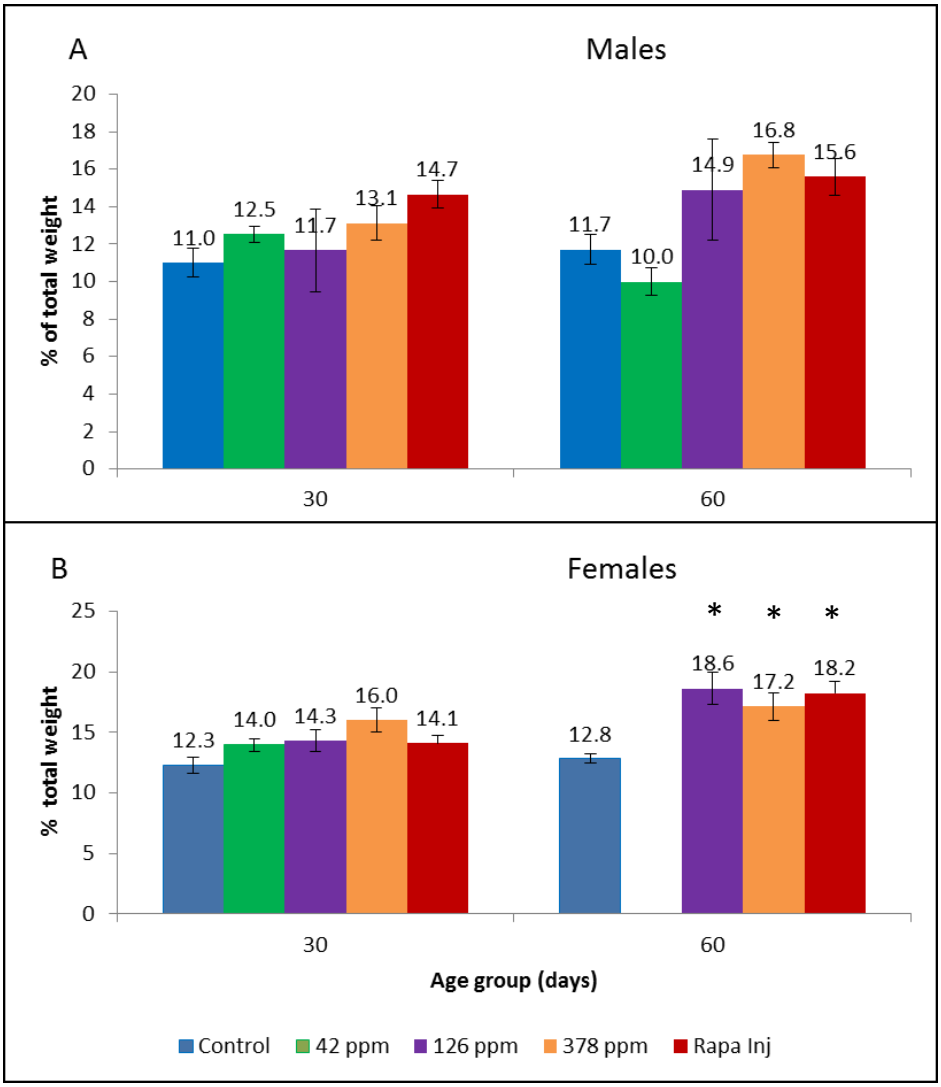

Figure 3.3. Fat mass in WT mice receiving dietary rapamycin treatments. Fat mass was measured by quantitative magnetic resonance (QMR). Average fat mass is represented as a percentage of total body weight at 30 or 60 day time points. Increased fat mass was apparent in both male and female WT mice treated with 126 ppm and 378 ppm dietary rapamycin compared to control diet treatment, especially at day 60. Fat mass percentages appeared similar to those resulting from daily rapamycin injection. Females receiving 126 or 378 ppm rapamycin treatments showed a significant increase in percent body fat compared to control treated mice, $F=8.988$, $p<0.001$. N=2 to 13 mice per treatment, error bars represent +/-SEM. . *indicates significant difference from same day control treated animals as tested through post-hoc pairwise comparison, $p<0.05$.

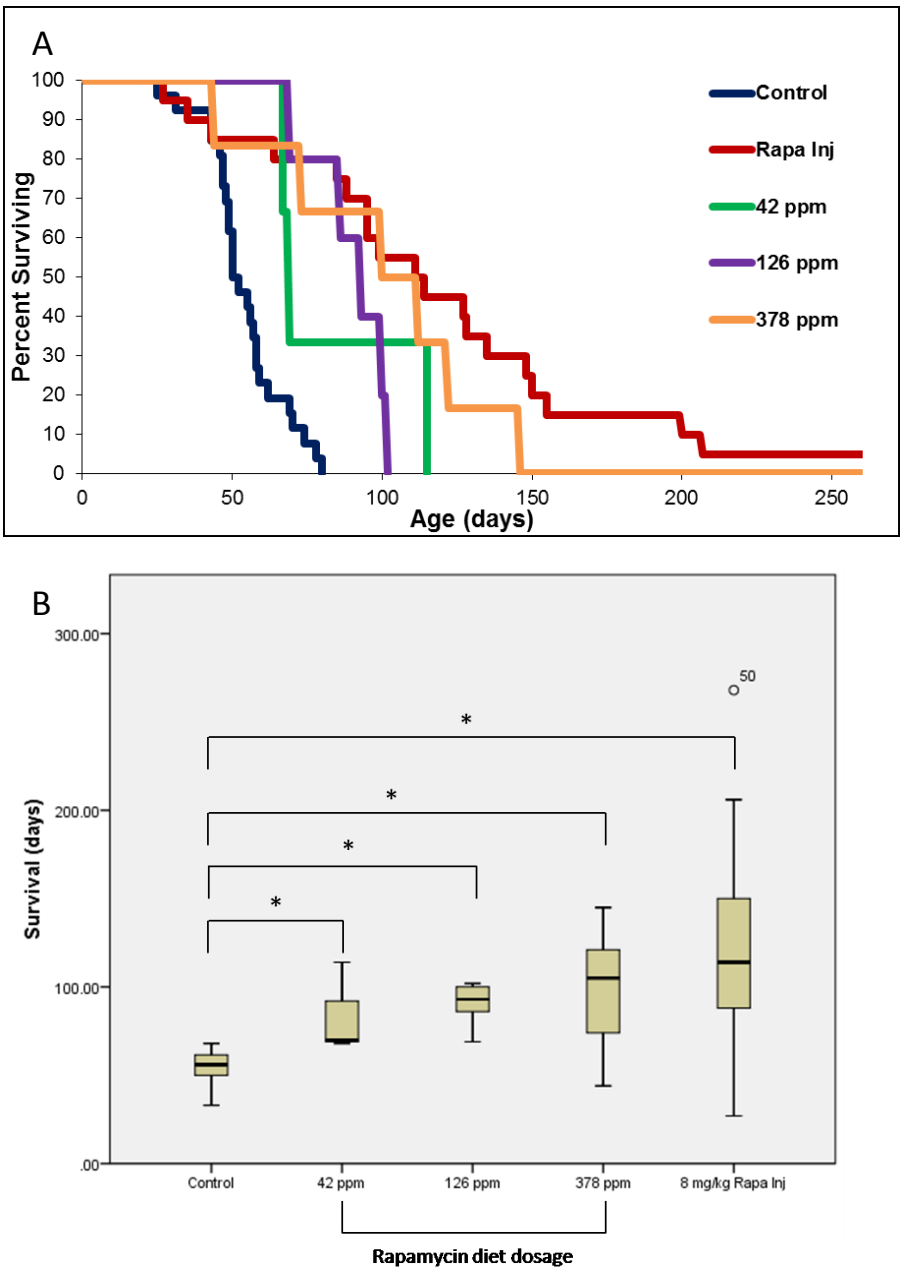

Figure 3.4. Dietary rapamycin improves survival in NDUFS4 KO mice. Dietary rapamycin treatment appeared to increase lifespan in KO mice in a dose-dependent manner. (A) Percent survival curves and (B) Boxplots of age of median survival. * indicates significant differences at $p<0.05$. N=3 to 21 mice. Median survival numbers are provided in Table 3.3C.

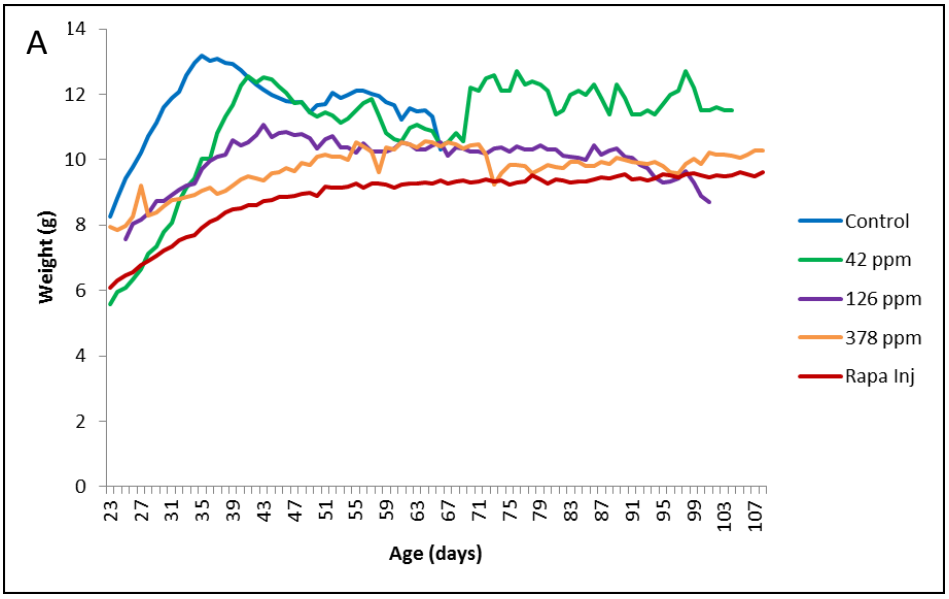

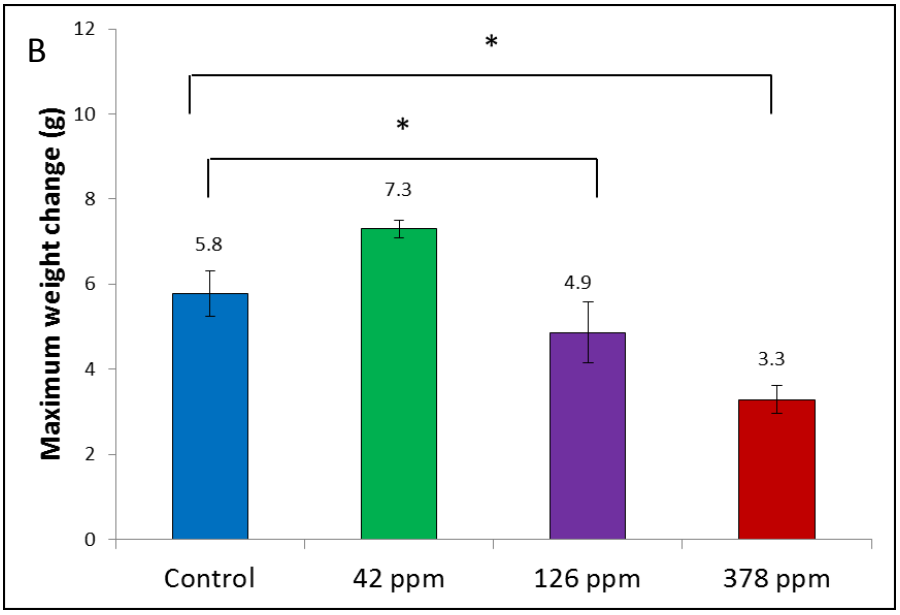

Figure 3.5. Dietary rapamycin attenuates weight change in NDUFS4 KO mice. (A) Weight tracking curves illustrate characteristic phenotype in control-treated KO mice, in which weight rapidly increases starting at P20 then peaks at P35, coinciding with onset of neurological symptoms. Rapamycin diet dosage at 42 ppm appeared to delay this weight phenotype, whereas 126 and 378 ppm dosages reduced weight change. (B) Average weight change across treatment groups. Individual changes were calculated by subtracting entry weights at weaning from maximum recorded weights. * indicates significant differences at $p<0.05$. N=3 to 20 mice, error bars represent SEM.

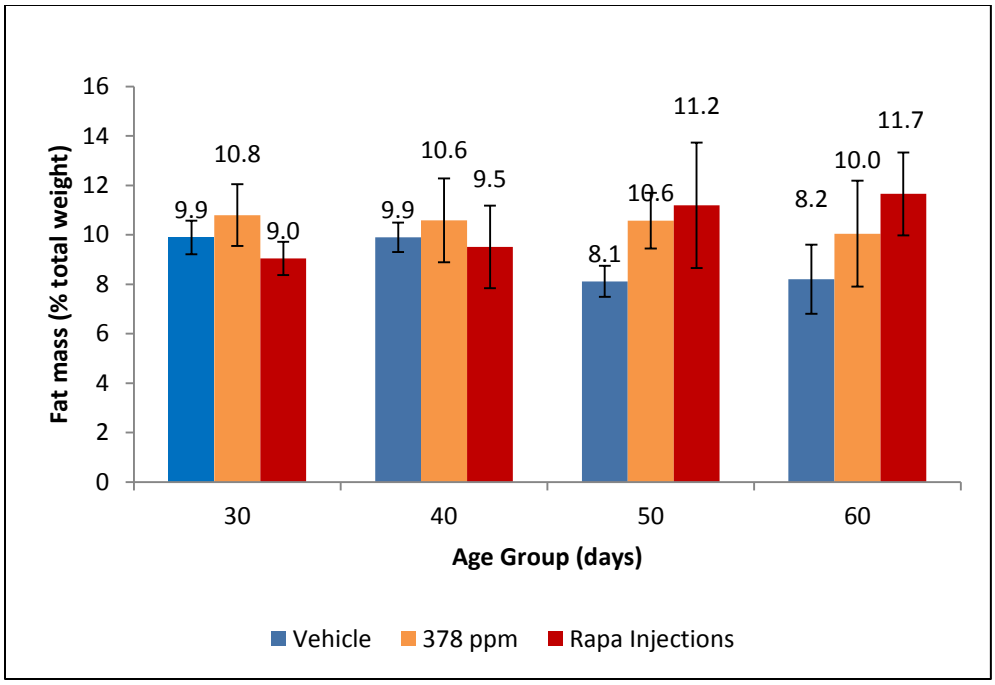

Figure 3.6. Dietary rapamycin treatment at 378 ppm rescues percentage of fat mass in NDUFS4 KO mice. Measurements of fat mass were taken every 10 days beginning at P30 until P60. Fat mass percentages for mice receiving daily IP injections of 8 mg/kg rapamycin is provided for comparison. 378 ppm of dietary rapamycin treatment increases fat mass in KO mice, especially at days 50 and 60, around the age of fatality for control treated mice.

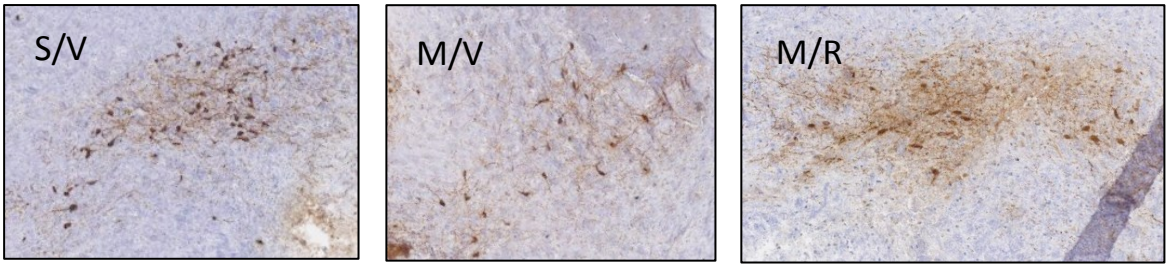

Figure 4.1. Rapamycin reduces MPTP-induced neurodegeneration in the substantia nigra (SN). Representative images of immunohistochemical staining for anti-tyrosine hydroxylase in presumptive SN. Saline-treated control animals show clear pattern of staining of both cell bodies and neurite projections (left panel). Acute MPTP insult results in decreased and diffuse staining (middle panel). Rapamycin treatment following MPTP exposure appears to partially rescue SN neurons (right panel). S/V = Saline/Vehicle, M/V = MPTP/Vehicle, M/R = MPTP/Rapamycin.

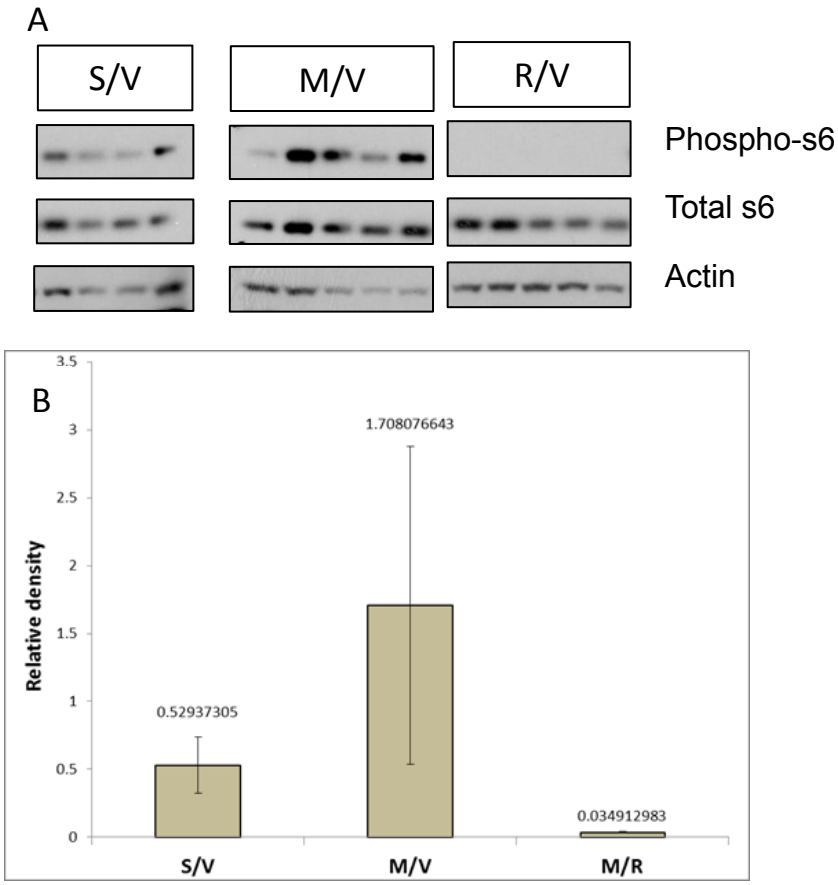

Figure 4.2. MPTP-induced upregulation of mTOR activity is decreased after rapamycin treatment. Western blotting for phospho-s6 was used as an indicator for mTORactivity. MPTP strongly increased levels of phospho-s6 relative to total s6 compared to control animals. Rapamycin treatment following acute MPTP insult appeared to completely abolish relative phospho-s6 activity. (A) Western blot images (B) Densitometry analysis. Error bars represent standard error of the mean. S/V = Saline/Vehicle, M/V = MPTP/Vehicle, M/R = MPTP/Rapamycin. N = 4 to 5 animals per group.

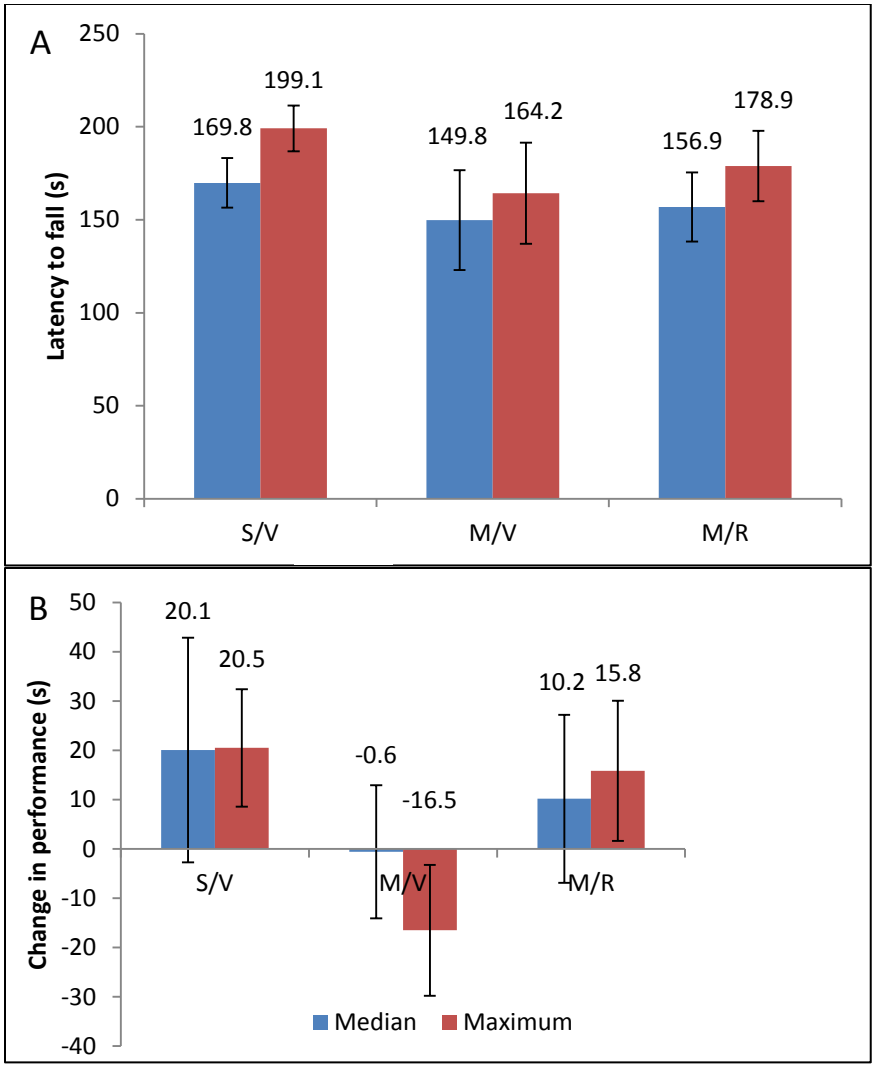

Figure 4.3. Overall rotarod performance across treatment conditions. (A) Rotarod performance was measured as latency to fall. S/V, M/V and M/R treatment groups did not show any significant differences in average latency times. Accounting for average changes from baseline performance (B) indicated the possibility of behavioral impairment as a result of MPTP insult and partial rescue from rapamycin treatment, but a high amount of variability in latency times was also evident. Error bars represent SEM. S/V = Saline/Vehicle, M/V = MPTP/Vehicle, M/R = MPTP/Rapamycin.

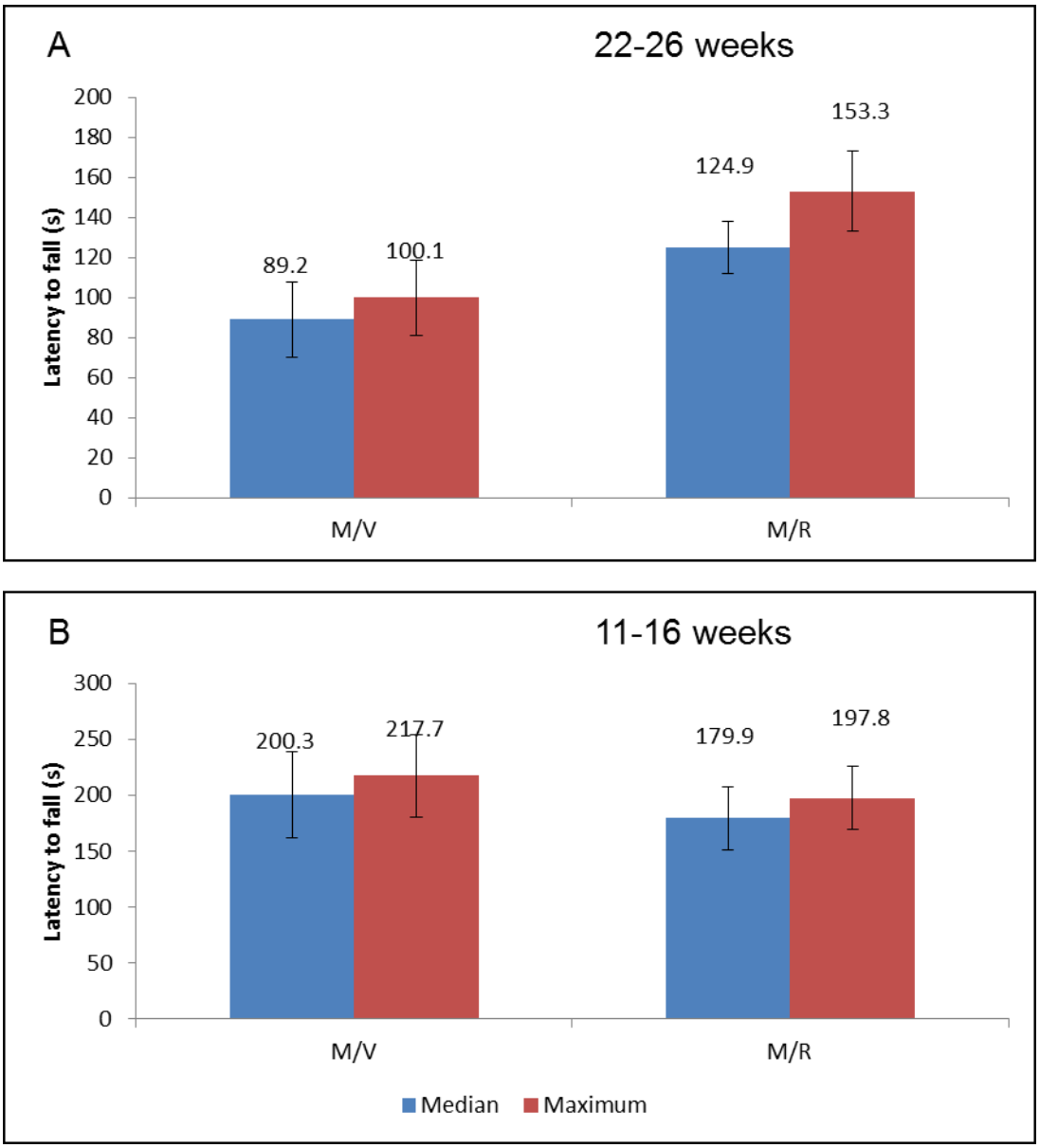

Figure 4.4. Rotarod performance split into adult (22-26 weeks) and juvenile (11-16 weeks) cohorts. (A) In the middle aged cohort, average median and maximum latency times were increased in rapamycin treated mice compared to controls after MPTP exposure. (B) Rapamycin treatment did not appear to improve performance in young mice after MPTP exposure. N=5 to 7 per group, error bars represent +/-SEM. S/V = Saline/Vehicle, M/V = MPTP/Vehicle, M/R = MPTP/Rapamycin

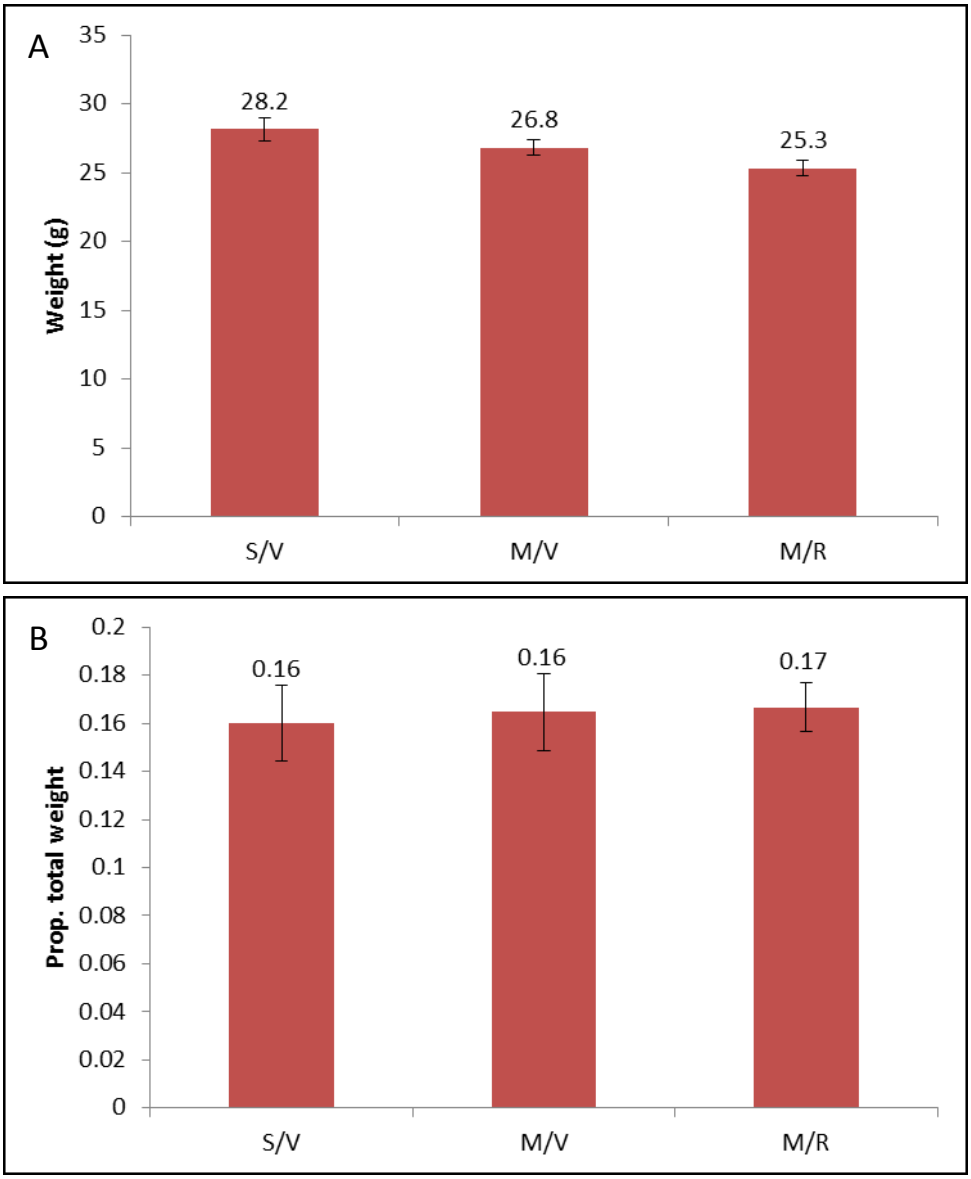

Figure 4.5. Acute MPTP exposure does not significantly alter body weight or fat mass in mice. (A) Average body weights were compared between treatment groups 14 days after MPTP or saline exposure. Mice treated with rapamycin after MPTP exposure (M/R mice) appeared to have reduced body weight compared to S/V and M/V groups. (B) Fat mass is shown as a proportion of total body weight. S/V = Saline/Vehicle, M/V = MPTP/Vehicle, M/R = MPTP/Rapamycin

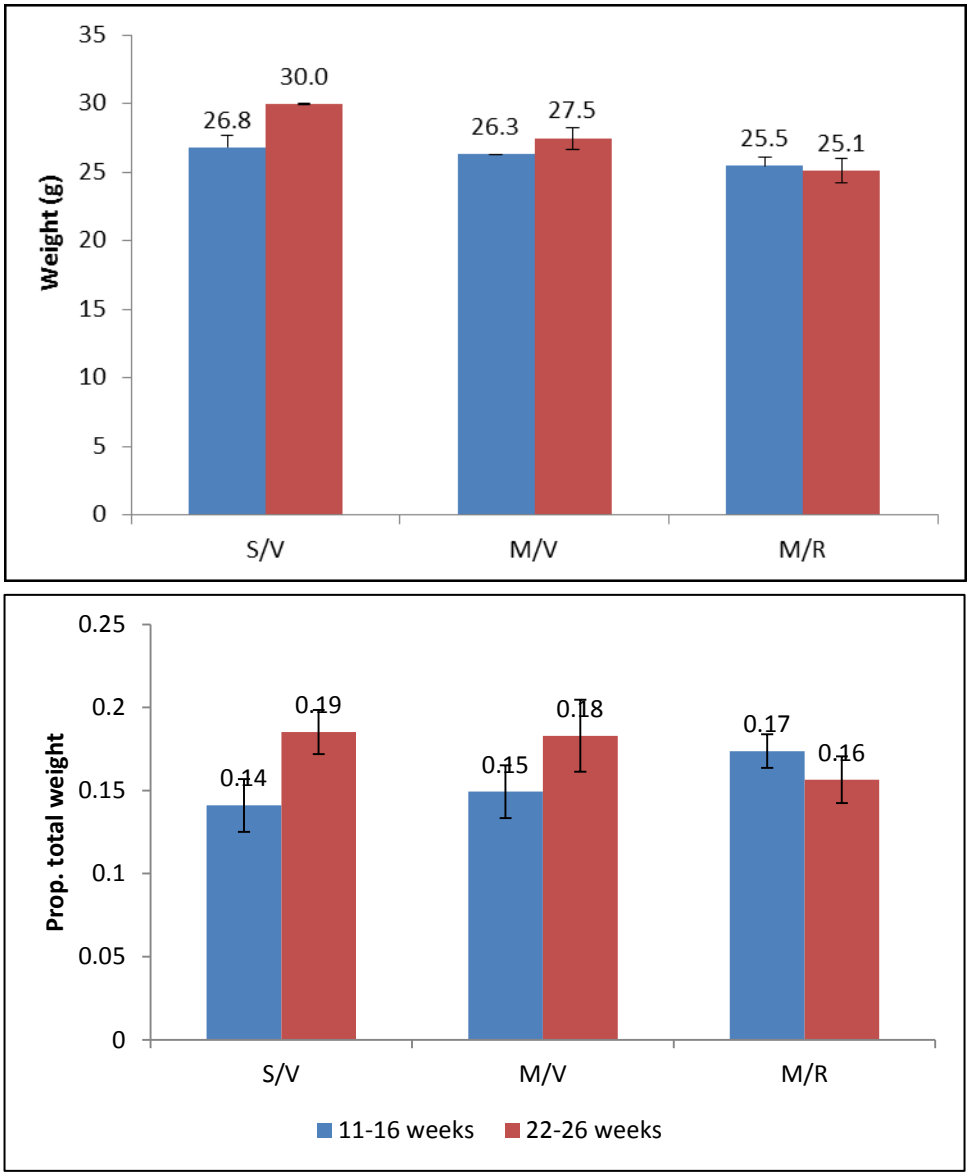

Figure 4.6. Comparison of weight and fat mass in treatment groups divided into age cohorts. No significant interaction between age and treatment type was detected. S/V = Saline/Vehicle, M/V = MPTP/Vehicle, M/R = MPTP/Rapamycin.

TABLES

	Malagelada et al. (2010)[141]	Liu et al. (2013)[142]	Yanos et al. (2014)
MPTP protocol	Acute regimen: 4 IP injections of 18 mg/kg at 2 hour intervals	Chronic regimen: 30 mg/kg/day for 7 days	Acute regimen: 4 IP injections of 18 mg/kg at 2 hour intervals
Rapamycin treatment	IP injection of 7.5 mg/kg, beginning 2 days before first MPTP/saline injection and continuing for 4 days	IV administration of 0.1 ml of 20 µg/ml rapamycin for 7 days after end of MPTP treatment	IP injection on of 8 mg/kg, beginning within 24 hours of acute MPTP exposure and continuing for 14-21 days
TH-immunostaining for dopaminergic neurons	Yes	Yes	Yes
Western blots for mTOR activity	No	No	Yes
Behavioral Assays	No	No	Yes
Assessment of body weight, fat mass	No	No	Yes

Table 4.1. Comparison of experimental approaches among research groups. Two studies have previously demonstrated that rapamycin treatment is effecting at reducing neurodegeneration in the substantia nigra of mice exposed to MPTP. The current study employs some novel assays that were not included in these prior studies.

REFERENCES

1. Johnson, S. C., Rabinovitch, P. S. & Kaeberlein, M. mTOR is a key modulator of ageing and age-related disease. *Nature* **493,** 338–45 (2013).
2. Stanfel, M. N., Shamieh, L. S., Kaeberlein, M. & Kennedy, B. K. The TOR pathway comes of age. *Biochim Biophys Acta* **1790,** 1067–74 (2009).
3. Zoncu, R., Efeyan, A. & Sabatini, D. M. mTOR: from growth signal integration to cancer, diabetes and ageing. *Nat Rev Mol Cell Biol* **12,** 21–35 (2011).
4. Wullschleger, S., Loewith, R. & Hall, M. N. TOR signaling in growth and metabolism. *Cell* **124,** 471–84 (2006).
5. Heitman, J., Movva, N. R. & Hall, M. N. Targets for cell cycle arrest by the immunosuppressant rapamycin in yeast. *Science* **253,** 905–9 (1991).
6. Sarbassov, D. D. *et al.* Rictor, a novel binding partner of mTOR, defines a rapamycin-insensitive and raptor-independent pathway that regulates the cytoskeleton. *Curr Biol* **14,** 1296–302 (2004).
7. Swiech, L., Perycz, M., Malik, A. & Jaworski, J. Role of mTOR in physiology and pathology of the nervous system. *Biochim Biophys Acta* **1784,** 116–32 (2008).
8. Sarbassov, D. D. *et al.* Rictor, a novel binding partner of mTOR, defines a rapamycin-insensitive and raptor-independent pathway that regulates the cytoskeleton. *Curr Biol* **14,** 1296–302 (2004).
9. Sarbassov, D. D., Guertin, D. A., Ali, S. M. & Sabatini, D. M. Phosphorylation and regulation of Akt/PKB by the rictor-mTOR complex. *Science* **307,** 1098–101 (2005).
10. Laplante, M. & Sabatini, D. M. mTOR Signaling in Growth Control and Disease. *Cell* **149,** 274–293 (2012).
11. Inoki, K., Li, Y., Zhu, T., Wu, J. & Guan, K. L. TSC2 is phosphorylated and inhibited by Akt and suppresses mTOR signalling. *Nat Cell Biol* **4,** 648–57 (2002).

12. Potter, C. J., Pedraza, L. G. & Xu, T. Akt regulates growth by directly phosphorylating Tsc2. *Nat Cell Biol* **4,** 658–65 (2002).

13. Vander Haar, E., Lee, S. I., Bandhakavi, S., Griffin, T. J. & Kim, D. H. Insulin signalling to mTOR mediated by the Akt/PKB substrate PRAS40. *Nat Cell Biol* **9,** 316–23 (2007).

14. Garami, A. *et al.* Insulin activation of Rheb, a mediator of mTOR/S6K/4E-BP signaling, is inhibited by TSC1 and 2. *Mol Cell* **11,** 1457–66 (2003).

15. Inoki, K., Li, Y., Xu, T. & Guan, K. L. Rheb GTPase is a direct target of TSC2 GAP activity and regulates mTOR signaling. *Genes Dev* **17,** 1829–34 (2003).

16. Tee, A. R., Anjum, R. & Blenis, J. Inactivation of the tuberous sclerosis complex-1 and -2 gene products occurs by phosphoinositide 3-kinase/Akt-dependent and -independent phosphorylation of tuberin. *J Biol Chem* **278,** 37288–96 (2003).

17. Long, X., Lin, Y., Ortiz-Vega, S., Yonezawa, K. & Avruch, J. Rheb binds and regulates the mTOR kinase. *Curr. Biol. CB* **15,** 702–713 (2005).

18. Gwinn, D. M. *et al.* AMPK phosphorylation of raptor mediates a metabolic checkpoint. *Mol Cell* **30,** 214–26 (2008).

19. Inoki, K. *et al.* TSC2 integrates Wnt and energy signals via a coordinated phosphorylation by AMPK and GSK3 to regulate cell growth. *Cell* **126,** 955–68 (2006).

20. Hresko, R. C. & Mueckler, M. mTOR.RICTOR is the Ser473 kinase for Akt/protein kinase B in 3T3-L1 adipocytes. *J Biol Chem* **280,** 40406–16 (2005).

21. Kim, E., Goraksha-Hicks, P., Li, L., Neufeld, T. P. & Guan, K.-L. Regulation of TORC1 by Rag GTPases in nutrient response. *Nat. Cell Biol.* **10,** 935–945 (2008).

22. Sancak, Y. *et al.* The Rag GTPases Bind Raptor and Mediate Amino Acid Signaling to mTORC1. *Science* **320,** 1496–1501 (2008).

23. Sancak, Y. *et al.* Ragulator-Rag complex targets mTORC1 to the lysosomal surface and is necessary for its activation by amino acids. *Cell* **141,** 290–303 (2010).

24. Zoncu, R. *et al.* mTORC1 senses lysosomal amino acids through an inside-out mechanism that requires the vacuolar H(+)-ATPase. *Science* **334,** 678–83 (2011).

25. Beretta, L., Gingras, A. C., Svitkin, Y. V., Hall, M. N. & Sonenberg, N. Rapamycin blocks the phosphorylation of 4E-BP1 and inhibits cap-dependent initiation of translation. *EMBO J* **15,** 658–64 (1996).

26. Haghighat, A., Mader, S., Pause, A. & Sonenberg, N. Repression of cap-dependent translation by 4E-binding protein 1: competition with p220 for binding to eukaryotic initiation factor-4E. *EMBO J* **14,** 5701–9 (1995).

27. Hara, K. *et al.* Regulation of eIF-4E BP1 phosphorylation by mTOR. *J Biol Chem* **272,** 26457–63 (1997).

28. Gingras, A. C., Kennedy, S. G., O'Leary, M. A., Sonenberg, N. & Hay, N. 4E-BP1, a repressor of mRNA translation, is phosphorylated and inactivated by the Akt(PKB) signaling pathway. *Genes Dev* **12,** 502–13 (1998).

29. Wang, X. *et al.* Regulation of elongation factor 2 kinase by p90(RSK1) and p70 S6 kinase. *EMBO J* **20,** 4370–9 (2001).

30. Holz, M. K., Ballif, B. A., Gygi, S. P. & Blenis, J. mTOR and S6K1 mediate assembly of the translation preinitiation complex through dynamic protein interchange and ordered phosphorylation events. *Cell* **123,** 569–80 (2005).

31. Mizushima, N. The role of the Atg1/ULK1 complex in autophagy regulation. *Curr Opin Cell Biol* **22,** 132–9 (2010).

32. Thoreen, C. C. *et al.* An ATP-competitive mammalian target of rapamycin inhibitor reveals rapamycin-resistant functions of mTORC1. *J Biol Chem* **284,** 8023–32 (2009).

33. Rubinsztein, D. C., Gestwicki, J. E., Murphy, L. O. & Klionsky, D. J. Potential therapeutic applications of autophagy. *Nat Rev Drug Discov* **6,** 304–12 (2007).

34. Neuhaus, P., Klupp, J. & Langrehr, J. M. mTOR inhibitors: an overview. *Liver Transpl* **7,** 473–84 (2001).

35. Cunningham, J. T. *et al.* mTOR controls mitochondrial oxidative function through a YY1–PGC-1α transcriptional complex. *Nature* **450,** 736–740 (2007).

36. Schieke, S. M. *et al.* The Mammalian Target of Rapamycin (mTOR) Pathway Regulates Mitochondrial Oxygen Consumption and Oxidative Capacity. *J. Biol. Chem.* **281,** 27643–27652 (2006).

37. Ramanathan, A. & Schreiber, S. L. Direct control of mitochondrial function by mTOR. *Proc. Natl. Acad. Sci.* **106,** 22229–22232 (2009).

38. Sarbassov, D. D. *et al.* Prolonged rapamycin treatment inhibits mTORC2 assembly and Akt/PKB. *Mol Cell* **22,** 159–68 (2006).

39. Fabrizio, P., Pozza, F., Pletcher, S. D., Gendron, C. M. & Longo, V. D. Regulation of longevity and stress resistance by Sch9 in yeast. *Science* **292,** 288–90 (2001).

40. Kaeberlein, M. *et al.* Regulation of yeast replicative life span by TOR and Sch9 in response to nutrients. *Science* **310,** 1193–6 (2005).

41. Vellai, T. *et al.* Genetics: influence of TOR kinase on lifespan in C. elegans. *Nature* **426,** 620 (2003).

42. Hansen, M. *et al.* Lifespan extension by conditions that inhibit translation in Caenorhabditis elegans. *Aging Cell* **6,** 95–110 (2007).

43. Kapahi, P. *et al.* Regulation of lifespan in Drosophila by modulation of genes in the TOR signaling pathway. *Curr Biol* **14,** 885–90 (2004).

44. Selman, C. *et al.* Ribosomal protein S6 kinase 1 signaling regulates mammalian life span. *Science* **326,** 140–4 (2009).

45. Robida-Stubbs, S. *et al.* TOR signaling and rapamycin influence longevity by regulating SKN-1/Nrf and DAF-16/FoxO. *Cell Metab* **15,** 713–24 (2012).

46. Bjedov, I. *et al.* Mechanisms of life span extension by rapamycin in the fruit fly Drosophila melanogaster. *Cell Metab* **11,** 35–46 (2010).

47. Harrison, D. E. *et al.* Rapamycin fed late in life extends lifespan in genetically heterogeneous mice. *Nature* **460,** 392–5 (2009).

48. Colman, R. J. *et al.* Caloric restriction delays disease onset and mortality in rhesus monkeys. *Science* **325,** 201–4 (2009).

49. Klass, M. R. Aging in the nematode Caenorhabditis elegans: major biological and environmental factors influencing life span. *Mech Ageing Dev* **6,** 413–29 (1977).

50. Kaeberlein, T. L. *et al.* Lifespan extension in Caenorhabditis elegans by complete removal of food. *Aging Cell* **5,** 487–94 (2006).

51. Lee, G. D. *et al.* Dietary deprivation extends lifespan in Caenorhabditis elegans. *Aging Cell* **5,** 515–24 (2006).

52. Kahn, A. J. Development, aging, and life duration: effects of nutrient restriction. *Am J Clin Nutr* **25,** 822–8 (1972).

53. Weindruch, R., Walford, R. L., Fligiel, S. & Guthrie, D. The retardation of aging in mice by dietary restriction: longevity, cancer, immunity and lifetime energy intake. *J Nutr* **116,** 641–54 (1986).

54. Lin, S. J., Defossez, P. A. & Guarente, L. Requirement of NAD and SIR2 for life-span extension by calorie restriction in Saccharomyces cerevisiae. *Science* **289,** 2126–8 (2000).

55. Meyer, T. E. *et al.* Long-term caloric restriction ameliorates the decline in diastolic function in humans. *J Am Coll Cardiol* **47,** 398–402 (2006).

56. Larson-Meyer, D. E. *et al.* Effect of 6-month calorie restriction and exercise on serum and liver lipids and markers of liver function. *Obes. Silver Spring* **16,** 1355–62 (2008).

57. Heilbronn, L. K. *et al.* Effect of 6-month calorie restriction on biomarkers of longevity, metabolic adaptation, and oxidative stress in overweight individuals: a randomized controlled trial. *JAMA* **295,** 1539–48 (2006).

58. Fontana, L., Meyer, T. E., Klein, S. & Holloszy, J. O. Long-term calorie restriction is highly effective in reducing the risk for atherosclerosis in humans. *Proc Natl Acad Sci U A* **101,** 6659–63 (2004).

59. Hansen, M. *et al.* A role for autophagy in the extension of lifespan by dietary restriction in C. elegans. *PLoS Genet* **4,** e24 (2008).

60. Fontana, L., Partridge, L. & Longo, V. D. Extending healthy life span--from yeast to humans. *Science* **328,** 321–6 (2010).

61. Kenyon, C. J. The genetics of ageing. *Nature* **464,** 504–12 (2010).

62. Takano, A. *et al.* Mammalian target of rapamycin pathway regulates insulin signaling via subcellular redistribution of insulin receptor substrate 1 and integrates nutritional signals and metabolic signals of insulin. *Mol Cell Biol* **21,** 5050–62 (2001).

63. Apfeld, J., O'Connor, G., McDonagh, T., DiStefano, P. S. & Curtis, R. The AMP-activated protein kinase AAK-2 links energy levels and insulin-like signals to lifespan in C. elegans. *Genes Dev* **18,** 3004–9 (2004).

64. Onken, B. & Driscoll, M. Metformin induces a dietary restriction-like state and the oxidative stress response to extend C. elegans Healthspan via AMPK, LKB1, and SKN-1. *PLoS One* **5,** e8758 (2010).

65. Anisimov, V. N. *et al.* Metformin slows down aging and extends life span of female SHR mice. *Cell Cycle* **7,** 2769–73 (2008).

66. Hudson, C. C. *et al.* Regulation of hypoxia-inducible factor 1alpha expression and function by the mammalian target of rapamycin. *Mol Cell Biol* **22,** 7004–14 (2002).

67. Mehta, R. *et al.* Proteasomal regulation of the hypoxic response modulates aging in C. elegans. *Science* **324,** 1196–8 (2009).

68. Zhang, Y., Shao, Z., Zhai, Z., Shen, C. & Powell-Coffman, J. A. The HIF-1 hypoxia-inducible factor modulates lifespan in C. elegans. *PLoS One* **4,** e6348 (2009).

69. Garelick, M. G. & Kennedy, B. K. TOR on the brain. *Exp Gerontol* **46,** 155–63 (2011).

70. Hoeffer, C. A. & Klann, E. mTOR signaling: at the crossroads of plasticity, memory and disease. *Trends Neurosci* **33,** 67–75 (2010).

71. Graber, T. E., McCamphill, P. K. & Sossin, W. S. A recollection of mTOR signaling in learning and memory. *Learn. Mem.* **20,** 518–530 (2013).

72. Jaworski, J. & Sheng, M. The growing role of mTOR in neuronal development and plasticity. *Mol Neurobiol* **34,** 205–19 (2006).

73. Casadio, A. *et al.* A transient, neuron-wide form of CREB-mediated long-term facilitation can be stabilized at specific synapses by local protein synthesis. *Cell* **99,** 221–37 (1999).

74. Yanow, S. K., Manseau, F., Hislop, J., Castellucci, V. F. & Sossin, W. S. Biochemical pathways by which serotonin regulates translation in the nervous system of Aplysia. *J Neurochem* **70,** 572–83 (1998).

75. Khan, A., Pepio, A. M. & Sossin, W. S. Serotonin activates S6 kinase in a rapamycin-sensitive manner in Aplysia synaptosomes. *J Neurosci* **21,** 382–91 (2001).

76. Beaumont, V., Zhong, N., Fletcher, R., Froemke, R. C. & Zucker, R. S. Phosphorylation and local presynaptic protein synthesis in calcium- and calcineurin-dependent induction of crayfish long-term facilitation. *Neuron* **32,** 489–501 (2001).

77. Tang, S. J. *et al.* A rapamycin-sensitive signaling pathway contributes to long-term synaptic plasticity in the hippocampus. *Proc Natl Acad Sci U A* **99,** 467–72 (2002).

78. Cammalleri, M. *et al.* Time-restricted role for dendritic activation of the mTOR-p70S6K pathway in the induction of late-phase long-term potentiation in the CA1. *Proc Natl Acad Sci U A* **100,** 14368–73 (2003).

79. Tsokas, P. *et al.* Local protein synthesis mediates a rapid increase in dendritic elongation factor 1A after induction of late long-term potentiation. *J Neurosci* **25,** 5833–43 (2005).

80. Schratt, G. M., Nigh, E. A., Chen, W. G., Hu, L. & Greenberg, M. E. BDNF regulates the translation of a select group of mRNAs by a mammalian target of rapamycin-phosphatidylinositol 3-kinase-dependent pathway during neuronal development. *J Neurosci* **24,** 7366–77 (2004).

81. Gong, R., Park, C. S., Abbassi, N. R. & Tang, S. J. Roles of glutamate receptors and the mammalian target of rapamycin (mTOR) signaling pathway in activity-dependent dendritic protein synthesis in hippocampal neurons. *J Biol Chem* **281,** 18802–15 (2006).

82. Lee, C. C., Huang, C. C., Wu, M. Y. & Hsu, K. S. Insulin stimulates postsynaptic density-95 protein translation via the phosphoinositide 3-kinase-Akt-mammalian target of rapamycin signaling pathway. *J Biol Chem* **280,** 18543–50 (2005).

83. Cracco, J. B., Serrano, P., Moskowitz, S. I., Bergold, P. J. & Sacktor, T. C. Protein synthesis-dependent LTP in isolated dendrites of CA1 pyramidal cells. *Hippocampus* **15,** 551–6 (2005).

84. Vickers, C. A., Dickson, K. S. & Wyllie, D. J. Induction and maintenance of late-phase long-term potentiation in isolated dendrites of rat hippocampal CA1 pyramidal neurones. *J Physiol* **568,** 803–13 (2005).

85. Banko, J. L., Hou, L., Poulin, F., Sonenberg, N. & Klann, E. Regulation of eukaryotic initiation factor 4E by converging signaling pathways during metabotropic glutamate receptor-dependent long-term depression. *J Neurosci* **26,** 2167–73 (2006).

86. Ran, I. *et al.* Persistent transcription- and translation-dependent long-term potentiation induced by mGluR1 in hippocampal interneurons. *J Neurosci* **29,** 5605–15 (2009).

87. Raab-Graham, K. F., Haddick, P. C., Jan, Y. N. & Jan, L. Y. Activity- and mTOR-dependent suppression of Kv1.1 channel mRNA translation in dendrites. *Science* **314,** 144–8 (2006).

88. Martin, S. J., Grimwood, P. D. & Morris, R. G. Synaptic plasticity and memory: an evaluation of the hypothesis. *Annu Rev Neurosci* **23,** 649–711 (2000).

89. Tischmeyer, W. *et al.* Rapamycin-sensitive signalling in long-term consolidation of auditory cortex-dependent memory. *Eur J Neurosci* **18,** 942–50 (2003).

90. Parsons, R. G., Gafford, G. M. & Helmstetter, F. J. Translational control via the mammalian target of rapamycin pathway is critical for the formation and stability of long-term fear memory in amygdala neurons. *J Neurosci* **26,** 12977–83 (2006).

91. Dash, P. K., Orsi, S. A. & Moore, A. N. Spatial memory formation and memory-enhancing effect of glucose involves activation of the tuberous sclerosis complex-Mammalian target of rapamycin pathway. *J Neurosci* **26,** 8048–56 (2006).

92. Neasta, J., Barak, S., Hamida, S. B. & Ron, D. mTOR complex 1: a key player in neuroadaptations induced by drugs of abuse. *J Neurochem* (2014). doi:10.1111/jnc.12725

93. Ehninger, D. *et al.* Reversal of learning deficits in a Tsc2+/- mouse model of tuberous sclerosis. *Nat Med* **14,** 843–8 (2008).

94. Labban, M., Dyer, J. R. & Sossin, W. S. Rictor regulates phosphorylation of the novel protein kinase C Apl II in Aplysia sensory neurons. *J Neurochem* **122,** 1108–17 (2012).

95. Huang, W. *et al.* mTORC2 controls actin polymerization required for consolidation of long-term memory. *Nat Neurosci* **16,** 441–8 (2013).

96. Um, S. H. *et al.* Absence of S6K1 protects against age- and diet-induced obesity while enhancing insulin sensitivity. *Nature* **431,** 200–5 (2004).

97. Blouet, C., Ono, H. & Schwartz, G. J. Mediobasal hypothalamic p70 S6 kinase 1 modulates the control of energy homeostasis. *Cell Metab* **8,** 459–67 (2008).

98. Mori, H. *et al.* Critical role for hypothalamic mTOR activity in energy balance. *Cell Metab* **9,** 362–74 (2009).

99. Cota, D. *et al.* Hypothalamic mTOR signaling regulates food intake. *Science* **312,** 927–30 (2006).

100. Mattson, M. P., Gleichmann, M. & Cheng, A. Mitochondria in neuroplasticity and neurological disorders. *Neuron* **60,** 748–66 (2008).

101. Martin, B., Mattson, M. P. & Maudsley, S. Caloric restriction and intermittent fasting: two potential diets for successful brain aging. *Ageing Res Rev* **5,** 332–53 (2006).

102. Mattson, M. P. *et al.* Neuroprotective and neurorestorative signal transduction mechanisms in brain aging: modification by genes, diet and behavior. *Neurobiol Aging* **23,** 695–705 (2002).

103. Weindruch, R. & Sohal, R. S. Seminars in medicine of the Beth Israel Deaconess Medical Center. Caloric intake and aging. *N Engl J Med* **337,** 986–94 (1997).

104. Duan, W. *et al.* Dietary restriction normalizes glucose metabolism and BDNF levels, slows disease progression, and increases survival in huntingtin mutant mice. *Proc Natl Acad Sci U A* **100,** 2911–6 (2003).

105. Steinkraus, K. A. *et al.* Dietary restriction suppresses proteotoxicity and enhances longevity by an hsf-1-dependent mechanism in Caenorhabditis elegans. *Aging Cell* **7,** 394–404 (2008).

106. Halloran, J. *et al.* Chronic inhibition of mammalian target of rapamycin by rapamycin modulates cognitive and non-cognitive components of behavior throughout lifespan in mice. *Neuroscience* **223,** 102–13 (2012).

107. Majumder, S. *et al.* Lifelong rapamycin administration ameliorates age-dependent cognitive deficits by reducing IL-1beta and enhancing NMDA signaling. *Aging Cell* **11,** 326–35 (2012).

108. Yang, S. B. *et al.* Rapamycin ameliorates age-dependent obesity associated with increased mTOR signaling in hypothalamic POMC neurons. *Neuron* **75,** 425–36 (2012).

109. Thies, W., Bleiler, L. & Alzheimer's, A. 2013 Alzheimer's disease facts and figures. *Alzheimers Dement* **9,** 208–45 (2013).

110. An, W. L. *et al.* Up-regulation of phosphorylated/activated p70 S6 kinase and its relationship to neurofibrillary pathology in Alzheimer's disease. *Am J Pathol* **163,** 591–607 (2003).

111. Lafay-Chebassier, C. *et al.* mTOR/p70S6k signalling alteration by Abeta exposure as well as in APP-PS1 transgenic models and in patients with Alzheimer's disease. *J Neurochem* **94,** 215–25 (2005).

112. Spilman, P. *et al.* Inhibition of mTOR by rapamycin abolishes cognitive deficits and reduces amyloid-beta levels in a mouse model of Alzheimer's disease. *PLoS One* **5,** e9979 (2010).

113. Caccamo, A., Majumder, S., Richardson, A., Strong, R. & Oddo, S. Molecular interplay between mammalian target of rapamycin (mTOR), amyloid-beta, and Tau: effects on cognitive impairments. *J Biol Chem* **285,** 13107–20 (2010).

114. Caccamo, A. *et al.* mTOR regulates tau phosphorylation and degradation: implications for Alzheimer's disease and other tauopathies. *Aging Cell* **12,** 370–80 (2013).

115. Yu, W. H. *et al.* Macroautophagy—a novel β-amyloid peptide-generating pathway activated in Alzheimer's disease. *J. Cell Biol.* **171,** 87–98 (2005).

116. Pei, J. J., Sjogren, M. & Winblad, B. Neurofibrillary degeneration in Alzheimer's disease: from molecular mechanisms to identification of drug targets. *Curr Opin Psychiatry* **21,** 555–61 (2008).

117. Griffin, R. J. *et al.* Activation of Akt/PKB, increased phosphorylation of Akt substrates and loss and altered distribution of Akt and PTEN are features of Alzheimer's disease pathology. *J Neurochem* **93,** 105–17 (2005).

118. Khurana, V. *et al.* TOR-mediated cell-cycle activation causes neurodegeneration in a Drosophila tauopathy model. *Curr Biol* **16,** 230–41 (2006).

119. Meske, V., Albert, F. & Ohm, T. G. Coupling of mammalian target of rapamycin with phosphoinositide 3-kinase signaling pathway regulates protein phosphatase 2A- and glycogen synthase kinase-3 -dependent phosphorylation of Tau. *J Biol Chem* **283,** 100–9 (2008).

120. Ozcelik, S. *et al.* Rapamycin Attenuates the Progression of Tau Pathology in P301S Tau Transgenic Mice. *PLoS ONE* **8,** e62459 (2013).

121. Gong, C.-X., Liu, F., Grundke-Iqbal, I. & Iqbal, K. Post-translational modifications of tau protein in Alzheimer's disease. *J. Neural Transm.* **112,** 813–838 (2005).

122. Oddo, S., Billings, L., Kesslak, J. P., Cribbs, D. H. & LaFerla, F. M. Abeta immunotherapy leads to clearance of early, but not late, hyperphosphorylated tau aggregates via the proteasome. *Neuron* **43,** 321–32 (2004).

123. Oddo, S. *et al.* Temporal profile of amyloid-beta (Abeta) oligomerization in an in vivo model of Alzheimer disease. A link between Abeta and tau pathology. *J Biol Chem* **281,** 1599–604 (2006).

124. Oddo, S. *et al.* Blocking Abeta42 accumulation delays the onset and progression of tau pathology via the C terminus of heat shock protein70-interacting protein: a mechanistic link between Abeta and tau pathology. *J Neurosci* **28,** 12163–75 (2008).

125. Oddo, S., Caccamo, A., Cheng, D. & LaFerla, F. M. Genetically altering Abeta distribution from the brain to the vasculature ameliorates tau pathology. *Brain Pathol* **19,** 421–30 (2009).

126. Ott, B. R. Cognition and behavior in patients with Alzheimer's disease. *J Gend Specif Med* **2,** 63–9 (1999).

127. Sims-Robinson, C., Kim, B., Rosko, A. & Feldman, E. L. How does diabetes accelerate Alzheimer disease pathology? *Nat Rev Neurol* **6,** 551–9 (2010).

128. Liu, Y., Liu, F., Grundke-Iqbal, I., Iqbal, K. & Gong, C. X. Brain glucose transporters, O-GlcNAcylation and phosphorylation of tau in diabetes and Alzheimer's disease. *J Neurochem* **111,** 242–9 (2009).

129. Talbot, K. *et al.* Demonstrated brain insulin resistance in Alzheimer's disease patients is associated with IGF-1 resistance, IRS-1 dysregulation, and cognitive decline. *J Clin Invest* **122,** 1316–38 (2012).

130. Moloney, A. M. *et al.* Defects in IGF-1 receptor, insulin receptor and IRS-1/2 in Alzheimer's disease indicate possible resistance to IGF-1 and insulin signalling. *Neurobiol Aging* **31,** 224–43 (2010).

131. O'Neill, C., Kiely, A., Coakley, M., Manning, S. & LongSmith, C. Insulin and IGF-1 signalling: longevity, protein homoeostasis and Alzheimer's disease. *Biochem. Soc. Trans.* **40,** 721 (2012).

132. Caccamo, A., Medina, D. X. & Oddo, S. Glucocorticoids exacerbate cognitive deficits in TDP-25 transgenic mice via a glutathione-mediated mechanism: implications for aging, stress and TDP-43 proteinopathies. *J Neurosci* **33,** 906–13 (2013).

133. Orr, M. E., Salinas, A., Buffenstein, R. & Oddo, S. Mammalian target of rapamycin hyperactivity mediates the detrimental effects of a high sucrose diet on Alzheimer's disease pathology. *Neurobiol Aging* **35,** 1233–42 (2014).

134. Kowal, S. L., Dall, T. M., Chakrabarti, R., Storm, M. V. & Jain, A. The current and projected economic burden of Parkinson's disease in the United States. *Mov. Disord.* **28,** 311–318 (2013).

135. Noyes, K., Liu, H., Li, Y., Holloway, R. & Dick, A. W. Economic burden associated with Parkinson's disease on elderly Medicare beneficiaries. *Mov. Disord.* **21,** 362–372 (2006).

136. Weintraub, D., Comella, C. L. & Horn, S. Parkinson's disease--Part 1: Pathophysiology, symptoms, burden, diagnosis, and assessment. *Am J Manag Care* **14,** S40–8 (2008).

137. Dorsey, E. R. *et al.* Projected number of people with Parkinson disease in the most populous nations, 2005 through 2030. *Neurology* **68,** 384–6 (2007).

138. Dauer, W. & Przedborski, S. Parkinson's disease: mechanisms and models. *Neuron* **39,** 889–909 (2003).

139. Levy, O. A., Malagelada, C. & Greene, L. A. Cell death pathways in Parkinson's disease: proximal triggers, distal effectors, and final steps. *Apoptosis* **14,** 478–500 (2009).

140. Tain, L. S. *et al.* Rapamycin activation of 4E-BP prevents parkinsonian dopaminergic neuron loss. *Nat Neurosci* **12,** 1129–35 (2009).

141. Malagelada, C., Jin, Z. H., Jackson-Lewis, V., Przedborski, S. & Greene, L. A. Rapamycin protects against neuron death in in vitro and in vivo models of Parkinson's disease. *J Neurosci* **30,** 1166–75 (2010).

142. Liu, K., Shi, N., Sun, Y., Zhang, T. & Sun, X. Therapeutic Effects of Rapamycin on MPTP-Induced Parkinsonism in Mice. *Neurochem. Res.* **38,** 201–207 (2013).

143. Malagelada, C., Ryu, E. J., Biswas, S. C., Jackson-Lewis, V. & Greene, L. A. RTP801 is elevated in Parkinson brain substantia nigral neurons and mediates death in cellular models of Parkinson's disease by a mechanism involving mammalian target of rapamycin inactivation. *J Neurosci* **26,** 9996–10005 (2006).

144. Webb, J. L., Ravikumar, B., Atkins, J., Skepper, J. N. & Rubinsztein, D. C. Alpha-Synuclein is degraded by both autophagy and the proteasome. *J Biol Chem* **278,** 25009–13 (2003).

145. Pan, T. *et al.* Rapamycin protects against rotenone-induced apoptosis through autophagy induction. *Neuroscience* **164,** 541–51 (2009).

146. Zhu, J. *et al.* Regulation of autophagy by extracellular signal-regulated protein kinases during 1-methyl-4-phenylpyridinium-induced cell death. *Am. J. Pathol.* **170,** 75–86 (2007).

147. Xilouri, M., Vogiatzi, T., Vekrellis, K., Park, D. & Stefanis, L. Abberant alpha-synuclein confers toxicity to neurons in part through inhibition of chaperone-mediated autophagy. *PLoS One* **4,** e5515 (2009).

148. Choi, K. C., Kim, S. H., Ha, J. Y., Kim, S. T. & Son, J. H. A novel mTOR activating protein protects dopamine neurons against oxidative stress by repressing autophagy related cell death. *J Neurochem* **112,** 366–76 (2010).

149. Lin, M. T. & Beal, M. F. Mitochondrial dysfunction and oxidative stress in neurodegenerative diseases. *Nature* **443,** 787–795 (2006).

150. Siddiqui, A., Hanson, I. & Andersen, J. K. Mao-B elevation decreases parkin's ability to efficiently clear damaged mitochondria: protective effects of rapamycin. *Free Radic. Res.* **46,** 1011–1018 (2012).

151. Ravikumar, B., Berger, Z., Vacher, C., O'Kane, C. J. & Rubinsztein, D. C. Rapamycin pre-treatment protects against apoptosis. *Hum Mol Genet* **15,** 1209–16 (2006).

152. Jiang, J., Jiang, J., Zuo, Y. & Gu, Z. Rapamycin protects the mitochondria against oxidative stress and apoptosis in a rat model of Parkinson's disease. *Int J Mol Med* **31,** 825–32 (2013).

153. Rieker, C. *et al.* Nucleolar Disruption in Dopaminergic Neurons Leads to Oxidative Damage and Parkinsonism through Repression of Mammalian Target of Rapamycin Signaling. *J. Neurosci.* **31,** 453–460 (2011).

154. Walker, F. O. Huntington's disease. *Lancet* **369,** 218–228 (2007).

155. Ehrlich, M. E. Huntington's disease and the striatal medium spiny neuron: cell-autonomous and non-cell-autonomous mechanisms of disease. *Neurother. J. Am. Soc. Exp. Neurother.* **9,** 270–284 (2012).

156. La Spada, A. R., Weydt, P. & Pineda, V. V. in *Neurobiol. Huntingt. Dis. Appl. Drug Discov.* (eds. Lo, D. C. & Hughes, R. E.) (CRC Press Llc., 2011). at <http://www.ncbi.nlm.nih.gov/books/NBK55992/>

157. Wacker, J. L., Zareie, M. H., Fong, H., Sarikaya, M. & Muchowski, P. J. Hsp70 and Hsp40 attenuate formation of spherical and annular polyglutamine oligomers by partitioning monomer. *Nat Struct Mol Biol* **11,** 1215–1222 (2004).

158. Ravikumar, B. *et al.* Inhibition of mTOR induces autophagy and reduces toxicity of polyglutamine expansions in fly and mouse models of Huntington disease. *Nat Genet* **36,** 585–95 (2004).

159. Kreiner, G. *et al.* A neuroprotective phase precedes striatal degeneration upon nucleolar stress. *Cell Death Differ* **20,** 1455–1464 (2013).

160. Berger, Z. *et al.* Rapamycin alleviates toxicity of different aggregate-prone proteins. *Hum. Mol. Genet.* **15,** 433–442 (2006).

161. Pandey, U. B. *et al.* HDAC6 rescues neurodegeneration and provides an essential link between autophagy and the UPS. *Nature* **447,** 860–864 (2007).

162. King, M. A. *et al.* Rapamycin Inhibits Polyglutamine Aggregation Independently of Autophagy by Reducing Protein Synthesis. *Mol. Pharmacol.* **73,** 1052–1063 (2008).

163. Van Slegtenhorst, M. *et al.* Identification of the tuberous sclerosis gene TSC1 on chromosome 9q34. *Science* **277,** 805–8 (1997).

164. Kandt, R. S. *et al.* Linkage of an important gene locus for tuberous sclerosis to a chromosome 16 marker for polycystic kidney disease. *Nat Genet* **2,** 37–41 (1992).

165. Osborne, J. P., Fryer, A. & Webb, D. Epidemiology of tuberous sclerosis. *Ann. N. Y. Acad. Sci.* **615,** 125–127 (1991).

166. Holmes, G. L. & Stafstrom, C. E. Tuberous sclerosis complex and epilepsy: recent developments and future challenges. *Epilepsia* **48,** 617–630 (2007).

167. Baybis, M. *et al.* mTOR cascade activation distinguishes tubers from focal cortical dysplasia. *Ann. Neurol.* **56,** 478–487 (2004).

168. Chan, J. A. *et al.* Pathogenesis of tuberous sclerosis subependymal giant cell astrocytomas: biallelic inactivation of TSC1 or TSC2 leads to mTOR activation. *J. Neuropathol. Exp. Neurol.* **63,** 1236–1242 (2004).

169. Meikle, L. *et al.* A mouse model of tuberous sclerosis: neuronal loss of Tsc1 causes dysplastic and ectopic neurons, reduced myelination, seizure activity, and limited survival. *J. Neurosci.* **27,** 5546–5558 (2007).

170. Meikle, L. *et al.* Response of a neuronal model of tuberous sclerosis to mammalian target of rapamycin (mTOR) inhibitors: effects on mTORC1 and Akt signaling lead to improved survival and function. *J. Neurosci.* **28,** 5422–5432 (2008).

171. Zeng, L., Xu, L., Gutmann, D. H. & Wong, M. Rapamycin prevents epilepsy in a mouse model of tuberous sclerosis complex. *Ann. Neurol.* **63,** 444–453 (2008).

172. Uhlmann, E. J. *et al.* Loss of tuberous sclerosis complex 1 (Tsc1) expression results in increased Rheb/S6K pathway signaling important for astrocyte cell size regulation. *Glia* **47,** 180–188 (2004).

173. Raffo, E., Coppola, A., Ono, T., Briggs, S. W. & Galanopoulou, A. S. A pulse rapamycin therapy for infantile spasms and associated cognitive decline. *Neurobiol Dis* **43,** 322–9 (2011).

174. Krueger, D. A. *et al.* Everolimus for subependymal giant-cell astrocytomas in tuberous sclerosis. *N. Engl. J. Med.* **363,** 1801–1811 (2010).

175. Kotulska, K. *et al.* Long-term effect of everolimus on epilepsy and growth in children under 3 years of age treated for subependymal giant cell astrocytoma associated with tuberous sclerosis complex. *Eur. J. Paediatr. Neurol.* **17,** 479–485 (2013).

176. Franz, D. N. Everolimus: an mTOR inhibitor for the treatment of tuberous sclerosis. *Expert Rev. Anticancer Ther.* **11,** 1181–1192 (2011).

177. Muncy, J., Butler, I. J. & Koenig, M. K. Rapamycin reduces seizure frequency in tuberous sclerosis complex. *J Child Neurol* **24,** 477 (2009).

178. Sengupta, S., Peterson, T. R., Laplante, M., Oh, S. & Sabatini, D. M. mTORC1 controls fasting-induced ketogenesis and its modulation by ageing. *Nature* **468,** 1100–1104 (2010).

179. Freeman, J. M. *The ketogenic diet: a treatment for children and others with epilepsy*. (Demos medical publishing, 2007).

180. McDaniel, S. S., Rensing, N. R., Thio, L. L., Yamada, K. A. & Wong, M. The ketogenic diet inhibits the mammalian target of rapamycin (mTOR) pathway. *Epilepsia* **52,** e7–e11 (2011).

181. Hagerman, R. J. & Hagerman, P. J. The fragile X premutation: into the phenotypic fold. *Curr Opin Genet Dev* **12,** 278–83 (2002).

182. Jacquemont, S., Hagerman, R. J., Hagerman, P. J. & Leehey, M. A. Fragile-X syndrome and fragile X-associated tremor/ataxia syndrome: two faces of FMR1. *Lancet Neurol.* **6,** 45–55 (2007).

183. Ronesi, J. A. & Huber, K. M. Metabotropic Glutamate Receptors and Fragile X Mental Retardation Protein: Partners in Translational Regulation at the Synapse. *Sci. Signal.* **1,** pe6 (2008).

184. Fragile X syndrome. *Genet. Home Ref.* (2014). at <http://ghr.nlm.nih.gov/condition/fragile-x-syndrome>

185. Bailey, D. B., Raspa, M., Bishop, E. & Holiday, D. No Change in the Age of Diagnosis for Fragile X Syndrome: Findings From a National Parent Survey. *Pediatrics* **124,** 527–533 (2009).

186. Feng, Y. *et al.* Fragile X Mental Retardation Protein: Nucleocytoplasmic Shuttling and Association with Somatodendritic Ribosomes. *J. Neurosci.* **17,** 1539–1547 (1997).

187. Garber, K., Smith, K. T., Reines, D. & Warren, S. T. Transcription, translation and fragile X syndrome. *Curr. Opin. Genet. Dev.* **16,** 270–275 (6).

188. Oberle, I. *et al.* Instability of a 550-base pair DNA segment and abnormal methylation in fragile X syndrome. *Science* **252,** 1097–102 (1991).

189. Dombrowski, C. *et al.* Premutation and intermediate-size FMR1 alleles in 10572 males from the general population: loss of an AGG interruption is a late event in the generation of fragile X syndrome alleles. *Hum Mol Genet* **11,** 371–8 (2002).

190. Bagni, C. & Greenough, W. T. From mRNP trafficking to spine dysmorphogenesis: the roots of fragile X syndrome. *Nat Rev Neurosci* **6,** 376–87 (2005).

191. O'Donnell, W. T. & Warren, S. T. A decade of molecular studies of fragile X syndrome. *Annu Rev Neurosci* **25,** 315–38 (2002).

192. Huber, K. M., Gallagher, S. M., Warren, S. T. & Bear, M. F. Altered synaptic plasticity in a mouse model of fragile X mental retardation. *Proc Natl Acad Sci U A* **99,** 7746–50 (2002).

193. Hoeffer, C. A. *et al.* Altered mTOR signaling and enhanced CYFIP2 expression levels in subjects with fragile X syndrome. *Genes Brain Behav* **11,** 332–41 (2012).

194. Nosyreva, E. D. & Huber, K. M. Metabotropic receptor-dependent long-term depression persists in the absence of protein synthesis in the mouse model of fragile X syndrome. *J Neurophysiol* **95,** 3291–5 (2006).

195. Sharma, A. *et al.* Dysregulation of mTOR signaling in fragile X syndrome. *J Neurosci* **30,** 694–702 (2010).

196. Farina, L. *et al.* MR Findings in Leigh Syndrome with COX Deficiency and SURF-1 Mutations. *Am. J. Neuroradiol.* **23,** 1095–1100 (2002).

197. Ostergaard, E. *et al.* Deficiency of the alpha subunit of succinate-coenzyme A ligase causes fatal infantile lactic acidosis with mitochondrial DNA depletion. *Am J Hum Genet* **81,** 383–7 (2007).

198. Darin, N., Oldfors, A., Moslemi, A. R., Holme, E. & Tulinius, M. The incidence of mitochondrial encephalomyopathies in childhood: clinical features and morphological, biochemical, and DNA anbormalities. *Ann. Neurol.* **49,** 377–383 (2001).

199. Rahman, S. *et al.* Leigh syndrome: clinical features and biochemical and DNA abnormalities. *Ann. Neurol.* **39,** 343–351 (1996).

200. Finsterer, J. Leigh and Leigh-like syndrome in children and adults. *Pediatr. Neurol.* **39,** 223–235 (2008).

201. Kerr, D. S. Review of clinical trials for mitochondrial disorders: 1997-2012. *Neurother. J. Am. Soc. Exp. Neurother.* **10,** 307–319 (2013).

202. Cooper, M. P. *et al.* Defects in energy homeostasis in Leigh syndrome French Canadian variant through PGC-1alpha/LRP130 complex. *Genes Dev.* **20,** 2996–3009 (2006).

203. Johnson, S. C. *et al.* mTOR inhibition alleviates mitochondrial disease in a mouse model of Leigh syndrome. *Science* **342,** 1524–8 (2013).

204. Kruse, S. E. *et al.* Mice with Mitochondrial Complex I Deficiency Develop a Fatal Encephalomyopathy. *Cell Metab.* **7,** 312–320 (2008).

205. Van Erven, P. M. *et al.* Leigh syndrome, a mitochondrial encephalo(myo)pathy. A review of the literature. *Clin. Neurol. Neurosurg.* **89,** 217–230 (1987).

206. Arii, J. & Tanabe, Y. Leigh syndrome: serial MR imaging and clinical follow-up. *AJNR Am. J. Neuroradiol.* **21,** 1502–1509 (2000).

207. Schleit, J. *et al.* Molecular mechanisms underlying genotype-dependent responses to dietary restriction. *Aging Cell* **12,** 1050–1061 (2013).

208. Quintana, A., Kruse, S. E., Kapur, R. P., Sanz, E. & Palmiter, R. D. Complex I deficiency due to loss of Ndufs4 in the brain results in progressive encephalopathy resembling Leigh syndrome. *Proc. Natl. Acad. Sci. U. S. A.* **107,** 10996–11001 (2010).

209. Breuer, M. E., Willems, P. H. G. M., Smeitink, J. A. M., Koopman, W. J. H. & Nooteboom, M. Cellular and animal models for mitochondrial complex I deficiency: a focus on the NDUFS4 subunit. *IUBMB Life* **65,** 202–208 (2013).

210. Scacco, S. *et al.* cAMP-dependent phosphorylation of the nuclear encoded 18-kDa (IP) subunit of respiratory complex I and activation of the complex in serum-starved mouse fibroblast cultures. *J. Biol. Chem.* **275,** 17578–17582 (2000).

211. Ramos, F. J. *et al.* Rapamycin reverses elevated mTORC1 signaling in lamin A/C-deficient mice, rescues cardiac and skeletal muscle function, and extends survival. *Sci. Transl. Med.* **4,** 144ra103 (2012).

212. Johnson, S. C., Rabinovitch, P. S. & Kaeberlein, M. mTOR is a key modulator of ageing and age-related disease. *Nature* **493,** 338–45 (2013).

213. Taylor, A. L., Watson, C. J. E. & Bradley, J. A. Immunosuppressive agents in solid organ transplantation: Mechanisms of action and therapeutic efficacy. *Crit. Rev. Oncol. Hematol.* **56,** 23–46 (2005).

214. Blagosklonny, M. V. Calorie restriction: decelerating mTOR-driven aging from cells to organisms (including humans). *Cell Cycle Georget. Tex* **9,** 683–688 (2010).

215. Patel, K. P., O'Brien, T. W., Subramony, S. H., Shuster, J. & Stacpoole, P. W. The spectrum of pyruvate dehydrogenase complex deficiency: clinical, biochemical and genetic features in 371 patients. *Mol. Genet. Metab.* **106,** 385–394 (2012).

216. Miller, R. A. *et al.* Rapamycin, but not resveratrol or simvastatin, extends life span of genetically heterogeneous mice. *J Gerontol Biol Sci Med Sci* **66,** 191–201 (2011).

217. Zhang, Y. *et al.* Rapamycin Extends Life and Health in C57BL/6 Mice. *J. Gerontol. A. Biol. Sci. Med. Sci.* **69A,** 119–130 (2014).

218. Neff, F. *et al.* Rapamycin extends murine lifespan but has limited effects on aging. *J. Clin. Invest.* **123,** 3272–3291 (2013).

219. Anisimov, V. N. *et al.* Rapamycin increases lifespan and inhibits spontaneous tumorigenesis in inbred female mice. *Cell Cycle* **10,** 4230–6 (2011).

220. Wilkinson, J. E. *et al.* Rapamycin slows aging in mice. *Aging Cell* **11,** 675–682 (2012).

221. Blagosklonny, M. V. Rapamycin extends life- and health span because it slows aging. *Aging* **5,** 592–8 (2013).

222. Richardson, A. Rapamycin, anti-aging, and avoiding the fate of Tithonus. *J. Clin. Invest.* **123,** 3204–3206 (2013).

223. Johnson, S. C., Martin, G. M., Rabinovitch, P. S. & Kaeberlein, M. Preserving Youth: Does Rapamycin Deliver? *Sci. Transl. Med.* **5,** 211fs40–211fs40 (2013).

224. Kaeberlein, M. mTOR Inhibition: From Aging to Autism and Beyond. *Scientifica* **2013,** e849186 (2013).

225. Anderson, S. L. *et al.* A novel mutation in NDUFS4 causes Leigh syndrome in an Ashkenazi Jewish family. *J. Inherit. Metab. Dis.* **31,** 461–467 (2008).

226. Budde, S. M. S. *et al.* Combined Enzymatic Complex I and III Deficiency Associated with Mutations in the Nuclear Encoded NDUFS4 Gene. *Biochem. Biophys. Res. Commun.* **275,** 63–68 (2000).

227. Budde, S. M. S., Heuvel, L. P. W. J. van den & Smeitink, J. A. M. The human complex I NDUFS4 subunit: from gene structure to function and pathology. *Mitochondrion* **2,** 109–115 (2002).

228. Budde, S. M. S. *et al.* Clinical heterogeneity in patients with mutations in the NDUFS4 gene of mitochondrial complex I. *J. Inherit. Metab. Dis.* **26,** 813–815 (2003).

229. Johnson, S. C. *et al.* mTOR Inhibition Alleviates Mitochondrial Disease in a Mouse Model of Leigh Syndrome. *Science* **342,** 1524–1528 (2013).

230. Meikle, L. *et al.* Response of a neuronal model of tuberous sclerosis to mammalian target of rapamycin (mTOR) inhibitors: effects on mTORC1 and Akt signaling lead to improved survival and function. *J. Neurosci. Off. J. Soc. Neurosci.* **28,** 5422–5432 (2008).

231. Yang, S.-B. *et al.* Rapamycin ameliorates age-dependent obesity associated with increased mTOR signaling in hypothalamic POMC neurons. *Neuron* **75,** 425–436 (2012).

232. Yu, Z. *et al.* Rapamycin and Dietary Restriction Induce Metabolically Distinctive Changes in Mouse Liver. *J. Gerontol. A. Biol. Sci. Med. Sci.* (2014). doi:10.1093/gerona/glu053

233. Sengupta, S., Peterson, T. R., Laplante, M., Oh, S. & Sabatini, D. M. mTORC1 controls fasting-induced ketogenesis and its modulation by ageing. *Nature* **468,** 1100–1104 (2010).

234. Fok, W. C. *et al.* Mice Fed Rapamycin Have an Increase in Lifespan Associated with Major Changes in the Liver Transcriptome. *PLoS ONE* **9,** e83988 (2014).

235. Langston, J. W., Ballard, P., Tetrud, J. W. & Irwin, I. Chronic Parkinsonism in humans due to a product of meperidine-analog synthesis. *Science* **219,** 979–980 (1983).

236. Forno, L. S., DeLanney, L. E., Irwin, I. & Langston, J. W. Similarities and differences between MPTP-induced parkinsonsim and Parkinson's disease. Neuropathologic considerations. *Adv. Neurol.* **60,** 600–608 (1993).

237. Nicklas, W. J., Youngster, S. K., Kindt, M. V. & Heikkila, R. E. MPTP, MPP+ and mitochondrial function. *Life Sci.* **40,** 721–729 (1987).

238. Markey, S. P., Johannessen, J. N., Chiueh, C. C., Burns, R. S. & Herkenham, M. A. Intraneuronal generation of a pyridinium metabolite may cause drug-induced parkinsonism. *Nature* **311,** 464–467 (1984).

239. Chan, P., DeLanney, L. E., Irwin, I., Langston, J. W. & Di Monte, D. Rapid ATP Loss Caused by 1-Methyl-4-Phenyl-1,2,3,6-Tetrahydropyridine in Mouse Brain. *J. Neurochem.* **57,** 348–351 (1991).

240. Fabre, E., Monserrat, J., Herrero, A., Barja, G. & Leret, M. L. Effect of MPTP on brain mitochondrial H2O2 and ATP production and on dopamine and DOPAC in the striatum. *J. Physiol. Biochem.* **55,** 325–331 (1999).

241. Hasegawa, E., Takeshige, K., Oishi, T., Murai, Y. & Minakami, S. 1-Methyl-4-phenylpyridinium (MPP+) induces NADH-dependent superoxide formation and enhances NADH-dependent lipid peroxidation in bovine heart submitochondrial particles. *Biochem. Biophys. Res. Commun.* **170,** 1049–1055 (1990).

242. Hasegawa, E. *et al.* A dual effect of 1-methyl-4-phenylpyridinium (MPP+)-analogs on the respiratory chain of bovine heart mitochondria. *Arch. Biochem. Biophys.* **337,** 69–74 (1997).

243. Przedborski, S. *et al.* Transgenic mice with increased Cu/Zn-superoxide dismutase activity are resistant to N-methyl-4-phenyl-1,2,3,6-tetrahydropyridine-induced neurotoxicity. *J. Neurosci.* **12,** 1658–1667 (1992).

244. Schapira, A. H. *et al.* Mitochondrial complex I deficiency in Parkinson's disease. *J. Neurochem.* **54,** 823–827 (1990).

245. Keeney, P. M., Xie, J., Capaldi, R. A. & Bennett, J. P. Parkinson's Disease Brain Mitochondrial Complex I Has Oxidatively Damaged Subunits and Is Functionally Impaired and Misassembled. *J. Neurosci.* **26,** 5256–5264 (2006).

246. An, W. L. *et al.* Up-regulation of phosphorylated/activated p70 S6 kinase and its relationship to neurofibrillary pathology in Alzheimer's disease. *Am J Pathol* **163,** 591–607 (2003).

247. Lafay-Chebassier, C. *et al.* mTOR/p70S6k signalling alteration by Abeta exposure as well as in APP-PS1 transgenic models and in patients with Alzheimer's disease. *J Neurochem* **94,** 215–25 (2005).

248. Pei, J. J., Sjogren, M. & Winblad, B. Neurofibrillary degeneration in Alzheimer's disease: from molecular mechanisms to identification of drug targets. *Curr Opin Psychiatry* **21,** 555–61 (2008).

249. Griffin, R. J. *et al.* Activation of Akt/PKB, increased phosphorylation of Akt substrates and loss and altered distribution of Akt and PTEN are features of Alzheimer's disease pathology. *J Neurochem* **93,** 105–17 (2005).

250. Khurana, V. *et al.* TOR-mediated cell-cycle activation causes neurodegeneration in a Drosophila tauopathy model. *Curr Biol* **16,** 230–41 (2006).

251. Ravikumar, B. *et al.* Inhibition of mTOR induces autophagy and reduces toxicity of polyglutamine expansions in fly and mouse models of Huntington disease. *Nat Genet* **36,** 585–95 (2004).

252. Nagatsu, T., Levitt, M. & Udenfriend, S. TYROSINE HYDROXYLASE. THE INITIAL STEP IN NOREPINEPHRINE BIOSYNTHESIS. *J. Biol. Chem.* **239,** 2910–2917 (1964).

253. Aviles-Olmos, I., Limousin, P., Lees, A. & Foltynie, T. Parkinson's disease, insulin resistance and novel agents of neuroprotection. *Brain* **136,** 374–384 (2013).

254. M Bousquet, I. S.-A. High-fat diet exacerbates MPTP-induced dopaminergic degeneration in mice. *Neurobiol. Dis.* **45,** 529–38 (2012).

255. Craft, S. & Stennis Watson, G. Insulin and neurodegenerative disease: shared and specific mechanisms. *Lancet Neurol.* **3,** 169–178 (2004).

256. Sedelis, M., Schwarting, R. K. & Huston, J. P. Behavioral phenotyping of the MPTP mouse model of Parkinson's disease. *Behav. Brain Res.* **125,** 109–125 (2001).

257. Jackson-Lewis, V. & Przedborski, S. Protocol for the MPTP mouse model of Parkinson's disease. *Nat. Protoc.* **2,** 141–151 (2007).

258. Gupta, M. *et al.* Aged mice are more sensitive to 1-methyl-4-phenyl-1,2,3,6-tetrahydropyridine treatment than young adults. *Neurosci. Lett.* **70,** 326–331 (1986).

259. Sugama, S. *et al.* Age-related microglial activation in 1-methyl-4-phenyl-1,2,3,6-tetrahydropyridine (MPTP)-induced dopaminergic neurodegeneration in C57BL/6 mice. *Brain Res.* **964,** 288–294 (2003).

260. Maiese, K., Chong, Z. Z., Shang, Y. C. & Wang, S. mTOR: on target for novel therapeutic strategies in the nervous system. *Trends Mol. Med.* **19,** 51–60 (1).

261. Ekberg, H. *et al.* Cyclosporine, tacrolimus and sirolimus retain their distinct toxicity profiles despite low doses in the Symphony study. *Nephrol. Dial. Transplant.* **25,** 2004–2010 (2010).